University Transportation Research Center - Region 2

Final Report

Correlation between Multiple Stress Creep Recovery (MSCR) Results and Polymer Modification of Binder

Performing Organization: Rowan University

September, 2013

Sponsor(s):
New Jersey Department of Transportation (NJDOT)
University Transportation Research Center - Region 2

University Transportation Research Center - Region 2

The Region 2 University Transportation Research Center (UTRC) is one of ten original University Transportation Centers established in 1987 by the U.S. Congress. These Centers were established with the recognition that transportation plays a key role in the nation's economy and the quality of life of its citizens. University faculty members provide a critical link in resolving our national and regional transportation problems while training the professionals who address our transportation systems and their customers on a daily basis.

The UTRC was established in order to support research, education and the transfer of technology in the field of transportation. The theme of the Center is "Planning and Managing Regional Transportation Systems in a Changing World." Presently, under the direction of Dr. Camille Kamga, the UTRC represents USDOT Region II, including New York, New Jersey, Puerto Rico and the U.S. Virgin Islands. Functioning as a consortium of twelve major Universities throughout the region, UTRC is located at the CUNY Institute for Transportation Systems at The City College of New York, the lead institution of the consortium. The Center, through its consortium, an Agency-Industry Council and its Director and Staff, supports research, education, and technology transfer under its theme. UTRC's three main goals are:

Research

The research program objectives are (1) to develop a theme based transportation research program that is responsive to the needs of regional transportation organizations and stakeholders, and (2) to conduct that program in cooperation with the partners. The program includes both studies that are identified with research partners of projects targeted to the theme, and targeted, short-term projects. The program develops competitive proposals, which are evaluated to insure the mostresponsive UTRC team conducts the work. The research program is responsive to the UTRC theme: "Planning and Managing Regional Transportation Systems in a Changing World." The complex transportation system of transit and infrastructure, and the rapidly changing environment impacts the nation's largest city and metropolitan area. The New York/New Jersey Metropolitan has over 19 million people, 600,000 businesses and 9 million workers. The Region's intermodal and multimodal systems must serve all customers and stakeholders within the region and globally.Under the current grant, the new research projects and the ongoing research projects concentrate the program efforts on the categories of Transportation Systems Performance and Information Infrastructure to provide needed services to the New Jersey Department of Transportation, New York City Department of Transportation, New York Metropolitan Transportation Council , New York State Department of Transportation, and the New York State Energy and Research Development Authorityand others, all while enhancing the center's theme.

Education and Workforce Development

The modern professional must combine the technical skills of engineering and planning with knowledge of economics, environmental science, management, finance, and law as well as negotiation skills, psychology and sociology. And, she/he must be computer literate, wired to the web, and knowledgeable about advances in information technology. UTRC's education and training efforts provide a multidisciplinary program of course work and experiential learning to train students and provide advanced training or retraining of practitioners to plan and manage regional transportation systems. UTRC must meet the need to educate the undergraduate and graduate student with a foundation of transportation fundamentals that allows for solving complex problems in a world much more dynamic than even a decade ago. Simultaneously, the demand for continuing education is growing – either because of professional license requirements or because the workplace demands it – and provides the opportunity to combine State of Practice education with tailored ways of delivering content.

Technology Transfer

UTRC's Technology Transfer Program goes beyond what might be considered "traditional" technology transfer activities. Its main objectives are (1) to increase the awareness and level of information concerning transportation issues facing Region 2; (2) to improve the knowledge base and approach to problem solving of the region's transportation workforce, from those operating the systems to those at the most senior level of managing the system; and by doing so, to improve the overall professional capability of the transportation workforce; (3) to stimulate discussion and debate concerning the integration of new technologies into our culture, our work and our transportation systems; (4) to provide the more traditional but extremely important job of disseminating research and project reports, studies, analysis and use of tools to the education, research and practicing community both nationally and internationally; and (5) to provide unbiased information and testimony to decision-makers concerning regional transportation issues consistent with the UTRC theme.

UTRC-RF Project No: 75144-05-20

Project Date: Setember 30, 2013

Project Title: Correlation between Multiple Stress Creep Recovery (MSCR) Results and Polymer Modification of Binderent of Complex Transportation Networks

Project's Website:
http://www.utrc2.org/research/projects/polymer-modification-binder

Principal Investigator:

Dr. Yusuf Mehta
Associate Professor
Department of Civil and Environmental Engineering
201 Mullica Hill Road
329 Rowan Hall
Glassboro, NJ 08028
Phone: (856) 256-5327
Email: Mehta@rowan.edu

Co-Author(s)

Aaron Nolan
Research Associate

- Eric DuBois
- Sara Zorn
- Eileen Batten
- Prashant Shirodkar
Undergraduate and Graduate Students
Department of Civil and Environmental Engineering
Rowan University Yang, Sami Demiroluk, Ender Morgul, Bekir Bartinering

Performing Organization: Rowan University

Sponsor(s):

New Jersey Department of Transportation (NJDOT)

University Transportation Research Center - Region 2, A Regional University Transportation Center sponsored by the U.S. Department of Transportation's Research and Innovative Technology Administration

To request a hard copy of our final reports, please send us an email at utrc@utrc2.org

Mailing Address:
University Transportation Reserch Center
The City College of New York
Marshak Hall, Suite 910
160 Convent Avenue
New York, NY 10031
Tel: 212-650-8051, Fax: 212-650-8374
Web: www.utrc2.org

Board of Directors

The UTRC Board of Directors consists of one or two members from each Consortium school (each school receives two votes regardless of the number of representatives on the board). The Center Director is an ex-officio member of the Board and The Center management team serves as staff to the Board.

City University of New York
Dr. Hongmian Gong - Geography
Dr. Neville A. Parker - Civil Engineering

Clarkson University
Dr. Kerop D. Janoyan - Civil Engineering

Columbia University
Dr. Raimondo Betti - Civil Engineering
Dr. Elliott Sclar - Urban and Regional Planning

Cornell University
Dr. Huaizhu (Oliver) Gao - Civil Engineering
Dr. Mark A. Turnquist - Civil Engineering

Hofstra University
Dr. Jean-Paul Rodrigue - Global Studies and Geography

Manhattan College
Dr. Anirban De - Civil & Environmental Engineering
Dominic Esposito - Research Administration

New Jersey Institute of Technology
Dr. Steven Chien - Civil Engineering
Dr. Joyoung Lee - Civil & Environmental Engineering

New York Institute of Technology
Dr. Nada Marie Anid - Engineering & Computing Sciences
Dr. Marta Panero - Engineering & Computing Sciences

New York University
Dr. Mitchell L. Moss - Urban Policy and Planning
Dr. Rae Zimmerman - Planning and Public Administration

Polytechnic Institute of NYU
Dr. John C. Falcocchio - Civil Engineering
Dr. Kaan Ozbay - Civil Engineering

Rensselaer Polytechnic Institute
Dr. José Holguín-Veras - Civil Engineering
Dr. William "Al" Wallace - Systems Engineering

Rochester Institute of Technology
Dr. J. Scott Hawker - Software Engineering
Dr. James Winebrake -Science, Technology, & Society/Public Policy

Rowan University
Dr. Yusuf Mehta - Civil Engineering
Dr. Beena Sukumaran - Civil Engineering

Rutgers University
Dr. Robert Noland - Planning and Public Policy

State University of New York
Michael M. Fancher - Nanoscience
Dr. Catherine T. Lawson - City & Regional Planning
Dr. Adel W. Sadek - Transportation Systems Engineering
Dr. Shmuel Yahalom - Economics

Stevens Institute of Technology
Dr. Sophia Hassiotis - Civil Engineering
Dr. Thomas H. Wakeman III - Civil Engineering

Syracuse University
Dr. Riyad S. Aboutaha - Civil Engineering
Dr. O. Sam Salem - Construction Engineering and Management

The College of New Jersey
Dr. Thomas M. Brennan Jr. - Civil Engineering

University of Puerto Rico - Mayagüez
Dr. Ismael Pagán-Trinidad - Civil Engineering
Dr. Didier M. Valdés-Díaz - Civil Engineering

UTRC Consortium Universities

The following universities/colleges are members of the UTRC consortium.

City University of New York (CUNY)
Clarkson University (Clarkson)
Columbia University (Columbia)
Cornell University (Cornell)
Hofstra University (Hofstra)
Manhattan College
New Jersey Institute of Technology (NJIT)
New York Institute of Technology (NYIT)
New York University (NYU)
Polytechnic Institute of NYU (Poly)
Rensselaer Polytechnic Institute (RPI)
Rochester Institute of Technology (RIT)
Rowan University (Rowan)
Rutgers University (Rutgers)*
State University of New York (SUNY)
Stevens Institute of Technology (Stevens)
Syracuse University (SU)
The College of New Jersey (TCNJ)
University of Puerto Rico - Mayagüez (UPRM)

** Member under SAFETEA-LU Legislation*

UTRC Key Staff

Dr. Camille Kamga: *Director, UTRC*
Assistant Professor of Civil Engineering, CCNY

Dr. Robert E. Paaswell: *Director Emeritus of UTRC and Distinguished* Professor of Civil Engineering, The City College of New York

Herbert Levinson: *UTRC Icon Mentor, Transportation Consultant and Professor Emeritus of Transportation*

Dr. Ellen Thorson: *Senior Research Fellow, University Transportation Research Center*

Penny Eickemeyer: *Associate Director for Research, UTRC*

Dr. Alison Conway: *Associate Director for New Initiatives and Assistant Professor of Civil Engineering*

Nadia Aslam: *Assistant Director for Technology Transfer*

Dr. Anil Yazici: *Post-doc/ Senior Researcher*

Nathalie Martinez: *Research Associate/Budget Analyst*

FHWA-NJ-2014-002

Correlation between Multiple Stress Creep Recovery (MSCR) Results and Polymer Modification of Binder

FINAL REPORT

September 30 2013

Submitted by

Yusuf Mehta, Ph.D., P.E.
Associate Professor

Aaron Nolan
Research Associate

Eric DuBois
Sara Zorn
Eileen Batten
Prashant Shirodkar
Undergraduate and Graduate Students
Department of Civil and Environmental Engineering
Rowan University

NJDOT Research Project Manager
Camille Crichton Summers

In cooperation with

New Jersey Department of Transportation
Bureau of Research

TECHNICAL REPORT
STANDARD TITLE PAGE

1. Report No. FHWA- NJ-2014-002	2.Government Accession No.	3. Recipient's Catalog No.
4. Title and Subtitle Correlation between Multiple Stress Creep Recovery (MSCR) Results and Polymer Modification of Binder		5. Report Date September 30 2013 6. Performing Organization Code
7. Author(s) Y. Mehta[1], A. Nolan[1], E. DuBois[1], S. Zorn[1], P. Shirodkar[1] 1. Rowan University		8. Performing Organization Report No.
9. Performing Organization Name and Address Rowan University College of Engineering Glassboro, NJ 08028		10. Work Unit No. 11. Contract or Grant No. 75144-05-20
12. Sponsoring Agency Name and Address New Jersey Department of Transportation PO 600 Trenton, NJ 08625 Federal Highway Administration U.S. Department of Transportation Washington, D.C. University Transportation Research Center City College of New York-Marshak 910 160 Convent Avenue, NewYork, NY 10031		13. Type of Report and Period Covered 14. Sponsoring Agency Code

15. Supplementary Notes

16. Abstract

Nationwide traffic loads are increasing, pushing conventional asphalt to its limit. In New Jersey matters are made worse by the heavy use of the Northeast Corridor. Polymer modification of asphalt, which can improve both low and high performance, is already available; however, in many cases traditional Superpave testing is not sensitive enough to quantify the impact of modification, dimensioning its use. Elastic Recovery and Forced Ductility, Superpave Performance Grade Plus tests, are sensitive to polymer modification but are time intensive and costly. These obstacles have lead the New Jersey Department of Transportation to require styrene-butadiene or styrene-butadiene-styrene to be incorporated in all modified binder to ensure performance, causing supply shortages and rising cost in the state. A relatively new test developed by the Federal Highway Administration, Multiple Stress Creep Compliance (MSCR) offers a simpler procedure using the Dynamic Shear Rheometer (DSR), thus it does not require the expense of purchase additional testing equipment. The objective of this study is to determine the feasibility of using MSCR as a specification for binder testing. Upon testing a variety of binders it has been determined that MSCR binder testing is sensitive to flow time results. Binders with non-recoverable compliance value (J_{nr}) of less than 0.5 kPa^{-1} appear to show better high temperature performance. The MSCR elastic curve requirement appears to be the most stringent of the requirements to evaluate elastic response as compared to elastic recovery at 25ºC and phase angle of 75º. An MSCR recovery at 3.2kPa greater than 40% will ensure that it is above the MSCR elastic recovery curve. This could serve as an alternative specification to the MSCR elastic recovery curve. The guidelines set forth by AASHTO MP 19-10, in which the binders are graded according to traffic (ESALs) by using J_{nr} is recommended. Additionally 1) The New Jersey DOT should use the access database system as a prescreening process for binder selection, alleviating extraneous binder testing and the cost associated with them. 2) New Jersey DOT could eliminate the use of elastic recovery, thus saving almost $15,000 dollars on capital cost of equipment and up to $500 per binder characterization considering labor and depreciation cost. These could lead to considerable savings of thousands of dollars over several years.; 3) Additional testing, including field performance should be conducted on binders with low J_{nr} (less than 0.5 kPa^{-1}) and with a lower PG-grade, such as PG 64-28 versus PG64-22. and 4) This can be addressed by closely looking at the ODSR result of binders. For example, at 64˚C, if the G*/sin(δ) is below 2.0 kPa, it is unlikely to pass a higher grade and withstand heavy traffic., and 5) Low non-recoverable creep compliance (Jnr < 0.5 kPa^{-1}) coupled with high MSCR recovery at 3.2 kPa (recovery greater than 40%) and G*/sin(δ) high enough to pass the next high grade will ensure that the binder selected will withstand heavy and extreme traffic levels.

17. Key Words: MSCR, binder specification, elastic recovery		18. Distribution Statement	
19. Security Classif (of this report) Unclassified	20. Security Classif. (of this page) Unclassified	21. No of Pages	22. Price

Form DOT F 1700.7 (8-69)

DISCLAIMER STATEMENT

"The contents of this report reflect the views of the author(s) who is (are) responsible for the facts and the accuracy of the data presented herein. The contents do not necessarily reflect the official views or policies of the New Jersey Department of Transportation or the Federal Highway Administration. This report does not constitute a standard, specification, or regulation."

Table of Contents

List of Figures

List of Tables

Executive Summary

Several states including New Jersey Department of Transportation (NJDOT) require the use of specific polymers, such as styrene-butadiene-styrene (SBS) or styrene-butadiene-rubber (SBR) in their polymer modified binders. The reasons for such a requirement is that these polymers have been known to perform well in the field and a there was a lack of appropriate parameter that is sensitive to polymer modification and can discern good and poor performing binders. Several states, such as New Jersey DOT use parameters measured in the PG plus tests, such as elastic recovery for polymer modified binders. For example, currently NDOT requires that elastic recovery should be more than 60%. In the past five years or so, a new test procedure multiple stress creep and recovery (MSCR) test was developed to capture the response of polymer modified binders. The two properties measured from this test is the non-recoverable compliance and the percent recovery at the end of 10 cycle of testing at 0.1 kPa followed by ten cycles of 3.2 kPa. The MSCR test, unlike the Superpave (AASHTO M320) is tested to failure. These high strain values are necessary to appropriately capture the response of the polymers in the binder. The objective of this study was to do a comprehensive laboratory evaluation of a broad range of neat and polymer modified binders recommend appropriate specifications for the PMB for the state of New Jersey.

The first phase of the research was to measure parameters from the Superpave (AASHTO M320), PG plus tests (Elastic recovery and force- ductility), and the MSCR test and compare the parameters measured between these test. The goal of the comparison was the neat, refinery provided binders, and in-house mixed PMB was to determine which parameters are most sensitive to polymer modification and would appropriately capture the elastic response contributed to the elastomers. The key findings of the study were that the percent recoveries of polymer modified binders at 3.2 kPa measured in MSCR vary significantly (as much as six to seven times) within the same performance grade. The addition of PPA in the 1.5% Elvaloy in NuStar 64-22 quadrupled the recovery measured in the MSCR test. However, such a dramatic improvement was not observed when Elastic Recovery was tested at 25°C. All received binders and the binder modified with PPA had recovery values greater than 60% while binders that graded at 64 and 70°C fell below the 60% recovery. All binders with a J_{nr} at 3.2kPa at 64 °C less than 0.6 kPa^{-1} exhibited elastic recovery more than 60%. All binders that had the MSCR recovery at 3.2 kPa greater than 40% was above the MSCR elastic recovery curve and all binders that were above the MSCR elastic recovery curve passed the elastic recovery requirement of 60%. Phase angle slightly increases with J_{nr}, and decrease with percentage of recovery. The peak ratio decreased with increase in non-recoverable compliance. Peak ratios and areas under the load displacement curve did not show sensitivity to performance grades. The area under the load-displacement curve was sensitive to the percent by volume of modifier added in the asphalt binders. One of the interesting findings of this analysis was that for the most part, low J_{nr} values translated to higher traffic grading as per AASHTO MP-19, except in some cases. For example, some polymer modified binders graded as PG 64-28, which were primarily designed to withstand low-temperature cracking graded as PG 64E. However, these binders would not be able to withstand the heavy traffic for which they would be graded. One way to resolve this to make sure that the $G^*/\sin(\delta)$ is high enough. The bottom-line from these findings showed that the non-recoverable creep compliance and the percent recovery at 3.2 kPa showed the potential of being sensitive to polymer modification and was more stringent than most of the other specifications typically used for PMB, such as elastic recovery at 60% and the phase angle of 75 degrees.

Based on the findings of the first phase, ten mixes were prepared with a broad range of binders and similar gradation. The purpose of the mix testing was to determine if low non-recoverable creep compliance would translate to better high temperature performance of the mix. The research team selected flow-time test because it also tested the sample to failure and appropriately captured binder behavior, especially in the secondary region of the flow-time test. The mix results confirmed that binders with low-non-recoverable compliance performed well in the flow-time test.

In addition, the research team analyzed the creep and recovery curve measured in the MSCR test to determine the individual components of the accumulated strain, such as linear elastic, non-linear elastic, linear viscoelastic, non-linear viscoelastic, and permanent strain. The goal was to better understand how different polymer components contribute to the strains. Elvaloy and PPA significantly impact the non-linear viscoelastic component of the strains.

The research team also did Gel Permeation Chromatography (GPC), Fourier Transform Infrared Spectroscopy (FTIR) analysis of neat, refinery produced and in-house polymer modified binders to determine the correlation between the molecular weight and amount of polymer with mechanical responses of the binder. Using, GPC, the research team was successful in determining whether or not a polymer is present within a binder, but not in determining the amount or type of polymer used. FTIR has the potential to be used in conjunction with GPC to be able to take any sample of polymer modified binder and find the type and concentration of polymer within that sample. The research team also attempted to determine the Saturates, Asphaltenes, Resins and Aromatics (SARA) of different polymer modified binders. The variability in the results was too high to make any significant correlation between polymer modification and the SARA components.

After conducting a thorough literature review, executing the proposed research plan and subsequent analysis of the results it is the recommendation of this paper for MSCR testing using the parameter J_{nr}, to become a standard means to evaluate polymer modified binders in New Jersey. The guidelines set forth by AASHTO MP 19-10, in which the binders are graded according to traffic (ESALs) by using J_{nr} are recommended. Additionally, a) the New Jersey DOT should use the access database system as a prescreening process for binder selection, alleviating extraneous binder testing and the cost associated with them; b) New Jersey DOT could eliminate the use of elastic recovery, thus saving almost $15,000 dollars on capital cost of equipment and up to $500 per binder characterization considering labor and depreciation cost. These could lead to considerable savings of thousands of dollars over several years; c) Additional testing, including field performance should be conducted on binders with low J_{nr} (less than 0.5 kPa^{-1}) and with a lower PG-grade, such as PG 64-28 versus PG64-22. This can be addressed by closely looking at the ODSR result of binders. For example, at 64˚C, if the $G^*/\sin(\delta)$ is below 2.0 kPa, it is unlikely to pass a higher grade and withstand heavy traffic; d) Low non-recoverable creep compliance ($J_{nr}<0.5kPa^{-1}$) coupled with high MSCR recovery at 3.2 kPa (recovery greater than 40%) and $G^*/\sin(\delta)$ high enough to pass the next high grade will ensure that the binder selected will withstand heavy and extreme traffic levels; and e) Most of the binders provided by the refinery do not have specific compositions. Some binders may have several polymers meeting the target specifications. Therefore, it is not known how other polymers influence the non-recoverable compliance. A detailed evaluation of the impact of a broad range of polymer modification on the non-recoverable compliance is needed. However, appropriate interlocking should be evaluated using direct measurement tools, such as the fluorescent microscope.

Chapter 1 Introduction

1.1 Background

The use of polymer modified binder has increased as conventional bitumen is pushed to its limits by ever increasing traffic demands. While there are a variety of modifiers, the New Jersey Department of Transportation (NJDOT) currently requires styrene-butadiene or styrene-butadiene-styrene to be incorporated in all modified binder, causing supply shortages and rising cost. The requirement is imposed by the NJDOT to ensure a level of quality because styrene-butadiene and styrene-butadiene-styrene have a proven record of performance because unlike conventional or "neat" binders, which have a standard measure of performance in the Superpave performance grading (PG), modified binders have several tests none of which are widely agreed upon. Superpave has attempted to incorporate elastic recovery (ER) and forced ductility (FD), which, are the most widely used tests for modified binders, in a newer grading scheme, called PG Plus grading, to recognize the benefits of the polymer modification. Unfortunately ER and FD are not very reliable indictors of performance and costly as they both require specialty equipment and are time intensive. The Multiple Stress Creep Compliance (MSCR) test, a new test developed by the Federal Highway Administration (FHWA), offers a simpler procedure that may hold the key to quantitatively rating modified binder for expected performance.

The MSCR test is performed on the Dynamic Shear Rheometer, a device already used for Superpave performance grading, and requires a fraction of the time it would take to run other tests. The MSCR parameter J_{nr} measures the non-recoverable creep compliance and is determined by dividing the non-recoverable (or permanent) shear strain by the applied shear stress. To determine if non-recoverable compliance can be utilized as a standard measure of performance of modified binder, testing and analysis will need to be conducted to quantify its sensitivity to mixture performance. If non-recoverable compliance of the binder correlates well with mixture performance this could open the door to the use of a wider variety of modified binders reducing the cost of modified binders, ultimately improve pavement performance by taking advantage of a broad range of polymers.

1.2 Objectives

To verify and qualify the MSCR parameter, non-recoverable compliance J_{nr}, as a standard measure of modified binder performance the following objectives will need to be achieved:

1. Determine from the existing literature the state of practice and the challenges and successes of using polymer and crumb rubber modified binders. This includes types of polymers, test methods to evaluate polymer modified binders; as well as, field and lab performance of mixtures.
2. Conduct traditional Superpave binder tests (AASHTO M 320 Table 1), Superpave PG Plus testing Elastic Recovery and Forced Ductility, to be compared to the non-recoverable creep compliance parameter J_{nr}.
3. Determine chemical compositions such as Saturates, Asphaltenes, Resins and Aromatic, molecular weight and wave numbers of certain polymers for select binders to determine modification type and content.
4. Perform performance testing to link the non-recoverable creep compliance parameter J_{nr} to performance.

   a. Dynamic Complex Modulus (DCM) testing will be conducted to determine the viscoelastic properties of asphalt mixes and will be used as an input for Mechanistic-Empirical Pavement Design Guide (MEPDG) analysis.
   b. Flow Time testing will be used to determine the Flow Time at which under a constant static load the asphalt sample begins to "flow" or deteriorate quickly.
5. Provide a final recommendation to the state of New Jersey if the non-recoverable creep compliance J_{nr} parameter can be used, with appropriate specification limits.
6. Develop a Microsoft access database of binder and mix data so that the state of New Jersey can select appropriate binders and mixtures that can meet the target values.

1.3 Research Approach

Task 1. Conduct literature review
First a thorough literature review was conducted to access the current state of practice. Polymer modification was defined, as well; the most commonly used modifiers were identified. Current testing methods, including MSCR testing, were reviewed for their prevalence and application. Available lab and field performance was evaluated for pertinent information.

Task 2. Conduct traditional Superpave test
Tradition Superpave lab testing commenced on a host of provided and in house modified binders to determine traditional parameters to later be correlated with chemical properties and Superpave PG Plus parameters.

Task 3. Conduct Superpave PG Plus testing
Superpave PG Plus testing method, such as Elastic Recovery, and Forced Ductility were conducted. These tests are already used in some states to measure parameters that are more sensitive to polymer modification. These results will be correlated with traditional Superpave test and MSCR tests.

Task 4. Conduct MSCR Testing
The bulk binder testing concluded with MSCR testing for the non-recoverable creep compliance, J_{nr}, and percentage recovery.

Task 5. Correlate parameters measured from different binder tests
The results of all binder testing were analyzed to clearly assess the impact of polymer modification and the correlation between each parameter measured in binder test and non-recoverable compliance (J_{nr}). In addition, non-linear viscoelastic parameters were determined using the creep and recovery curve measured in MSCR.

Task 6. Conduct GPC, FTIR and SARA Analysis
Additionally the use of Gel Permeation Chromatography (GPC), Fourier Transform Infrared Spectroscopy (FTIP) and Saturates, Asphaltenes, Resins and Aromatic (SARA) analysis was investigated to determine the feasibility of use to determine polymer type and content.

Task 7. Conduct mix performance testing

Once binder testing was complete, performance testing was conducted on select binders based on their J_{nr} to determine whether low non-recoverable creep compliance of binders will lead to poor high temperature performance of mixtures. Dynamic complex modulus testing was initially considered to evaluate mix performance but ultimately Flow Time testing was conducted as the main parameter to evaluate performance of mix. The higher strains of Flow Time testing, which leads to failure of the test samples, was selected in favor of the low, nondestructive, stresses in which DCM testing is conducted under.

Task 8. Correlate mix and binder test results

The results of all testing were analyzed to assess the impact of polymer modification and the connection to J_{nr} on high temperature mix performance.

Task 9. Develop a database

The results of all tests will be compiled into Microsoft access database of binder and mix data for use in industry. The database will allow the state agency to query binder and mix data based on the Superpave and AASHTO M320 specifications.

Task 10. Recommendations

Finally, a recommendation for the use of J_{nr} as a design specification was developed. The specification will include recommended ranges of use and a comparison to the current standard.

1.5 Scope of work

The scope of the work is presented below in Table 1, with the test performed, its specification, the property it determines and the number of binders tested. The number of binders tested for each procedure was dependent on the availability of the binder.

Table 1. Scope of Work

Test	Specification	Property
Superpave	AASHTO M320	High temperature true grade
Superpave	AASHTO M320	Low temperature true grade
Elastic Recovery	AASHTO T301	Percent Recovery (%)
Forced Ductility	AASHTO T300	Peak Ratio
MSCR	AASHTO TP 70	J_{nr} (kPa^{-1}) and Percent Recovery (%)
GPC		Molecular Weight (M_w)
SARA	D 4124 – 01	SARA Composition
DCM	T 342	Dynamic Complex Modulus
Flow Time	TP79-11	Flow Time (sec)

1.6 Significance

The direct impact of this study is the creation of a new specification for the use of polymer modified binders that would alleviate the need to perform Elastic Recovery or Force Ductility. The new testing method is less costly and is performed quicker than the previous methods, thus, allowing industry to implement them more readily. The NJDOT can then use the specification to allow contractors the use of a wider variety of polymer modifiers. More variety should alleviate the supply shortages of SBS and drive down the price of polymer modification. Pavement performance should generally be improved as polymer modification becomes a more affordable option, and is thus made more available.

The cost implications of utilizing MSCR testing over Elastic Recovery can be divided into two categories: expense per test and apparatus expense. The contributing factor to the difference in expense per test is time per test. MSCR testing requires approximately 15 minutes while a single elastic recovery test requires 4 hours from start to finish. It should be noted that although the Elastic Recovery sample must be monitored during the entire testing process there are stages that a lab technician could be performing another task but from experience it can be expected to require approximately half of the 4 hours. MSCR testing is conducted using the Dynamic Shear Rheometer, which is already a commonly used piece of equipment for Superpave testing, while the Elastic Recovery test would require the purchase of a ductilometer, which is priced at about $15,000. Therefore the savings of eliminating elastic recovery binder testing would be approximately $500 per binder characterization in addition to the capital cost mentioned earlier.

Chapter 2 Literature Review

2.1 Polymer Modifiers

Bitumen obtained from distillation of crude oil is a flexible material with a density of 1g/cm^3 at room temperature. But at low temperatures it becomes brittle and high temperatures flows like a viscous liquid. The physical, mechanical and rheological properties of the bitumen primarily depend on its colloidal structure, linked to the chemical composition especially to the proportion of asphaltenes and maltenes. Asphaltenes are polar materials of high molecular weight (10,000 to 100,000) that are insoluble in n-heptane, a non-polar solvent, and is the straight chain alkane with chemical formula $H_3C(CH_2)_5CH_3$ or C_7H_{16} [1]and constitutes 5% to 25% of the bitumen. Maltenes are constituted by resins, aromatic and saturated oils that are soluble in n-heptane and possess low molecular weight. Several polymers (thermoplastics and elastomers) are mixed with bitumen in proportions below 10% to improve the properties of the binder [2] [3].

The polymers used for bitumen modification are divided into two groups, namely elastomers and plastomers. Approximately 75% of modified binders are classified as elastomers, 15% as plastomers and 10% either rubber or miscellaneously modifiers.

Elastomers used in bitumen modification are styrene-butadiene-styrene (SBS), natural rubber, reclaimed tire rubber/crumb rubber, Polybutadiene, Polyisoprene, Isobutene isoprene copolymer, Polychloropren and styrene butadiene rubber (SBR) [4] [5]. In the elastomeric group styrenic block copolymers like SBS have shown the greatest potential when blended with bitumen. The polymers that are classified as plastomers or thermoplastics are Ethyl-vinyl-acetate (EVA), Polyvinyl chloride (PVC), Ethylene propylene (EPDM), Ethylene Acrylate Copolymer and ethylene butyl acrylate (EBA) [5] [6].

2.2 Different Types of Polymers

2.2.1 Styrene Butadiene- Rubber (SBR)

Styrene Butadiene Rubber (SBR) has been widely used as an asphalt modifier as it has been documented: to improve the low-temperature ductility, increase viscosity and elastic recovery; as well as, improves adhesive and cohesive properties of the mixes. The rubber particles are very small and uniform, leading to rapid dispersion and a homogenous mixture. A study by Florida Department of Transportation (DOT) showed that adding SBR increases elasticity, improves adhesion and cohesion, and reduces the rate of oxidation, reducing the effects of aging. Texas DOT found that cement-SBR coated aggregates increased stability when used in HMA. However, it has shown relatively poor tensile strength and poor resistance to cracking [7] [8] [9] [10] [11].

2.2.2 Styrene-Butadiene-Styrene (SBS)

Styrene Butadiene Styrene (SBS) is a tri-block copolymer or a thermoplastic rubber which significantly increases strength at higher temperatures as well as flexibility at lower temperatures [12]. The molecular structure of SBS can be linear or radial. In linear SBS, two polystyrene (PS) blocks are placed at the ends with polybutadiene (PB), an elastomeric block, in the middle. In radial SBS, the molecule of SBS has a star structure with more than three polystyrene blocks. The polar and rigid polystyrene (PS) blocks in SBS make the polymer binder system more resistant to deformation. More polar groups in the polymer provide stronger interactions between the polymer, the asphaltene and the polar aromatic components of asphalt.

[13]. Therefore, SBS can improve the mechanical properties and rheological behavior of conventional asphalt compositions as it is provided with a two-phase morphology. The glassy polystyrene (PS) domains are connected together by the rubbery polybutadiene (PB) segments. [14] [15].

The researchers found that the polystyrene end blocks impart the strength to the polymer while the rubbery matrix blocks of polybutadiene gave the material its exceptional viscosity. That means the glassy ST domains of SBS increase the stiffness of asphalt for high temperature use, whereas the rubbery BT midblocks resist thermal cracking at low service temperatures. They also found that maltene, the soluble fraction extracted from the asphalt by n-heptane, interacts preferentially with the polybutadiene unit of SBS whereas asphaltene, the insoluble fraction, interacts predominantly with the polystyrene unit [16] [17]. Viscosity increases with interactions of asphaltene with polystyrene (PS) units of SBS [18] [17] [4].

2.2.3 Elvaloy

Elvaloy is a terpolymer comprising of ethylene, normal butylacrylate and glycidyl methacrylate (GMA). The molecular weight and comonomer levels may vary during manufacturing of polymers. It has an active ingredient, ethylene glycidyl acrylate (EGA) that chemically reacts with asphalt and becomes stable. The modified binder is elastically improved and more resilient. The GMA portion of the molecule is responsible for this reaction. Elvaloy copolymers react with asphalt and form a polymer linked asphalt system with improved performance properties. The epoxide ring in the glycidal structure undergoes an additional reaction with various functional groups in a typical asphaltene molecule. The asphaltenes which can have carboxylic acid functionality open the epoxy ring and form an aromatic ester. Polymers with higher levels of GMA were evaluated in asphalt. These polymers allow the use of fewer polymers to give the same response in high temperatures [5]. The reaction mechanism of Elvaloy with asphaltene is shown in Figure 1 below.

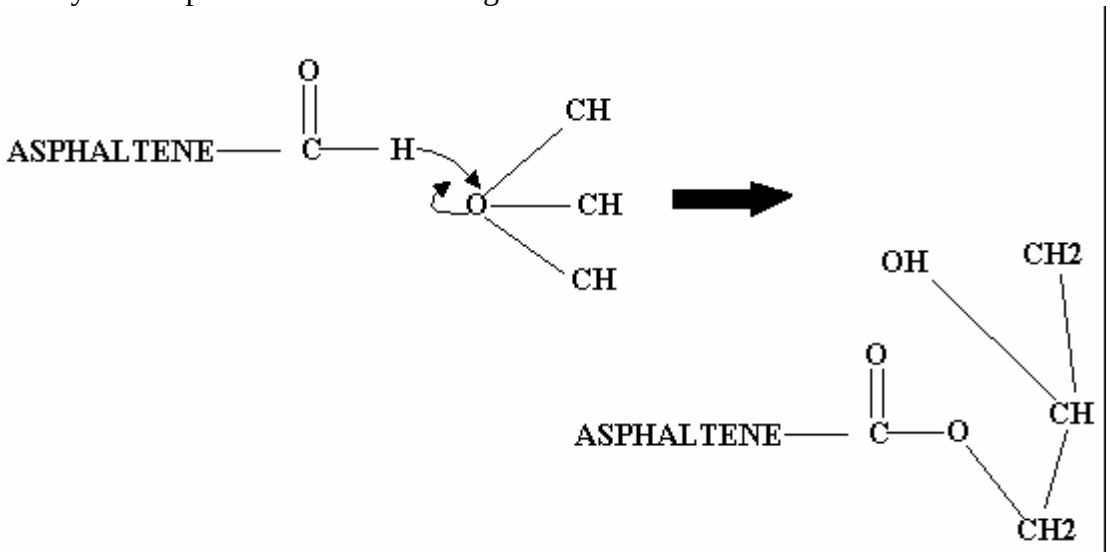

Figure 1. Reaction Mechanism of Elvaloy with [5]

2.2.4 Ethylene Vinyl Acetate (EVA)

EVA is a semi crystalline copolymer and is one of the principal plastomers used to improve both the workability of asphalt during construction and its deformation resistance in service [19]. The EVA polymers are classified as plastomers as they modify bitumen by

formation of a tough and rigid network to resist deformation. The characteristics of EVA fall between those of low density polyethylene, semi rigid translucent product and those of a transparent rubbery material, like plasticized PVC and certain types of rubbers.

2.2.5 Polyphosphoric Acid (PPA) and Gilsonite

Polyphosphoric acid is a liquid mineral polymer having generic composition $H_{n+2}P_nO_{3n+1}$. PPA has a minimum of two phosphorus atoms and a minimum average molecular weight of 258 [20]. Gilsonite is a resinous hydrocarbon that occurs naturally and could be used as a modifier [20].

2.2.6 Crumb Rubber Modifiers (CRM)

Crumb Rubber Modifiers (CRM), are the product of ground tire rubbers that are then added to asphalt to introduce an environmentally friendly method of recycling tires while improving asphalt performance. CRM has been documented to improve rutting resisting properties as well as fatigue life. CRM increases the stiffness and elasticity at high service temperatures while at very low service temperatures stiffness is reduced. However, there is no established procedure for proper use of CRM and consequently obtaining an optimum modification of properties is difficult [21]. This difficulty is due in part to the lack of a test sensitive to polymer modifications impact on performance.

2.3 Testing Methods

Polymer modification is a documented method to improve mix performance; however, the current Superpave binder specification (AASHTO M-320, *Specification for Performance Graded Asphalt Binders*) does not adequately ensure that modified binders will perform well in intended applications. As a result, many state DOTs have added additional tests, to complement the Superpave binder specification, in an attempt to ensure that an acceptable modifier is included in the binder. These "Superpave Plus" tests do not relate directly to performance, but only relate to the presence of a particular modifier in the binder [22]. Several state agencies (Figure 2), including New Jersey, have developed a PG "plus" specification that complements the current Superpave specifications to ensure that a preferred binder is selected.

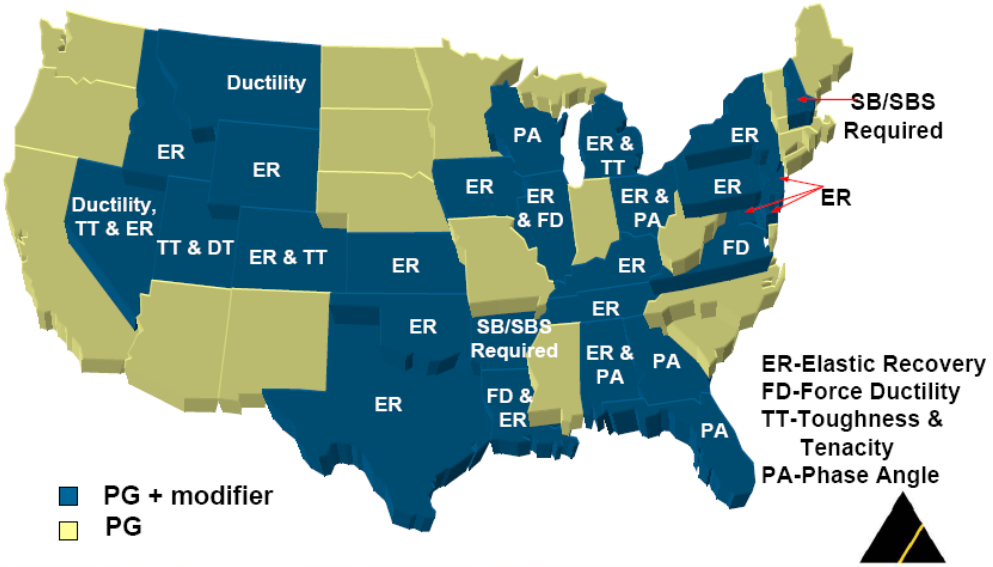

Figure 2. States with PG-Plus Specification [23]

The PG "plus" specifications includes one or more of the following tests 2,3,18:
1. Elastic Recovery (ASTM 6084 Standard Method of Test for Elastic Recovery Test of Bituminous Materials by Means of a Ductilometer) (Used by 42% of state agencies, including New Jersey)
2. Toughness and Tenacity (ASTM D5801-95R01 Test Method for Toughness and Tenacity of Bituminous Materials) (Used by 10% of state agencies)
3. Direct Tension (AASHTO MP1A Direct Tension Test) (Used by 10% of state agencies)
4. Force Ductility (ASTM STP 203-19 Force Ductility of Polymer Modified Binder)
5. Zero Shear Viscosity (used extensively in Europe)
6. Multiple Stress Creep Recovery Testing of Asphalt Binders (recently developed by FHWA)
In many cases not only is there little agreement between experts on the reliability to predict performance of some of the PG plus tests, there is also contradictory finding like in the case of the force ductility test. In a study conducted by the University of Wisconsin, "no correlations could be found to indicate the relevance of the ductility in terms of fatigue or rutting resistance of asphalt" [24]. The MSCR test, a new test, recently developed, could potentially replace many PG-Plus tests as a reliable indicator of performance.

2.3.1 Superpave AASHTO M320

Asphalt binders are required to meet present Superpave binder specifications (AASHTO M-320, 2001). The Superpave Performance Grade (PG) System focuses on climate effects, construction, aging (during construction and in-service), traffic speed, and traffic volume. Justifications for these focuses are that the behavior of asphalt binders depends on temperature, time of loading, and aging. Properties related to pavement performance are based on rheology; the study of flow and deformation. Tests used in PG specifications are Rotational Viscosity (RV) for construction (workability), Dynamic Shear Rheometer (DSR) for rutting and fatigue, and Bending Beam Rheometer (BBR) for thermal cracking. [25]

Three aging levels are used for the PG tests. Original or virgin binders are tested for RV and DSR (for rutting at high temperatures). Rolling Thin Film Oven (RTFO) aged binders are tested for DSR (for fatigue at high temperatures) and BBR. Binders aged in the Pressurized Aging Vessel (PAV) are tested for DSR (for fatigue at intermediate temperatures) and BBR. RTFO is a short term aging method designed to imitate aging undergone by hot mixing and construction. PAV is designed for long term aging resulting from in-service use.

Superpave Performance Grade (PG), AASHTO M-320, specifications used today to categorize asphalt binders are based on unmodified asphalt binders. AASHTO M-320 includes original DSR, RTFO DSR, PAV DSR, BBR, and RV. Since the introduction of polymer modifiers, AASHTO M-320 has not been able to adequately characterize the performance of modified binders in the field. In response, states have added Superpave Plus tests to ensure the presence of polymer modification. Superpave Plus tests may include Elastic Recovery (ER) ASTM D113-86, Force Ductility AASHTO T-300, and Multiple Stress Creep Recovery (MSCR) which was developed by the FHWA. New Jersey currently uses Elastic Recovery [4].

2.3.2. Multiple Stress Creep Recovery Testing of Asphalt Binders

The Multiple Stress Creep Recovery (MSCR) test, a new test developed by the FHWA, has been shown to be sensitive to polymer modification in many studies, including a University of Massachusetts Dartmouth study that tested a base binder that was then modified, separately, with two different polymers and different proportions. Both MSCR parameters: non-recoverable

creep compliance, or J_{nr}, and percentage of elastic recovery improved with the addition of polymer and with the increase of polymer [26]. In the case of many of the other tests, specialized equipment is required, which is often very expensive; however, MSCR testing can be conducted using the same sample and dynamic shear rheometer (DSR) equipment as the AASHTO M320 specification test [27] [28] [29] [30]. This would allow for the new testing method to be integrated into practice fairly seamlessly in comparison to a test that would require the purchasing of more equipment.

The MSCR test is performed using the DSR by applying a controlled shear stress of 0.1 kPa using a haversine load for 1 second followed by a 9-second rest period. During each cycle, the asphalt binder reaches a peak strain, and then recovers before the shear stress is applied again. Figure 3 is a typical plot of the first 10 cycles. The difference between the peak strain and the final strain is divided by the peak strain to get the percentage of elastic recovery for each cycle, calculated in Equations 1 and 2. Ten creep-recovery cycles are used, at 0.1 kPa shear stress, and the average elastic recovery is determined. Immediately after ten cycles are completed at shear stress value of 0.1 kPa, the testing continues with an additional ten creep-recovery cycles, using a shear stress value of 3.2 kPa. The average creep recovery is calculated from Equations 3 and 4 and non-recoverable creep compliance is calculated using Equations 5-8.

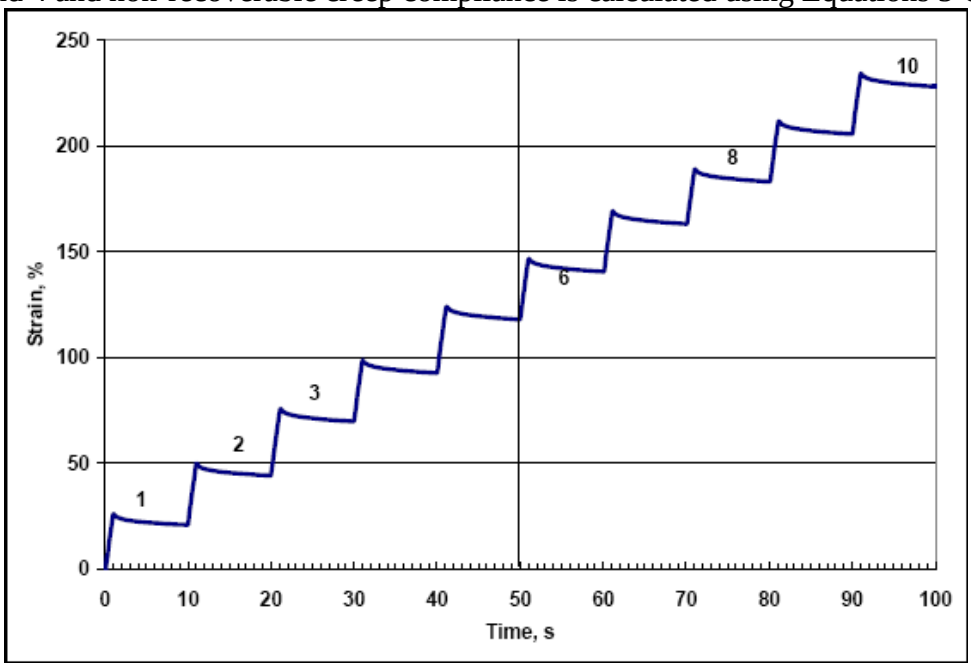

Figure 3. Typical plot of the first 10 cycles of MSCR testing [31]

Equation 1 $\in_r (\mathbf{0.1}, \boldsymbol{N}) = \frac{(\boldsymbol{\epsilon_1 - \epsilon_{10}}) * \mathbf{100}}{\boldsymbol{\epsilon_1}}$ for N= 1 to1 0

Equation 2 $\in_r (\mathbf{3.2}, \boldsymbol{N}) = \frac{(\boldsymbol{\epsilon_1 - \epsilon_{10}}) * \mathbf{100}}{\boldsymbol{\epsilon_1}}$ for N= 11 to 20

Equation 3 $\boldsymbol{R_{0.1}} = \frac{\boldsymbol{SUM}(\in_r (\mathbf{0.1}, \boldsymbol{N}))}{\mathbf{10}}$ for N=1 to 10

Equation 4 $\boldsymbol{R_{3.2}} = \frac{\boldsymbol{SUM}(\in_r (\mathbf{3.2}, \boldsymbol{N}))}{\mathbf{10}}$ for N=11 to 20

Equation 5 $\boldsymbol{J_{nr}}(\mathbf{0.1}, \boldsymbol{N}) = \frac{\boldsymbol{\epsilon_{10}}}{\mathbf{0.1}}$

Equation 6 $\boldsymbol{J_{nr}}(\mathbf{3.2}, \boldsymbol{N}) = \frac{\boldsymbol{\epsilon_{10}}}{\mathbf{3.2}}$

Equation 7 $J_{nr0.1} = \frac{SUM(J_{nr}(0.1,N))}{10}$ for N = 1 to 10

Equation 8 $J_{nr3.2} = \frac{SUM(J_{nr}(3.2,N))}{10}$ for N = 11 to 20

The high temperature specification parameter in Table 1 of AASHTO M320—G*/sin δ—has been shown to relate poorly to rutting for many "premium grade" modified asphalt binders. This has led to the development of the multiple stress creep-recovery (MSCR) test as a potential replacement for the conventional G*/sin(δ) test in the specification. From the MSCR test, the new high temperature specification parameter is determined by dividing the non-recoverable (or permanent) shear strain by the applied shear stress, calculated from Equation 5 and 6 for each stress level and an average of the stress level for Equations 7 and 8. The result is called the non-recoverable creep compliance, or J_{nr}. The binder can then be graded with J_{nr}, falling into traffic levels that are broken into ranges of equivalent single axle loads (ESALs), Table 2. For example a binder tested at 64˚C and 3.2 kPa with a resulting J_{nr} of 0.75 kPa^{-1}would be graded as a PG64H capable of 10 million or greater ESALs. This grading process elevates the need to temperature bump binders when heavy traffic is expected, which is the case under the current standards, instead J_{nr} make the distinction based on expected performance.

Table 2. Traffic Grading according to Jnr

Jnr (3.2kPa)	Temperature	Traffic	ESALs
≤4.0	64	Standard	<10 million
≤2.0	64	Heavy	10-30 million
≤1.0	64	Very Heavy	>30 million
≤0.5	64	Extremely Heavy	>30 million Standing traffic

While the MSCR test (AASHTO TP70) can be used to generate the J_{nr} value, it can also be used to determine the elasticity of the asphalt binder by measuring the recovery percentage from peak loading. In this, the test operates similarly to other PG-Plus tests, such as the Elastic Recovery test (AASHTO T301), in ensuring the degree of elasticity response due to polymer modification in an asphalt binder. Research conducted by the Federal Highway Administration has correlated J_{nr} and recovery values from the MSCR test for many modified asphalt binders. Based on this data, minimum recovery values can be specified for certain values of J_{nr}. Asphalt binders that fall below the curve in Figure 4 are considered to have low elasticity; those that are above the curve are considered to have high elasticity.

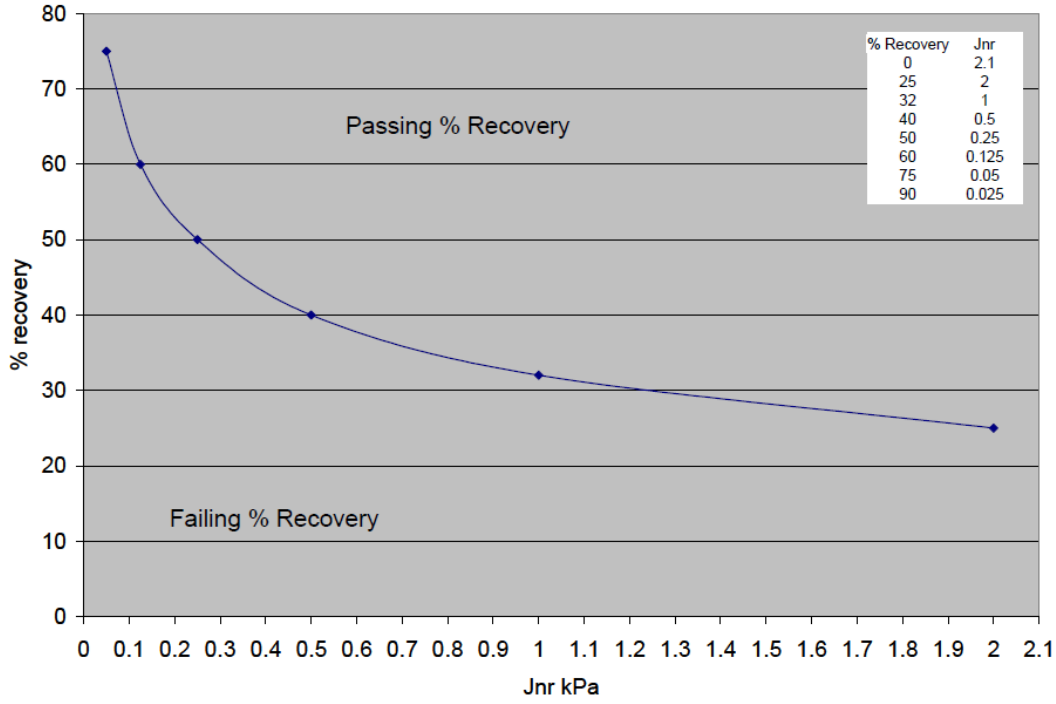

Figure 4. Percentage recovery versus J_{nr} [31]

The high temperature binder specification parameter from the MSCR test is J_{nr}. If the asphalt binder meets the appropriate J_{nr} specification, then it should be expected that it will minimize its contribution to rutting. In addition, if the user agency wants to verify the presence of a polymer and/or evaluate the elasticity of the binder adding the appropriate MSCR recovery value as a minimum requirement is an option [18]. However, the appropriate specification limits and test reproducibility needs to be evaluated.

2.3.3 MSCR Curve

Recently, Huang et al, developed a methodology to characterize the creep and recovery curve into linear viscoelastic, non-linear viscoelastic, and permanent strain (PS) components [32]. The PS is not measured under steady state. There is a need to determine if the parameters of the entire creep and recovery curve rather than just the two parameters that are currently used would help better characterize the behavior of polymer modified binder. The findings from Huang et al's study provide an opportunity to characterize the entire creep and recovery curve from the MSCR tests and determine the sensitivity of the parameters to type and amount of polymer modification.

Huang et al. studied the MSCR test cycles using Schapery's non-viscoelastic model for different binders, and found that some asphalt binders exhibited linear viscoelastic behavior throughout the MSCR test, while some exhibited non-linear viscoelastic response during loading and/or unloading [33]. This MSCR test was conducted using multiple stress levels (25, 50, 100, 200, 400, 800, 1600, 3200, 6400, 12800, and 25600 Pa) unlike the conventional procedure that uses two stress levels (100 and 3200 Pa). The non-linear viscoelastic parameters were determined using recovery strains, which has a larger number of data points (90) as compared to creep strains (10). This was done to get a better fit. In the proposed study, the concept was

adopted from Huang's, but it was modified slightly to characterize each creep and recovery curve in the MSCR test into linear viscoelastic, non-linear viscoelastic, and PS.

2.3.3.1 Linear Viscoelastic (LVE) Parameter

The creep compliance is determined from the 1-second creep curve using the following equation.

Equation 9 $$J(t) = \frac{\gamma(t)}{\tau}$$

Where: J(t) = creep compliance, 1/kPa;

$\gamma(t)$ = strain, %;

τ = creep shear stress, kPa.

If the material is linear viscoelastic, the recovery curve can be predicted using the following equation 10. The recovery curve at any time t can be calculated by the superposition of the strain from the positive creep stress at time t=0 to time t=t seconds and negative creep stress from time t=1 second to t= t seconds.

Equation 10 $$\gamma_{recoverable}(t) = \tau J(t) - \tau J(t-1)$$

Creep compliance can be calculated by fitting equation 9 or equation 10 to the measured data. Since there are 90 points in the recovery curve as compared to 10 data points in the creep curve, more accurate parameters of creep compliance can be calculated by fitting equation 10 to the measured recovery curve. More data points could easily be acquired for the creep portion. However, the purpose was to characterize the curve accurately using existing MSCR data and avoid any additional testing.

2.3.3.2 Non-linear Viscoelastic Component

To determine the non-linear viscoelastic parameter, the creep and recovery curve at 3.2 kPa was analyzed. If the material is not linear viscoelastic, then the recovery curve from equation 10 will not fit the measured recovery curve. The non-linear viscoelastic parameters were introduced to better fit the recovery data. The authors conducted an analysis of the 10 cycles at 0.1 kPa and observed almost negligible non-linear viscoelastic response. In other words, the response was independent of the time history. Considering that the responses were LVE, the authors felt comfortable in not including response of MSCR data due to 0.1 kPa,

2.3.3.3 Parameter G_1

The parameter G_1 is determined by fitting the recovery curve of the first 1 seconds using equation 11. The creep compliance J(t) is determined from the steps above.

Equation 11 $$\gamma_{recoverable}(t) = G_1[\tau J(t) - \tau J(t-1)]$$

2.3.3.4 Parameter G_2 and G_3

The parameter G_2 provides a vertical shift to match the recovery curve at the recovery point of 2 seconds. The parameter G_2 is the time independent component of the recovery curve between 2 and 10 seconds (See Figure 5). The parameter G_3 changes the slope of the recovery curve between 2 and 10 seconds. The parameter G_3 is the time dependent component of the recovery curve between 2 and 10 seconds. The sensitivity of the recovery curve to the three non-linear

viscoelastic parameters is explained later. Parameters G_2 and G_3 are determined using equation 12.

Equation 12 $\boldsymbol{\gamma_{recoverable}(t) = G_2\,[\tau\,J(2) - \tau\,J(1)] + G_3[\tau\,J(t) - \tau\,J(t-1)]}$

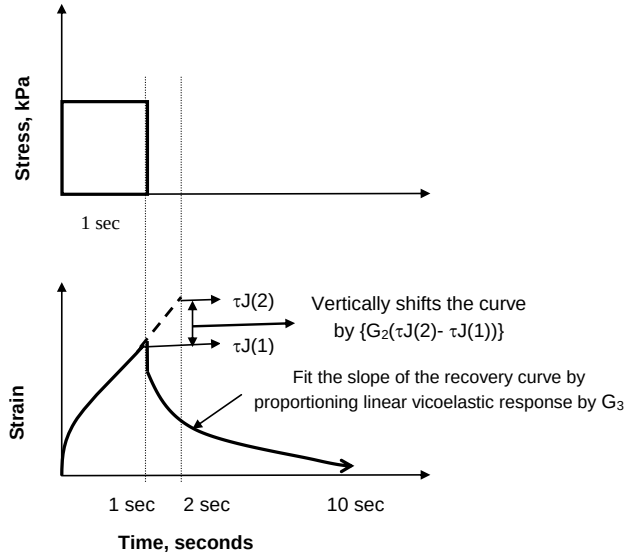

Figure 5. Schematic of a 1-second creep and 9 -second recovery curve at 3.2 kPa for Non-Linear Viscoelastic Curve (not to scale)

4.2.3 Permanent Strain (PS)

The non-recoverable strain at the end of 10 seconds may not all be attributed to PS because all the recoverable strain from the linear and non-linear viscoelastic component may not have recovered at the end of 10 sec. The PS is calculated by subtracting the measured non-recoverable recovery from the calculated recovery at 10 sec (shown in Figure 6).

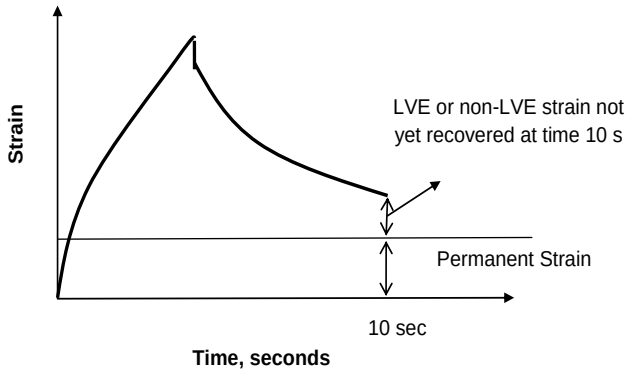

Figure 6. Schematic showing recovery at the end of 1-second creep and 9-second recovery at 3.2 kPa (not to scale)

As described above, the creep and recovery curve can be characterized in three components: linear viscoelastic, non-linear viscoelastic, and PS. The detailed methodology developed to characterize the entire creep and recovery curve based on the concept explained above is outlined below.

2.3.3 Elastic Recovery

This test is performed by pulling a binder briquette specimen a rate of 5 cm/min with a ductilometer. Upon reaching 20 cm the sample is no longer elongated and after five minutes the sample is severed. The sample then remains in the ductilometer for one hour, to allow the sample to retract. The elongated sample is finally measured by releasing the ductilometer and matching the severed ends so that they just touch. In addition to a lengthy testing procedure the preparation of the binder specimen requires at least two and a half hours, to pour, trim and equilibrate the sample to the ductilometer bath.

Elastic recovery (ER) is the degree to which a substance recovers to its original shape after release of stress. A certain degree of ER is desirable in pavement to avoid permanent deformation. The ER is measured with an instrument called a ductilometer. ER is used to test the polymer modified binders by different departments of transportation. Most recently, the test is typically being performed at 25˚C on RTFO aged material at 5 cm/min to 20 cm. A state agency will allow a modified binder if it produces an elastic recovery greater than an agency specified percentage.

2.3.4 Forced Ductility

The Force Ductility test, AASHTO T-300, measures the tensile properties of polymer modified asphalt binders. During testing, a specimen is elongated at a constant rate of 2 in/min to produce a load versus time relationship which is converted to a load versus displacement relationship [34]. Using this data, the peak ratio and area under the force displacement curve can be calculated. Peak ratio is the ratio of the force of the second peak and the initial peak. The initial peak is the first high peak and the second peak is the first succeeding lower peak as shown in Figure 7.

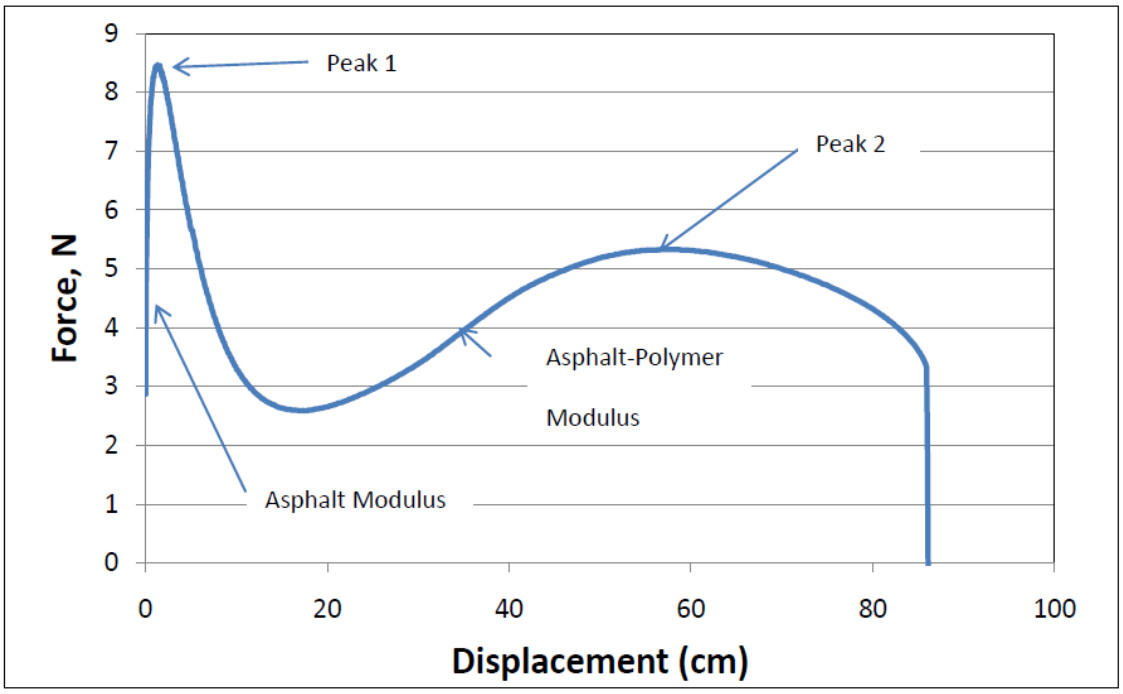

Figure 7. Typical Forced Ductility data plot

2.3.5 Gel Permeation Chromatography

Asphalt is a mixture of a wide variety of hydrocarbons; the molecular structure of asphalt affects the physical and aging properties as well as how the molecules interact with each other and with aggregates. The Gel Permeation Chromatography (GPC) test is used to measure the molecular size distribution of a substance using silica gel porous columns or styragel columns through which the sample solution is pumped. The response obtained by the detector of the GPC is recorded as the elution time increase [35]. High-pressure gel permeation chromatography (HP_GPC) separates an asphalt binder into fractions of a variety of molecular sizes and thus establishes a profile of molecular size distribution. This is plotted with detector responses on an ordinate and elution times on an abscissa. The GPC profile of an asphalt binder is classified into three groups: large (LMS), medium (MMS), and small molecular size (SMS) [36]. Past research focused on the characterization of asphalt binders as a tool and the links between the GPC results and both the physical properties of the binders and the field performance of the pavements.

Researchers found that GPC could be used to identify differences in a binder source and to detect the presence of modifiers or fillers. It was also determined the molecular size distribution of asphalt has a direct effect on the asphalts physical properties. However, they also concluded that results are conflicting on whether HP-GPC analysis can help identify the performance of asphalt-aggregate mixtures [36].

Shen et al, 2006, conducted research on recycling of laboratory prepared reclaimed asphalt pavement mixtures containing crumb rubber modified binders in hot-mix asphalt. The researchers in this study used GPC to measure the molecular size distribution of the substance with silica gel porous columns through which the sample solution is pumped. The response obtained by the detector of the GPC is recorded as the elution time increase. From previous research it was concluded that a sample mix could be used to obtain GPC information instead of the binder being extracted and the test being performed on the recovered materials. Shen et al used the same technique to obtain GPC results from the mixtures. A sample of asphalt mix was first weighed and allowed to dissolve in a tetrahydrofuran solvent with the asphalt concentration in the solvent being adjusted to 1/400. The solution was then drawn with an injector and filtered through a 0.45-μm filter to ensure the purity of the solution. After that, 0.5 ml of the solution was immediately drawn and injected into the GPC system. The solution was pumped through the gel permeation columns and allowed to flow at a rate of 1ml/min. The test was conducted at 35°C for 30 min for each injection. They used three duplicate injections for each mixture. The GPC results from this research showed that the molecular size distributions of the recycled mixtures were very similar to those of the virgin mixtures regardless of the aggregate type. Also, the differences in larger molecular size (LMS) between the virgin and the recycled mixtures were minute.

Woo et al, 2007, studied the loss of polymer-modified binder quality with oxidative aging. The molecular size distribution of asphalt materials was measured using a Waters gel permeation chromatograph (GPC) system. It has two types of detectors, namely refractive index detector and an intrinsic viscosity detector. They used a mass of 0.2 g of material and dissolved in 10 ml of tetrahydrofuran. This solution was passed by columns at a flow rate of 1.0 ml/min after being filtered through a 0.4μm polytetrafluoroethylene syringe filter. The GPC results from this study indicated the degradation in the molecular size by change in the polymer peak.

Shen et al, 2006, studied HP-GPC aging of recycled crumb rubber modified binders with rejuvenating agents. They used GPC to characterize the aging process of blends of aged CRM binders containing rejuvenating agents. They discovered that the compositional changes of the

blends of aged binders and rejuvenating agents due to the aging processes proposed by SHRP binder specifications RTFO and RTFO+PAV, were well reflected by GPC results. Also, it was found that there was a good correlation between the large molecular size (LMS) and the performance properties of the blends. Researchers in the past have studied the rheological properties of binders using GPC and have concluded that aging of a binder causes an increase in the LMS and a decrease in the MMS and SMS. The changes in molecular size could result in a significant change in the asphalt binder consistency and therefore its physical properties.

The GPC testing equipment Shen et al used for this study consisted of a solution injection unit connected to six silica gel porous columns through which the sample solution is pumped. This pore arrangement allows larger molecules of a sample to flow through a differential refractometer detector first, followed by progressively smaller molecules. This detector continuously scales the number of molecules flowing through as a function of time, automatically recording a continuous tracing of time versus the number of flowing molecules. They conducted GPC testing on sample solutions with a concentration of 1/400 (namely, 0.0080 g of asphalt binder in a 3.2 g solvent) after they were filtered with a 0.45μm filter.

Shen et al indicated that an increase in the percentage of LMS in the binders caused an increase in the rutting resistance ability of the aged CRM binders and the two control binders that were used. This was comparable for both rejuvenating agents and the binder sources. They also suggested that a precise amount of rejuvenating agents should be added so that the proper rutting resistance properties of the blends will be obtained. Also, in this particular study, they have found that a decrease in % LMS of the blends by addition of a rejuvenating agent caused a decrease in the G*Sin δ, which improved the fatigue resistance properties of the binders.

Masson et al, 2007, conducted a study on early thermal degradation of bituminous sealants resulting from improper installation. Bituminous sealants are mixtures of bitumen with a rubbery material (like SB copolymer, ground tire rubber or both.) and filler (most often limestone). GPC allows for the fractionation of the sealant bitumen and SB copolymer based on molecular sizes.

The test results were expressed in minutes, which were converted to molecular weight with the help of a calibration curve [37].

Masson et al performed GPC on a Waters chromatograph equipped with four Styragel columns (HR-1, -3, -4 and -5). These columns covered a molecular mass range of about 100g/mol to 2000kg/mol. The reported signal was that of a 2% (weight/volume) sealant solution in tetrahydrofuran (THF) as obtained from an ultraviolet detector set at 210nm. The sealants were left to dissolve for one hour in Tetrahydrofuran before they were passed through a 0.45μm pore-size filter and injected on the columns held at 40°C. The GPC results from this study indicated that the copolymer chain lengths were shortened by heat.

Bianchetto et al, 2007 [35], conducted a study on the effect of calcareous fillers on bituminous mix aging. Aging is one of the many reasons for the failure of bituminous wearing courses. The addition of filler to the mixes can improve the physical properties. Bianchetto et al ,2007, determined the molecular weights and distributions by gel permeation chromatography that used LKB-2249 equipment, with μ-Styragel columns (105 and 102 A0) and a Shimadzu ultraviolet detector at 254 nm. Tetrahydrofuran was used as a solvent. The chromatographic tests provided clear evidence of the advantages of using limestone as mineral filler to improve the aging resistance of conventional bitumen. They also observed that the complex shear modulus (G*) increases more slowly and the phase angle (δ) decreases more slowly because of aging. [38]

2.3.6 Fourier transform infrared spectroscopy (FTIR)

GPC is good for finding molecular weight distribution, and can be used to find the amount of polymer within a sample so long as the exact polymer used is known. However, another test is needed to be able to find the polymer content of any sample tested. This test is FTIR. The test is run by heating a binder to 163˚C and then pressing a small amount onto a piece of wax paper. The sample is then pressed onto the FTIR machine onto its diamond crystal and a pressure is applied. Usually, a spectroscopy process would work by shining one specific wavelength of light through the sample and testing the absorbance only at that wavelength. However, FTIR works differently. The light shined through the sample is of many different wavelengths at the same time. The wavelengths of light are switched for each data point and the computer works backwards to find the absorbance at each tested wavelength. The computer software supplies a plot of its own, and also a file that can be used in Microsoft Excel to plot the data.

2.3.7 Saturates, Aromatics, Resins, and Asphaltenes (SARA)

Binders are made up of four major components: saturates, aromatics, resins, and asphaltenes. The amount of each within a binder could determine how it will act under physical stress and its environment. SARA Analysis is a test in which the four components of a binder are separated and weighed to find the mass fraction of each within a binder. The main objective is to see if adding a polymer to a binder will change the percentages of the binder components itself, possibly affecting its physical performance.

The test is performed by dissolving a 2-3 gram sample in 100 times its weight in n-heptane. After this, saturates, aromatics, and resins are dissolved into the solvent. However, the asphaltenes are insoluble in n-heptane, and form a cake like material within the container. The slurry is passed through a Gooch crucible vacuum apparatus. At this point in time the asphaltenes have been separated and can be weighed. The solution of the remaining three components is reduced to 20 mL by evaporation and then poured into an alumina filled column about 3 feet in height.

At this point in time a beaker is placed underneath the column to collect saturates. More n-heptane plus toluene is added to the column and the beaker is left until all passes through. Then the beaker is switched for a fresh one and toluene and methanol are added. The second beaker is left until all dripping from the column has stopped and a third fresh beaker is placed underneath. This second beaker catches the aromatics fraction of the binder. After the third beaker is placed underneath, trichloroethylene is added to the column and the rest of the sample drips through the bottom into the beaker. This is the resins fraction. The ratio and volume of solvents for each step are shown in Table 3. The beakers and the crucible are left to dry and then can be weighed to find mass fraction.

Table 3. Solvents used to recover fractions

Column Feed Volumes Eluent Solvent	**Fractions received in tarred containers of eluate**		
	mL	**Fraction**	**Total mL**
n-Heptane	65		
Toluene	35	**Saturates**	100
Toluene	100		
Methanol/toluene 50/50	100	**Naphthalene aromatics (NA)**	200
Trichloroethylene	200		
Column hold up		**Polar aromatics (PA)**	200 hold up

2.3.8 Dynamic Complex Modulus (DCM)

The new AASHTO Mechanistic-Empirical (M-E) Design Guide uses the dynamic complex modulus as the primary test protocol to characterize the modulus response of hot mix asphalt. Dynamic complex modulus or E* is the ratio of stress to strain under dynamic conditions, refer to Equation 13.

Equation 13 $$|E^*| = \frac{\sigma}{\varepsilon}$$

Where σ = the amplitude of stress

ε = the amplitude of strain

The test was conducted at three temperatures 4, 20, and 40 °C, as well as multiple frequencies ranging from 0.1 to 10 Hz. Subsequently, a master curve was developed using the procedure in AASHTO PP-62, [39] developed to extrapolate more data points.

2.3.9 Mechanistic Empirical Pavement Design Guide (MEPDG)

MEPDG software evaluates the major flexible pavement distresses, permanent deformation (rutting), and fatigue cracking (alligator and longitudinal cracking). The software uses traffic data, climatic data, the structure of the pavement, and asphalt layer properties to predict performance [40]. For the asphalt layer properties data, MEPDG has three levels of inputs with level 3 using default values for Performance Grades, level 2 using some binder properties and level 1 using dynamic complex modulus test results and binder information [40] .

2.3.10 Flow Time

The mixtures described previously were tested in accordance with AASHTO TP79-11 Standard Method of Test for Determining the Dynamic Modulus and Flow Number for Hot Mix Asphalt (HMA) Using the Asphalt Mixture Performance Tester (AMPT). Flow time is a quick and simple measurement of the resistance of AC mixtures to permanent deformation for rutting evaluation. MSCR testing was conducted in accordance with AASHTO TP70-12 to determine the J_{nr} parameter.

During this uniaxial static creep test, the specimen is subjected to a constant compressive load of 600 KPa (30 psi) at a test temperature of 52.5^{o}C (130^{o}F). For this study, the test was performed without confining pressure. While MSCR testing uses standard values during testing, the temperature of 52.5^{o}C (130^{o}F) for flow time testing was selected to match conditions in New Jersey. Flow time was conducted for 10,000 seconds or until the sample failed due to cracking initiation. The resulting axial strain is measured as a function of time and numerically differentiated to calculate the flow time which is defined as the time corresponding to the minimum rate of change of axial strain. The flow time is found by fitting the axial strain model (Equation 14) to the axial strain data using nonlinear least squares, then determining the inflection point (flow time) from the second derivative of the model (Equation 15).

Equation 14 $$\varepsilon = At^B - C\,(e^{Dt} - 1)$$

Equation 15 $$\frac{d^2\varepsilon}{dt^2} = AB(B-1)t^{B-2} - CD^2e^{Dt}$$

where:

ε = axial strain, microstrains

t = time, seconds

A, B, C, and D = fitting coefficients

The total compliance at any given time, D(t), is calculated as the ratio of the measured strain (ε_t) to the applied stress σ_0 (Equation 16).

Equation 16 $$\mathbf{D(t)} = \frac{\boldsymbol{\varepsilon_t}}{\boldsymbol{\sigma_0}}$$

Tests in the AMPT were conducted on 100 mm (4 in) diameter by 150 mm (6 in) high test specimens that are cored and cut from larger 150 mm (6 in) diameter by 170±mm (6.75 in) high gyratory specimens prepared in a Superpave gyratory compactor to target 7% air voids. Specimens are prepared according to AASHTO PP 60 *Provisional Standard Practice for Preparation of Cylindrical Performance Test Specimens Using the Superpave Gyratory Compactor (SGC).* (FHWA 2013)

Figure 8 shows a typical result of the flow time test. The plot is divided into three basic regions or stages of deformation: primary, secondary, and tertiary. The primary region is where the strain rate decreases sharply and is associated with a densification type of permanent deformation. This behavior continues until the mixture reaches an optimum density level that is followed by the secondary region of the curve where the strain rate remains almost constant under the applied static load. As loading continues within the secondary region, densification will continue until a point is reached where the mixture becomes unstable and significant deformation occurs reaching the tertiary region. The time corresponding to the start of the tertiary zone is referred to as the flow time. Flow time can therefore be considered as the time when the rate of change of compliance is the lowest. The slope represents the rate of change in permanent deformation as a function of the change in loading time. High flow times and low slopes are desired properties for rutting resistant mixtures.

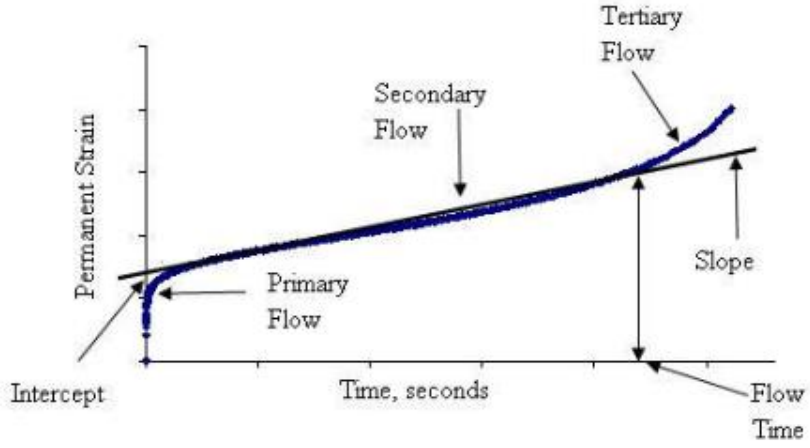

Figure 8. Typical flow time test result

2.4 Laboratory Performance of Modified Binders

Laboratory evaluation of the modified bitumen containing styrene-ethylene-butylene-styrene (SEBS), ethylene vinyl acetate (EVA) and ethylene butyl acrylate (EBA) copolymers [7] [8] [4] indicated that the morphology and storage stability of the modified binders were largely dependent on the polymer content and were influenced by the characteristics of the base bitumen and the polymers. At a low polymer content (3% by weight), the modified binders showed dispersed polymer particles in a continuous bitumen matrix [7] [8] [4] [41]. At a sufficiently high polymer content (6% by weight), a continuous polymer phase was observed. Regardless of the nature of the two phases, the storage stability of the modified binders decreased as polymer content increased.

Polymer modification improved bitumen rheological properties such as increased elastic responses at high temperatures and reduced creep stiffness at low temperatures. The degree of improvement generally increased with polymer content, but varied with bitumen source/grade and polymer type [41] [42] [43]. Polymer modification also influenced bitumen aging properties. Evaluation of aging effects was dependent on testing conditions (e.g. temperature and frequency).

The source of asphalt and polymer significantly impacts the dispersion properties of SBS particles [42]. If there are two, interlocked continuous polymer phases, rather than one continuous polymer phase, this will lead to a more homogenous mixture; leading to higher stiffness and hence lower rutting resistance.

The NJDOT currently requires the use of SB or SBS formulations for all polymer modified binders to ensure mix performance due to the lack of a standardized test to determine the expected performance of other polymers. By Requiring SB or SBS for all polymer modified binders the NJDOT is effectively limiting the use of other polymers and creating supply shortages of SB and SBS, thus increasing the cost of polymer modified binders. This has created the need to develop/identify a test method to evaluate the performance of polymer modified binders.

2.5 Morphology of Polymer Modified Binder

A fluorescent microscopy is used to investigate the morphology of the PMB's by determining the state of dispersion of the polymer within the base bitumen. It is also used to characterize the nature of the continuous and discontinuous phases as it allows the observation of the homogeneity and the structure in the raw state. This technique is based on the principle that polymers swells due to the absorption of some of the constituents of the base bitumen and also due to the fluorescent effect. The bitumen rich phase looks darker and the polymer rich phase appears light as seen in Figure 9. [6]

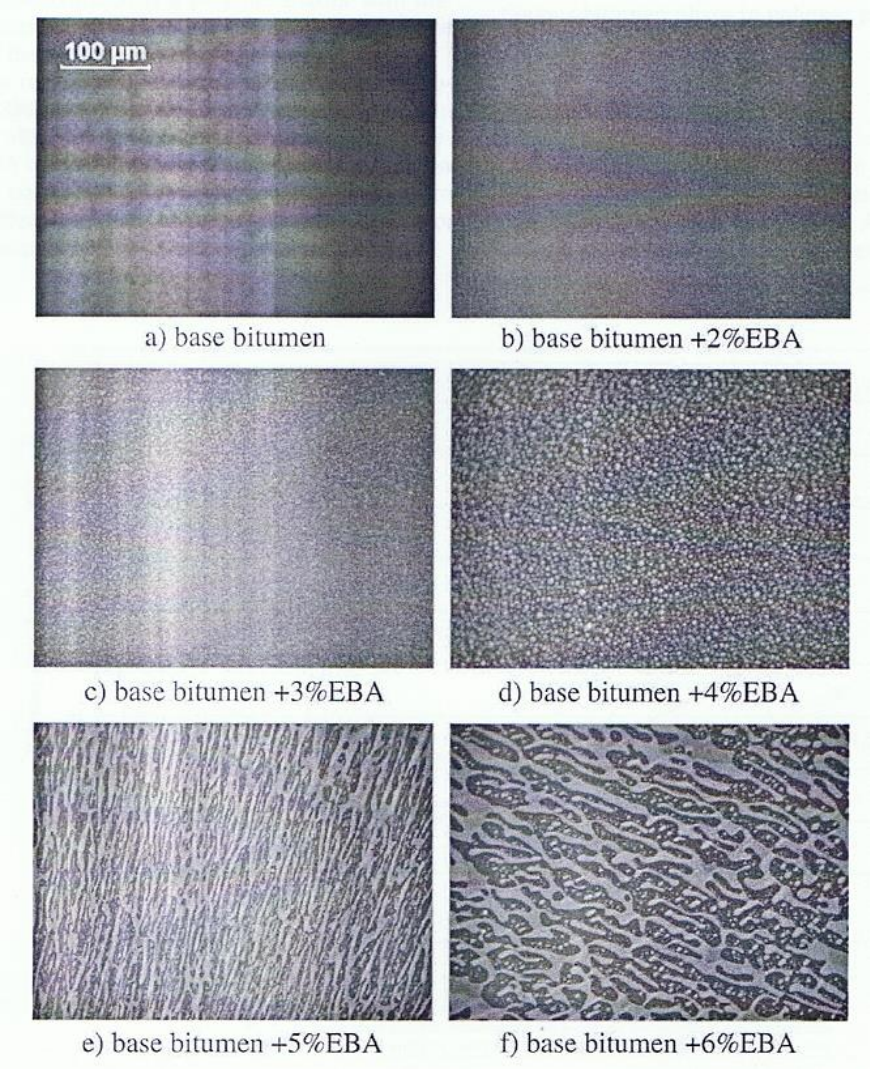

Figure 9. Fluorescent images of EBA Polymer Modified Binder samples with 100x magnification [6]

2.5.1 Qwin-Plus image processing and analysis

The Qwin-Plus image analyzer is software that is capable of providing full measurements of polymer distribution. Digital image processing and analysis techniques were used to quantify the polymer distribution area throughout the PMB's. This polymer distribution area is expressed as the relative proportion of the polymer phase to composite image which is based on each of the polymer contents. After the images are captured by camera, they are transformed to the grey scale. Using the algorithms in the Qwin-Plus software, operations like shading corrections, brightness or contrast optimizing , sharpen and enhancement are applied to transform the original image to binary image which has areas/features of either black (0) or white phases (1) as seen in Figure 10. The main purpose of this is to isolate the polymers from composite images and prepare images that are ready for quantified measurements. Hence, following the image processing, the percent area distribution of polymer phase through the base bitumen can be calculated for each polymer type and content (Figure 11). [6]

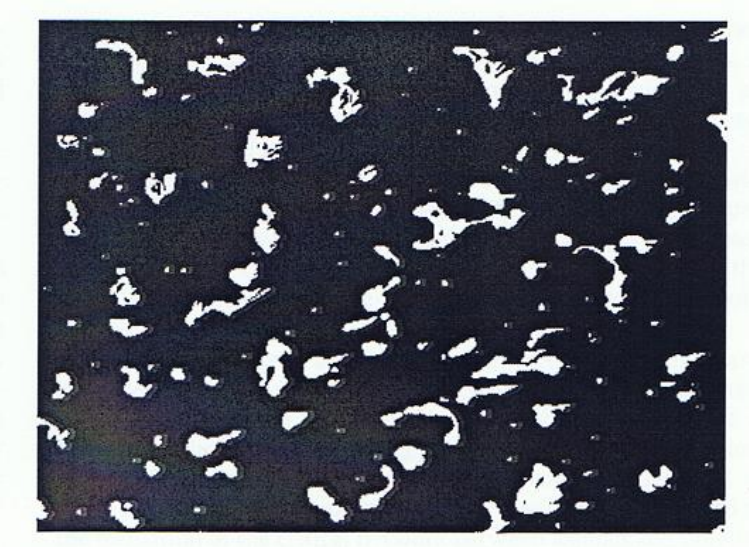

Figure 10. An example of an image transformed to binary image of black and white phases [6]

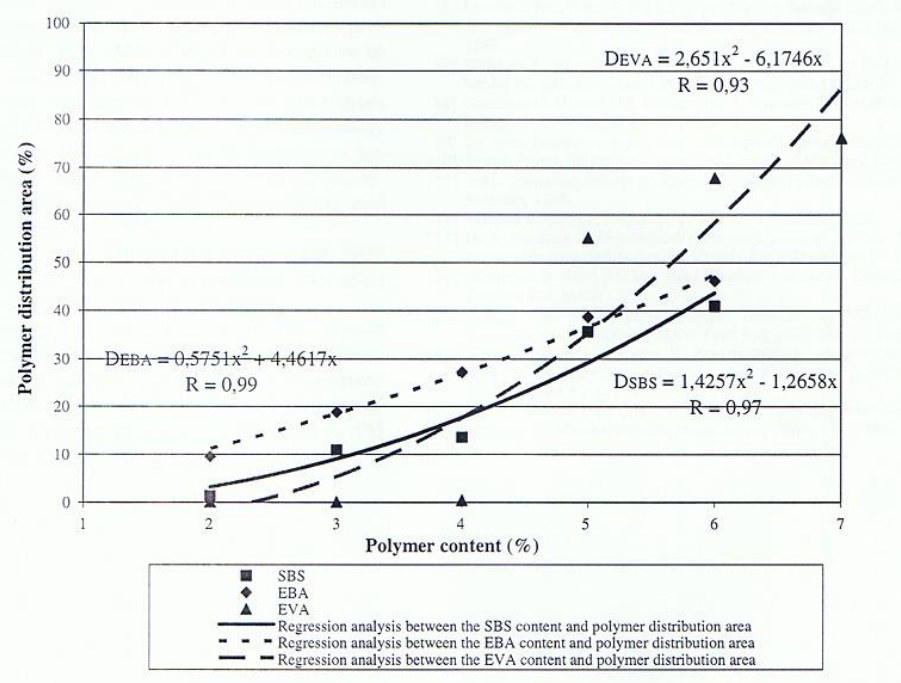

Figure 11. Area of distribution of SBS, EVA and EBA based polymers in base bitumen [6]

2.6 Effect of aging on modified binders

Cortozo et al, 2004, studied the change in the properties of SBS modified asphalts under different aging conditions using rolling thin film oven test and pressure aging vessel [44]. The SBS modified asphalts used for their study were AM1, AM2 and AM3. They used size exclusion chromatography and infrared spectroscopy to determine the effect of different molecular weight and architecture of SBS during thermo oxidative degradation. After RTFO ageing on asphalt, the penetration and torsional elastic recovery values decreased while softening points increased which indicates hardening of material during the RTFO process (Table 4). They observed a decrease in viscosity of the modified asphalts with increase in temperature (12). There was an

increase in viscosity after RTFO and PAV which indicate hardening of asphalts during both processes (Figure 12). Also the modification of the rheological properties of asphalts during aging process depends on the structural characteristics of that polymer.

The constituents of asphalt occur in a broad range of molecular weights, shapes and chemical functionalities. These characteristics are responsible for different interactions between molecules like pi-pi interactions between aromatic rings, van-der-Waals interactions between aliphatic chains, polar interactions like hydrogen bonding and ionic bonding involving heteroatoms. A heteroatom is any atom that is not carbon or hydrogen but atoms typically like nitrogen, oxygen, sulfur, phosphorus, chlorine etc., [45]. These interactions are critical to the physical and mechanical properties of the asphalt.

The chemical modification that takes place during aging is the formation of oxidation products coming from the asphalt and from the degradation of the polymer which gives rise to insoluble cross-linking products. The products of thermo oxidative degradation are low molecular weight polymers from chain scission (i.e. polymer degradation) and reaction products from polymeric radical asphalt reactions.

Table 4. Physical characteristics of unaged and RTFO aged asphalt

Physical characteristics of unaged and RTFOT aged asphalts

Asphalt	Penetration (0.1 mm)	Softening point (°C)	Torsional elastic recovery (%)
AM1	36	65	46
AM1/RTFOT	29	65	44
AM2	37	67	61
AM2/RTFOT	30	68	55
AM3	39	63	50
AM3/RTFOT	33	66.5	40

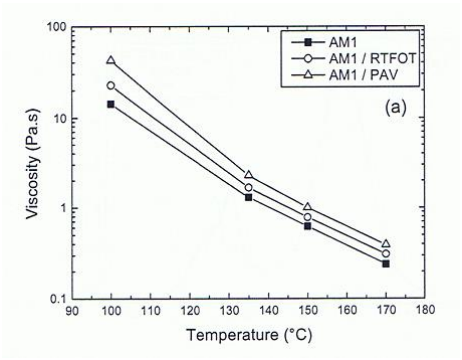

(a)

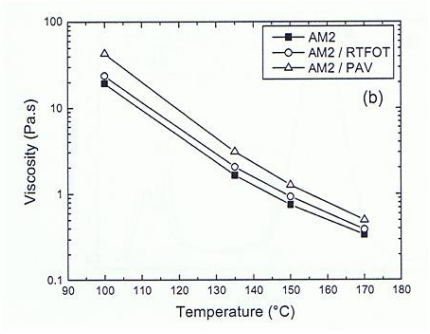

(b)

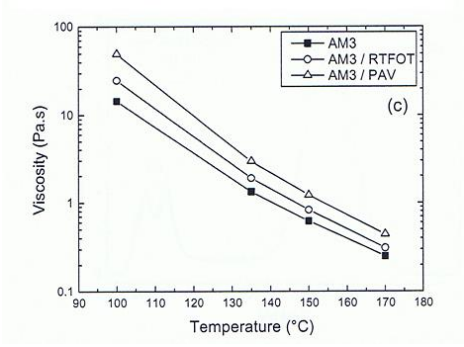

(c)

Figure 12. Rotational viscosities of SBS modified asphalt versus temperature before and after aging: (a) AM1, (b) AM2 and (c) AM3 [44]

Mouillet et al, 2007 [41], studied if PMB's aging is a consequence of bitumen aging, polymer aging or a combination of both [46]. Aging is a complex process and the principle cause of aging in service of bituminous binders is the oxidation by oxygen from the air of certain molecules. This oxidation results in the formation of highly polar and strongly interacting oxygen containing functional groups. The short term aging is assessed by RTFO and long term aging by PAV to simulate the short term and long term aging in the field. PMB's have a biphasic structure with polymer nodules dispersed in a continuous bitumen phase or a bitumen phase dispersed within a continuous polymer phase or even two interlocked continuous phases.

Specific structural indices were used to find the effect of aging of pure copolymers followed by infrared analysis. The polymer infrared bands were used to define the indices, as the ratio of the bands to the sum of the absorption bands between 3100 and 2700 cm-1. The index for SBS is given as: carbonyl species at 1740 cm^{-1} (appearing after aging), trans-butadiene at 965

cm^{-1} and styrene at 700 cm^{-1}. The index for EVA is : vinyl acetate at 1740 cm^{-1} and CH_2 chains of ethylene at 724 cm^{-1}.

It was observed that for SBS aging there was an increase in the carbonyl species index and a decrease in butadiene related index with the index of styrene remaining almost stable as seen in the Figure 13 below. The structural index is expressed as wt. % on Y-axis as shown in Figures 13 & 14. Aging of SBS alone occurs through oxidation of the unsaturated polybutadiene blocks which could lead to chains scission (polymer degradation).

The aging pattern for EVA alone is stability content of the vinyl acetate oxygenated species and aliphatic long chains as shown in Figure 14 below. There is a relative stability of the copolymer under PAV conditions up to 25 hours of aging due to the saturated part of EVA. The copolymers are able to be oxidized as a chemical degradation of the Vinyl Acetate patterns but at temperatures higher than 180 °C.

The SBS modified bitumen binders tend to become more homogenous upon aging due to some polymer degradation (chain scission) and a better compatibility of the smaller polymer chains with the oxidized bitumen molecules. Unstable SBS polymers become more compatible with aged bitumen.

The trend of EVA modified bitumen is that the binder becomes less homogenous upon aging due to a lower compatibility of the polymer chains remaining stable under aging with the oxidized bitumen molecules. Stable EVA polymers become less compatible with the aged bitumen. But the cross linked binders are less sensitive to aging due to their more homogenous quasi mono-phase structure before aging which protects them from phase exchanges.

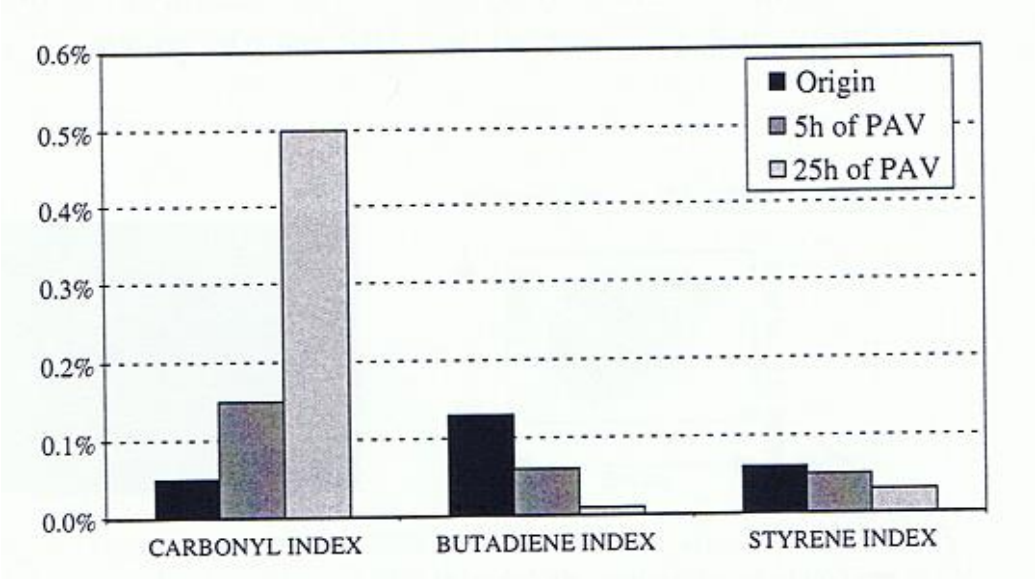

Figure 13. Evolution of SBS structural indices after aging [46]

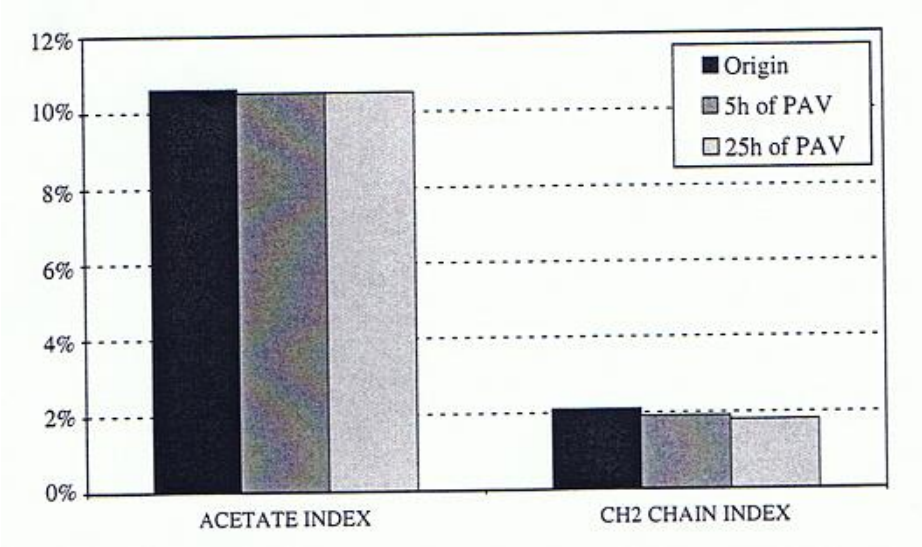

Figure 14. Evolution of EVA structural indices after aging [46]

2.6.1 Laboratory Evaluation of Short Term Aging Using GPC

Lee et al, 2009, investigated the effects of short-term aging on nine asphalt mixtures, out of which three were control mixtures (PG64-22), three were SBS modified (PG76-22) and three were rubber-modified (PG76-22) [47]. They designated the SBS modified binders as SM. The control and SM binders were collected from three different binder sources and were designated as A, B & C. Five short term aging treatments were used and RTFO aging was done on all the nine binders. GPC was used to detect molecular size distribution change of asphalt binder during the aging process. Increase in large molecular size (LMS) generally results in an increase in viscosity and stiffness of the asphalt binder. This change in viscosity of binder due to aging is predicted by other researchers as well.

They used GPC equipment for chromatographic analysis of binders. A differential refractive index meter was used as a detector. A series of two styragel HR 3 and 4E columns were used for separating constituents of asphalt binder by molecular size. The columns were kept at 35°C throughout the test. Tetrahydrofuran (THF) was allowed to flow at a rate of 1ml/min. The concentration rate was 0.25% by weight of binder.

For short term aged mixtures, a specific quantity of asphalt mixture was taken and dissolved into THF in a beaker. To have the concentration of the dissolution the same for all the testing (0.25% by weight), the binder content of the mixture had to be obtained. To carry this out, they used the ignition oven test (AASHTO T 308-04) for the mixture passing 4.75mm sieve. The unaged and RTFO aged binders specific quantity of binder was collected and dissolved in THF at 0.25% by weight concentration rate. This concentration was achieved by dissolving 0.008 g of binder sample in 3.2g of THF solvent. Each sample dissolved in THF was filtered through 0.45µm syringe filter to inject into the injection module. For each test a 50 µl of dissolved sample was injected. They observed that the test took 30 min and elution started at 11 min from injection and ended at 21 min. They repeated testing for each sample three times and average LMS was considered. For polymer modified asphalt, the materials that were greater than the filter size were screened before injection. So the binder and polymeric materials that were smaller than the filter pore size were allowed to pass through the columns. LMS calculation is dependent on parameters such as detector, solvent, column type, column age and data acquisition software.

As mentioned above, GPC was used to study the short term oven aging on the asphalt binders. They concluded that the commonly used short term aging methods in the laboratory which are 154°C oven aging for 2 hours and a 135°C oven aging for 4 hours are not significantly different for the nine binders. They found that RTFO aging method had less aging effect based on the LMS ratios than the short term oven aging method as seen in Figures 15 and 16. The longer aging period and the higher aging temperatures led to an increase in the LMS ratios as seen in Figure 17 below.

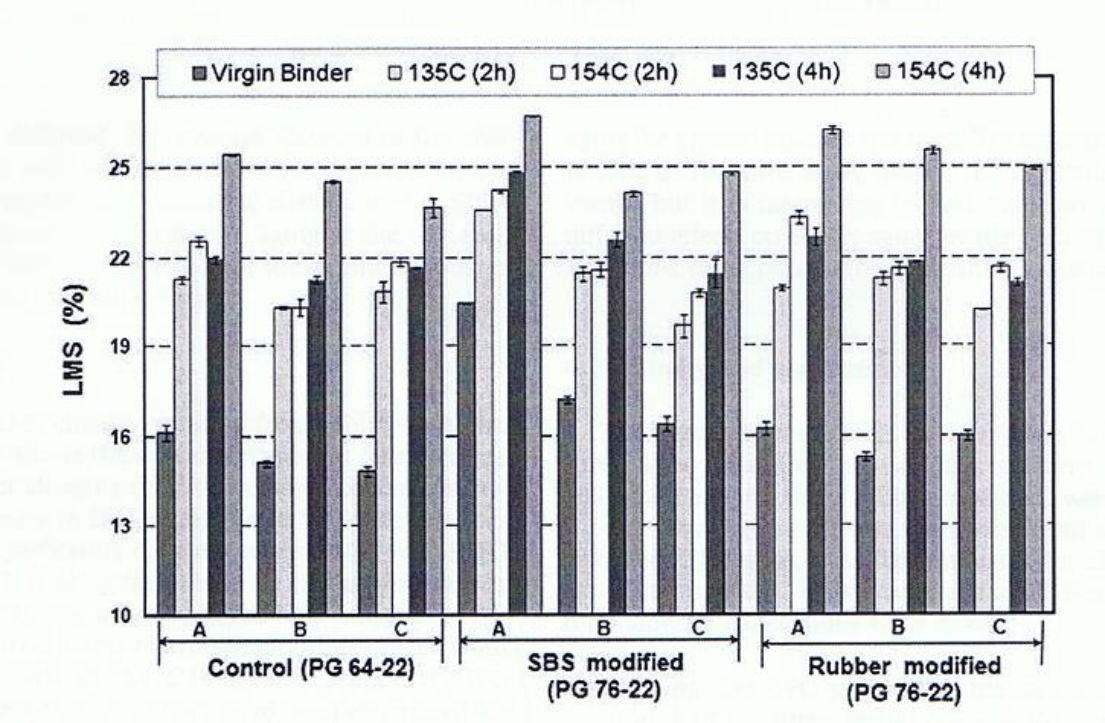

Figure 15. LMS change by percentage for short-term oven aging [47]

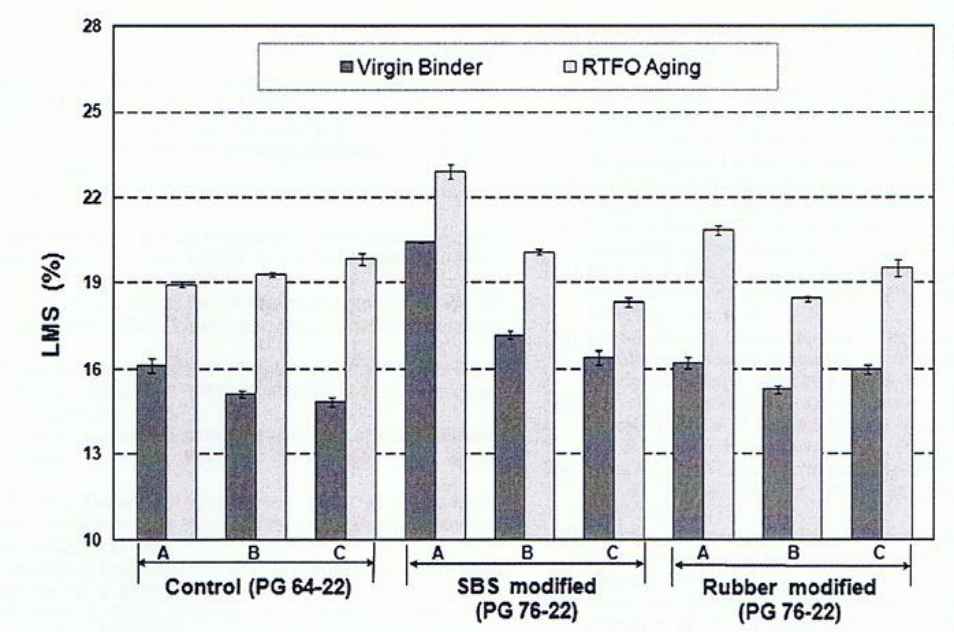

Figure 16. LMS change by percentage from rolling-thin film oven aging (RTFO) [47]

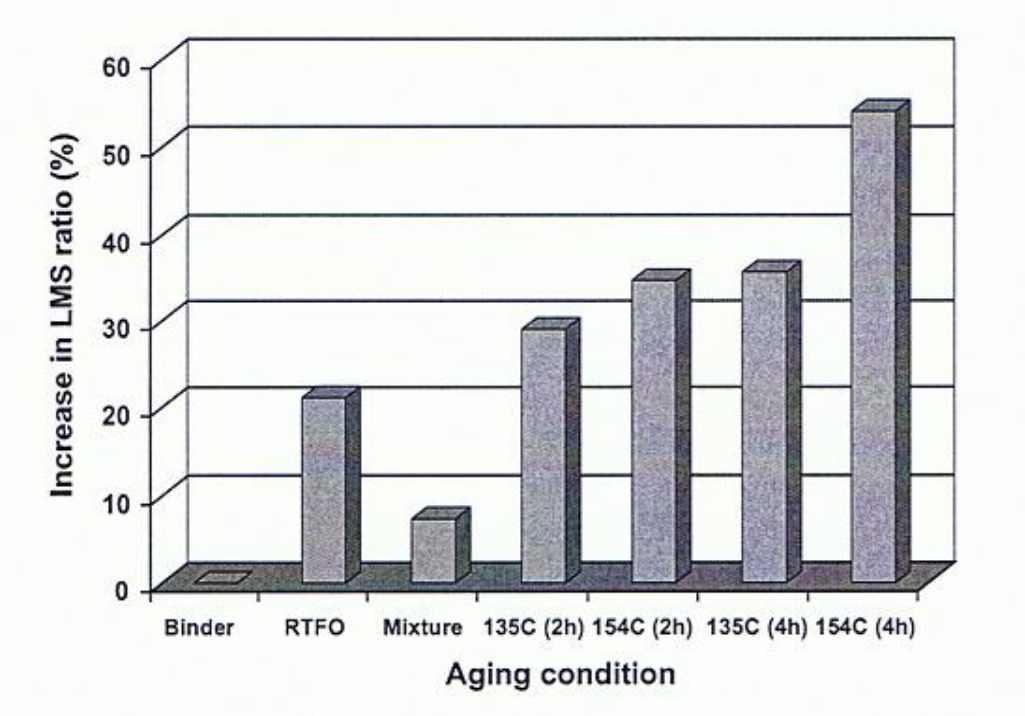

Figure 17. Aging effect (increase in LMS ratio) by aging condition [47]

2.6.2 Effect of Short Term and Long Term Aging

Haddadi et al, 2008, studied the effect of short term aging in the mixing process of the binder through penetration and softening measurement after RTFO (Table 5) [19]. Aging of PMB's caused a decrease in penetration and an increase in softening point indicating that binder hardens due to oxidative aging. They observed that by adding EVA the resistance to oxidative degradation of the used (aged) bitumen was improved.

The properties of the modified binders are significantly improved when a continuous polymer phase is formed. The amount of EVA required ensuring the formation of its continuous phase depends on the chemical composition of the asphalt, swelling potential of the polymer and the bitumen-polymer compatibility. The chemical composition of the PMB's reveal an increase in asphaltenes due to the shifting of lower molecular weight fractions towards higher molecular weight fractions i.e. oils towards resins and resins towards asphaltenes. As asphaltenes content increases the compatibility between bitumen and polymer increases.

Table 5. Penetration and softening point of the base and the EVA modified bitumen's before and after RTFO [19]

	EVA content (%)			
	0	3	5	7
Penetration				
Before RTFOT	88	71	54	48
After RTFOT	53	49	41	37
Softening				
Before RTFOT	45	52	62	67
After RTFOT	54	60	68	73
ΔSP(°C)	9	8	6	6

Sengoz and Isikyakar, 2008, studied the relationship between the polymer content and indirect tensile strength (ITS) results of the short and long term aged samples. The indirect tensile strength (ITS) of the SBS modified mixtures was higher than the unmodified mixtures which can be attributed to the increased stiffness of the SBS modified bitumen. The ITS values increased with increasing polymer content up to 5% and there was a decrease at 6% (Figure 18). It was noted as the tensile strength of the modified mixtures increased, as compared to the tensile strength of the unmodified binder, the cohesive strength of the modified mixtures increased. [6]

From Figures 18 and 19, for the specimen prepared with the base bitumen, as aging time increased from unaged to long term aged condition, the ITS values increased. This increase in indirect tensile strength is an indicator of the effect of aging. Aging is represented by stiffening of the asphalt cement, higher viscosity and more brittle condition. The aged mixture is more susceptible to cracking and deterioration due to wear and moisture compared to unaged mixture. But the rate of aging decreased with the addition of polymers (Figure 19). The ratio of the ITS of short and long term aged polymer modified mixture to the ITS of the unaged mixture are called aging indices. As shown in Figure 20, the aging indices decrease with increasing polymer content. Also no change is observed on the aging indices above 5% of SBS polymer content which implies that 5% SBS content is the optimum that minimizes the effect of aging and provides reasonable service life of the mixture.

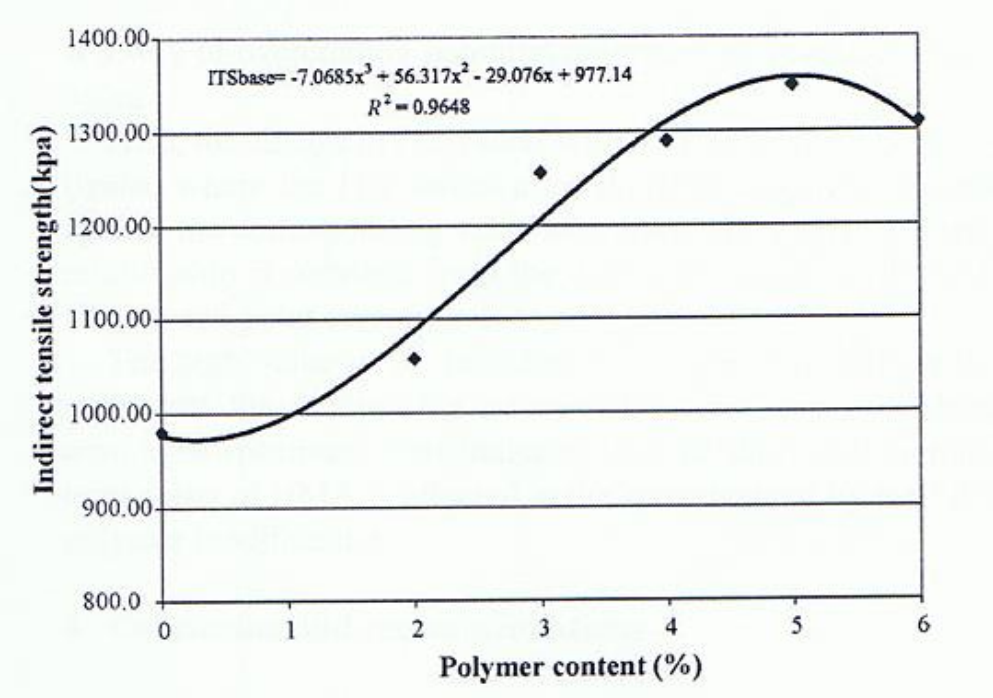

Figure 18. Indirect Tensile Strength of polymer modified HMA [6]

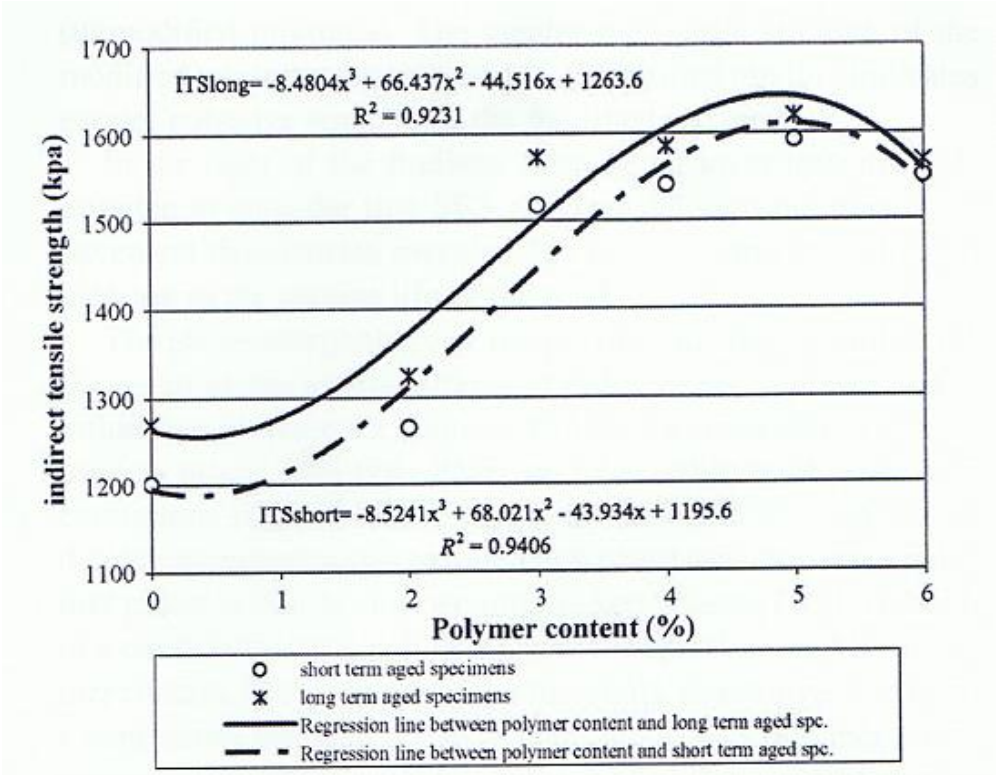

Figure 19. Relationship between the polymer content and indirect tensile strength of short and long term aged specimens [6]

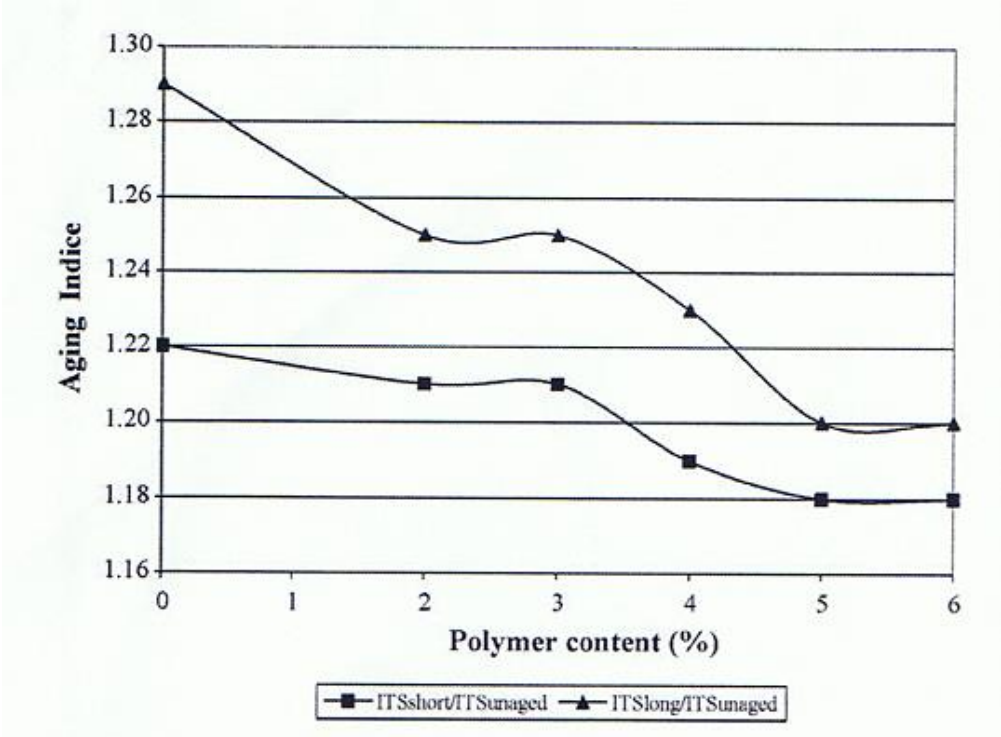

Figure 20. Aging indices corresponding to polymer content [6]

Ruan et al, 2003, studied the effect of long term oxidation on the rheological properties of PMA's. The modifiers used were SBR, SBS and tire rubber. The unmodified asphalt was

modified with 3%SBR, 3%SBS and 5% tire rubber plus 2%SBS. They found that SBS is less efficient at increasing asphalt ductility than SBR particularly with little oxidation as seen in Figure 21. This is due to the difference in the structures of SBR and SBS which results in the difference in interactions between them and the asphalt. SBS has two polystyrene blocks and SBR has one. The polar and rigid polystyrene block makes the polymer binder system more resistant to deformation. More polar groups in the polymer make stronger interactions between the polymer, the asphaltene, and the polar aromatic components of asphalt. It also makes SBS modified asphalt difficult to flow and builds stress easily when undergoing extension. [48]

Sulfur is used to form cross-links (vulcanization) between the polymer chains of SBR and BR which gives higher elasticity and greater tensile strength. Aging improves the temperature susceptibility of asphalt binders and damages the polymer network. So if the oxidative aging is extended, ductility decreases, counteracting the benefit of polymer modification. This is due to stiffening of the asphalt base material and to some extent degradation of the polymer. In a study by Airey, 2003, aging of SBS PMB tends to reduce the molecular size of the SBS copolymer with a decrease in elastic response of the modified bitumen.

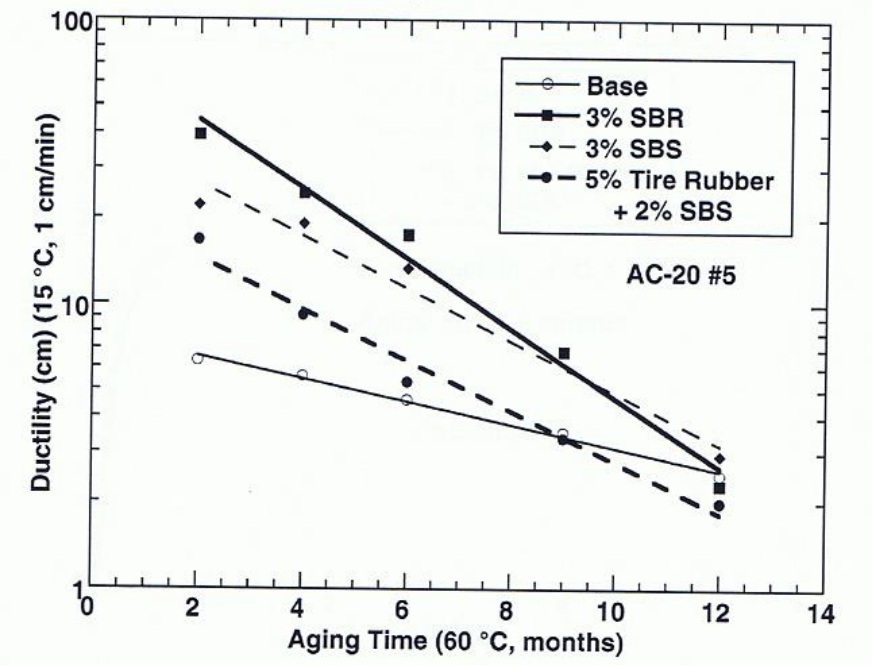

Figure 21. Decreases in ductility with aging time [48]

Khodaii and Mehrara, 2009, evaluated the permanent deformation of unmodified and SBS modified asphalt mixtures using dynamic creep test. Based on their study, they found that the coarse graded asphalt mixtures have more resistance to permanent deformation than the dense graded mixtures (Figure 22). This can be due to lower dependency on mastic properties especially at higher temperatures. They also studied that among the three types of mixtures they used with 4%, 5% and 6% of SBS polymer, the mixture with 5% SBS had the most improved mechanical behavior (Figure 23). [49]

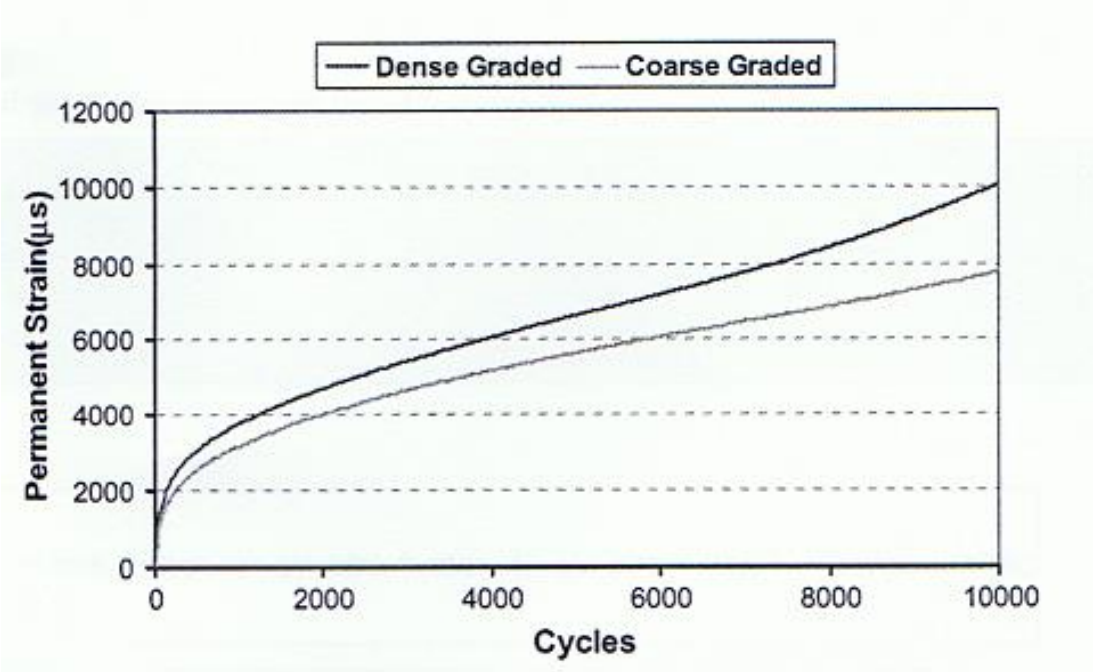

Figure 22. Creep curve for unmodified coarse and dense graded samples at 40˚C and 200 kPa stress level [49]

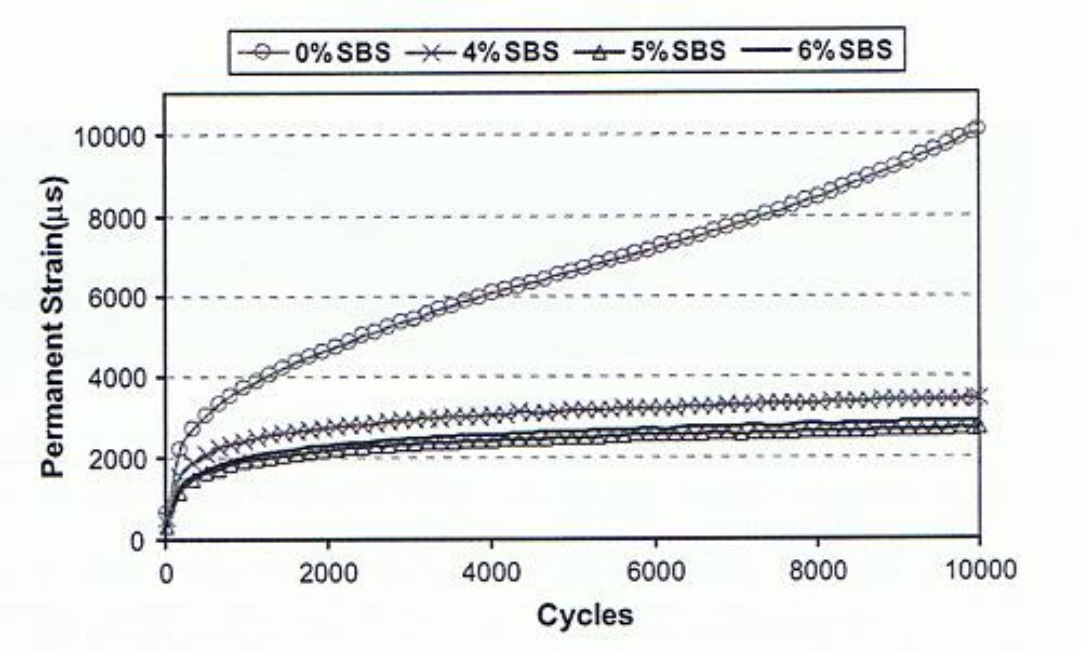

Figure 23. Creep curve for modified mixtures with different amounts of SBS at 40˚C and 200 kPa stress level [49]

Tayfur et al, 2005, evaluated mechanical properties of control and modified asphalt mixtures. The study focused on hot mix asphalt permanent deformation resistance of a conventional and five modified asphalt mixtures. The modifiers used were amorphous polyalphaolefin, cellulose fiber, polyolefin, bituminous cellulose fiber and SBS. They conducted indirect tensile strength, indirect tensile, static creep, repeated creep and LCPC wheel tracking tests under different loading conditions and temperatures. The indirect tensile strength of the modified mixtures was

higher than the control mix which implies that modified mixtures appear to be capable of withstanding larger tensile strains prior to cracking (Figure 24). Also modified mixtures showed more resistance to the permanent deformation in LCPC wheel tracking test at 60 °C. The researchers thought that modifiers contribute much to adhesion ability among aggregates of hot asphalt mixtures. [50]

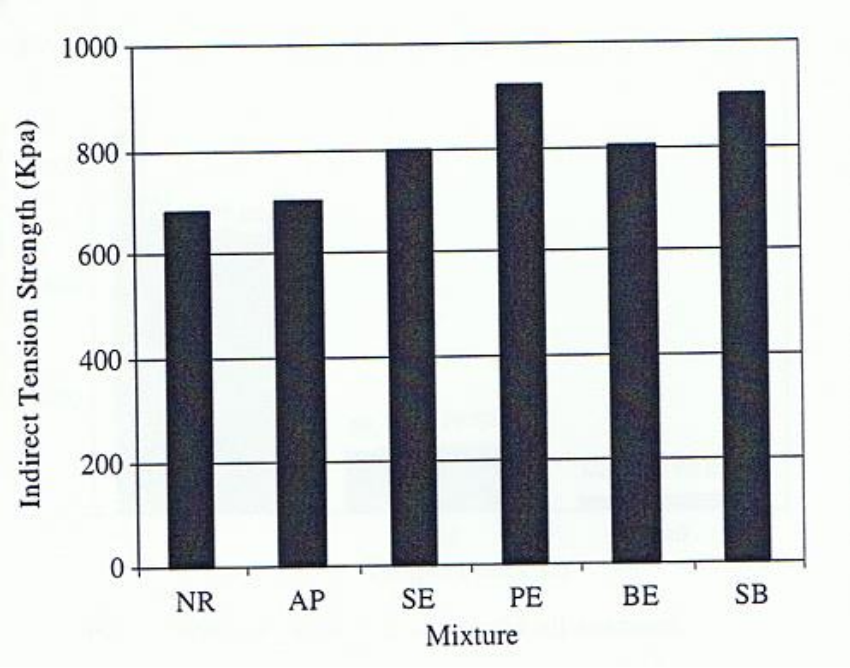

Figure 24. Indirect tension strength of the mixtures [50]

2.6.3 Storage Stability and Compatibility of Polymer Modified Binder

According to Gonzalez et al, 2004, the major problem of the PMB is the morphological stability during prolonged storage at high temperatures. The major cause of instability is due to the Brownian coalescence followed by gravitational flocculation and later creaming. Particularly in the case of CRM, the denser polymer particles settle at the bottom of the tank. Stability tests were performed both with the oscillatory flow and microscopy tests to analyze elastic modulus G' and loss modulus G". The difference between G' and G" from the top and bottom of the tube is the indication of phase separation. They analyzed the G' versus frequency of two samples containing 3% virgin EVA CP-636 as shown in Figure 25. After 24 hours of storage at 165°C, the elastic modulus of the upper part of the sample was higher than that of the lower part which indicates a coarsening effect due to coalescence of the EVA particles. The bad stability as seen in Figure 25 was also noticed in the blend containing 3% of recycled EVA, Figure 24. But good stability results were obtained for blends containing 1% of either recycled EVA or virgin EVA as seen in Figure 25. No phase separation was observed even after 4 days at 165°C (Figure 27). [51]

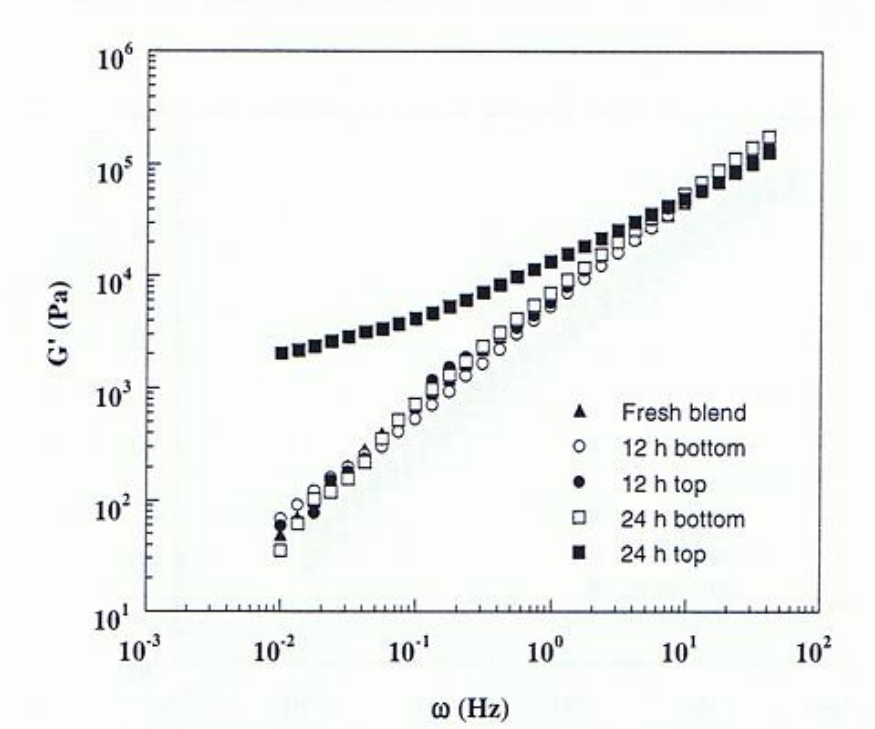

Figure 25. Elastic modulus as a function of frequency at T=165˚C for top and bottom sections of bitumen +3% EVA CP-636 [51]

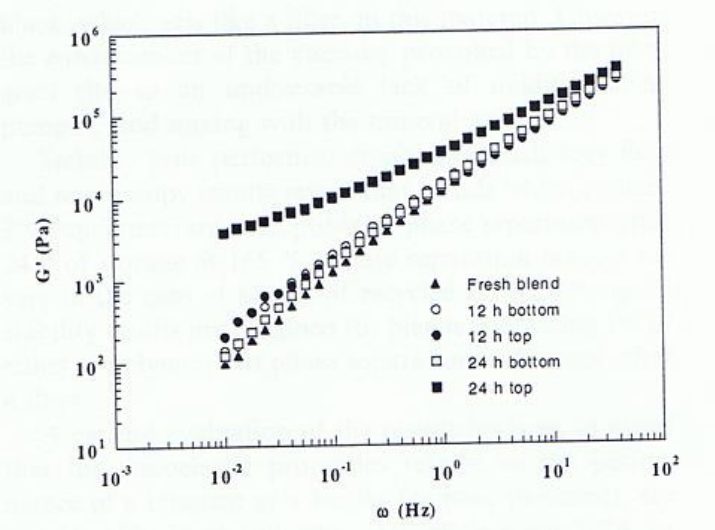

Figure 26. Elastic modulus as a function of frequency at T=165˚C for top and bottom parts of bitumen +3% recycled EVA [51]

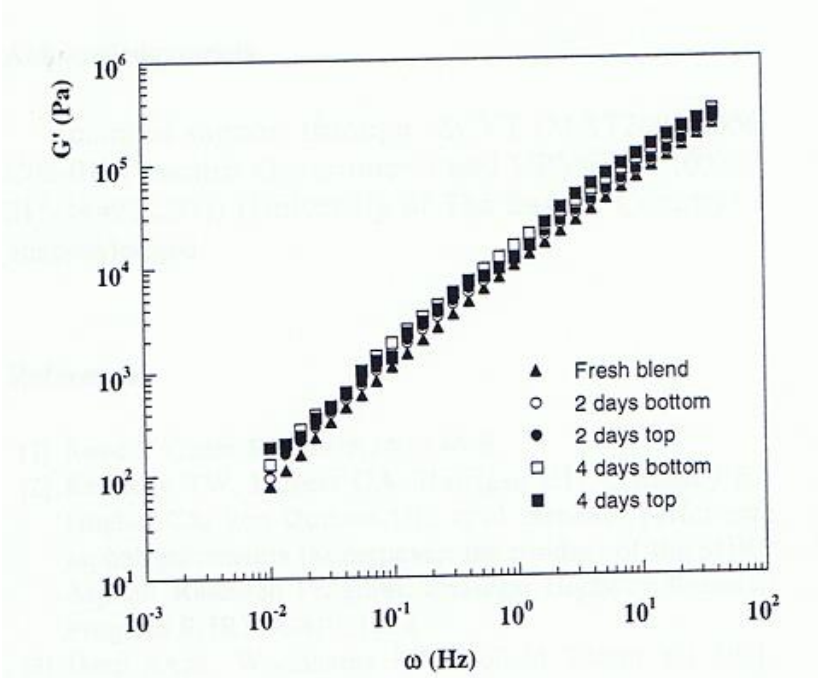

Figure 27. Elastic modulus as a function at T=165˚C for top [51]

According to the studies of Khodaii and Mehrara, 2009, and Sengoz and Isikyakar, 2008, all SBS modified asphalt mixtures provided adequate stability. Also the stability increased with increase in SBS content up to 5% and decreased thereafter as seen in Figure 28 below [6]. Based on the data, the researchers concluded that 5% could be evaluated as optimum SBS content. The values of storage stability were determined from the difference between the softening point temperatures of PMB samples taken from the top and bottom of the cylindrical molds of 32-mm diameter and 160-mm height. They were stored in an oven vertically at 163°C for 48 hours.

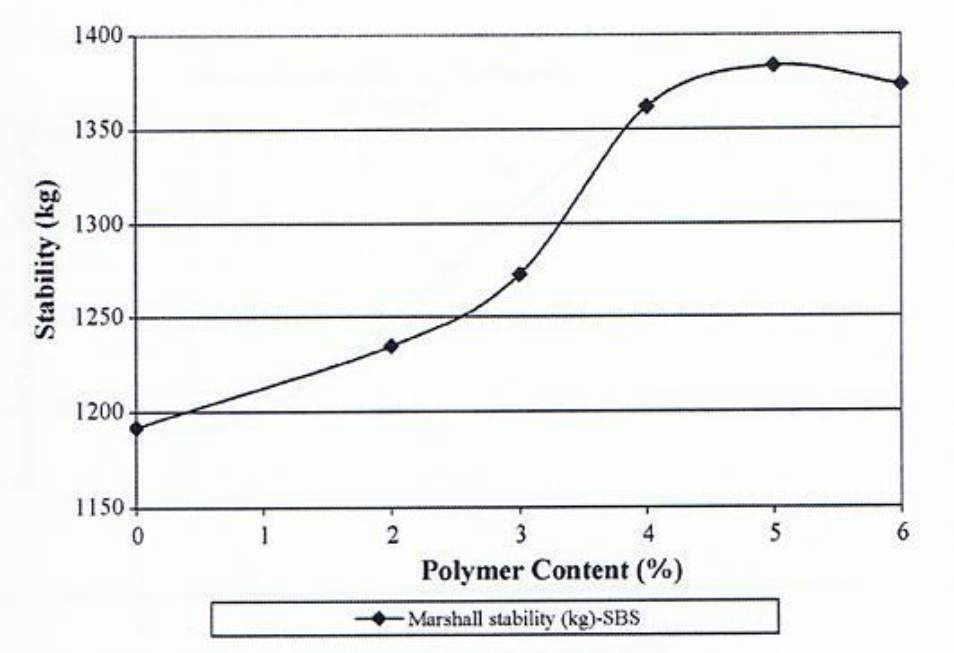

Figure 28. Marshall stability values of polymer modified HMA [6]

Wen et al, 2002, studied the high temperature storage stability of SBS tri-block copolymer modified asphalt [52]. Due to poor compatibility between SBS and asphalt the storage stability is usually poor at elevated temperatures for SBS modified asphalt. The structure of SBS affects the compatibility and storage stability of SBS modified asphalts. SBS modified asphalt without sulfur is unstable and has phase separation at elevated temperatures. The mechanism for the gross phase separation is called Brownian flocculation. They observed that the stability of PMA was improved by the addition of elemental sulfur and the blend with sulfur can be stored at high temperature.

In the storage stability test, the sample was poured into a 32mm diameter aluminum foil tube which is 160mm in height. After closing the tube, it is stored vertically at 163°C for 48 hours in an oven. Then the tube was cooled to ambient temperature and was cut horizontally into three equal sections. They measured the difference in softening points between the top and the bottom sections of the tube. If the difference is less than 2.5°C, the sample was considered to have good storage stability as seen in Figure 29 below. [52]

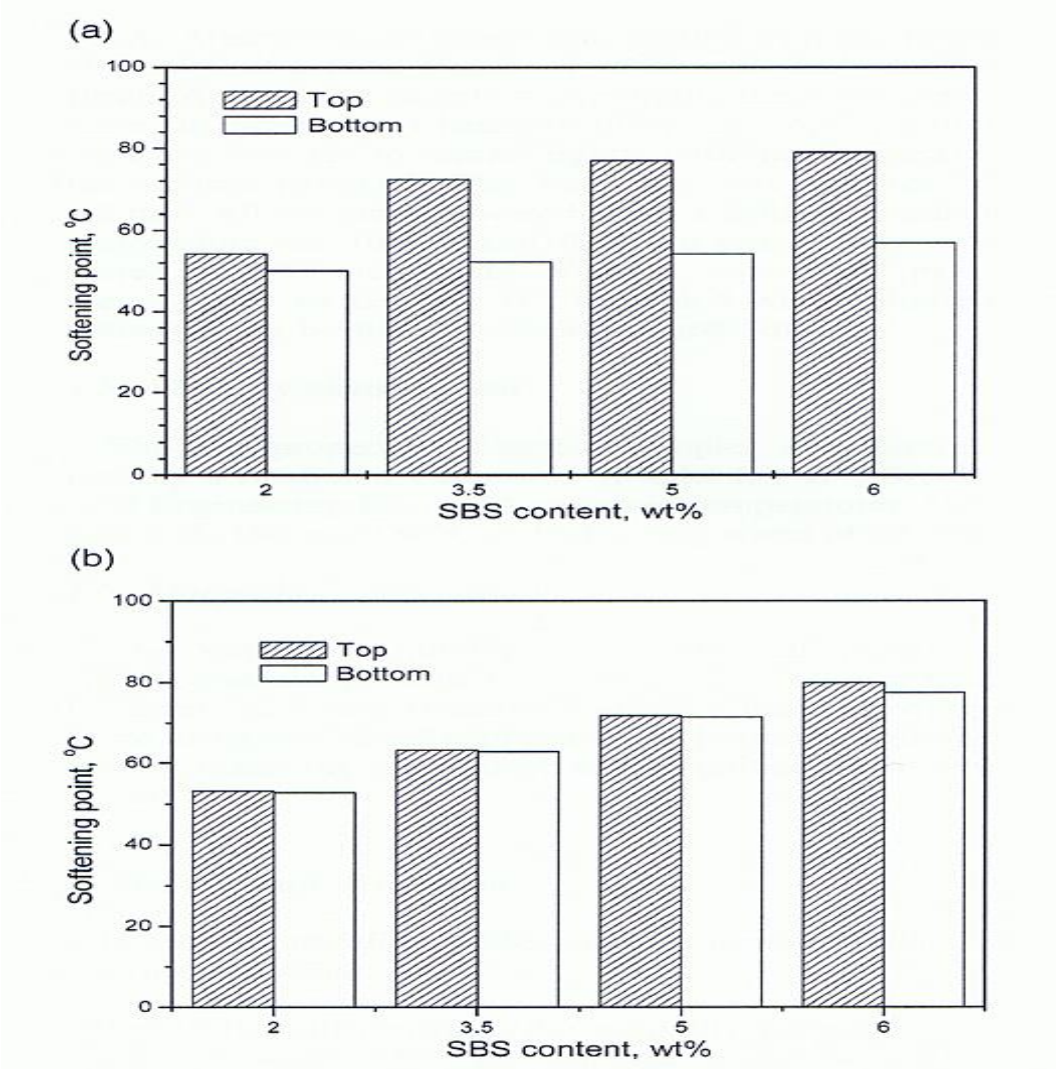

Figure 29. Effect of sulfur on storage stability of SBS- modified asphalt (Asphalt 100, SBS 1301, 3.5 wt.%, sulfur 5.0 wt.% based on SBS). (a) Before adding sulfur; (b) After adding sulfur [52]

According to a study by Fu et al, 2007 on the storage stability and compatibility of asphalt modified binder, the performance of SBS copolymer modified asphalt binder at high temperature was improved significantly with the addition of SBS-g-M grafted with vinyl monomer under gamma rays irradiation [15]. The difference between the softening points between the top and bottom sections of the tube, measured according to the rule of isolation degree measurement was not more than 2.5°C even after four months of storage at room temperature as seen in the Table 6 below.

Table 6. The isolation degree of PMA measured before and after stored for 4 months [15]

The isolation degree of PMA measured before and after stored for 4 months

Samples	Softening point upper part/°C	Softening point below part/°C	The temperature gap between upper and below part/°C
1#(A)	53.2	51.7	1.5
1#(B)	54.8	52.5	2.3
2#(A)	60.6	60.4	0.2
2#(B)	62.6	61.4	1.2

A: Fresh blending; B: Stored 4 months.

It was difficult to disperse 6% of SBS even under high shear stress and high temperature of 170°C as seen in Figure 30. With increased storage time, SBS particles dispersed finely throughout the asphalt but without being stabilized in the asphalt matrix (Figure 32). But when 6% SBS-g-M was added to the binder, it dispersed homogenously in the asphalt binder under the same high shear stress and at the same high temperature. As storage time increased from 1-hour to 24 hours, the particle size became much smaller and SBS-g-M dispersed even more homogenous which indicates that SBS-g-M has high temperature storage stability (Figure 30). Therefore, the compatibility and storage stability are improved with SBS-g-M (Figure 30) when compared to SBS modified asphalt binder (Figure 29 above). As mentioned earlier, this storage stable SBS-g-M- modified asphalt binder was prepared with the addition of polar monomer grafted SBS in gamma rays irradiation method. The addition of SBS-g-M improves the binder as a blended system forms a more perfect network in modified asphalt binder which makes the binder perform well at high temperatures and also reduce temperature susceptibility as seen in Figures 31, 32 and 33. [15]

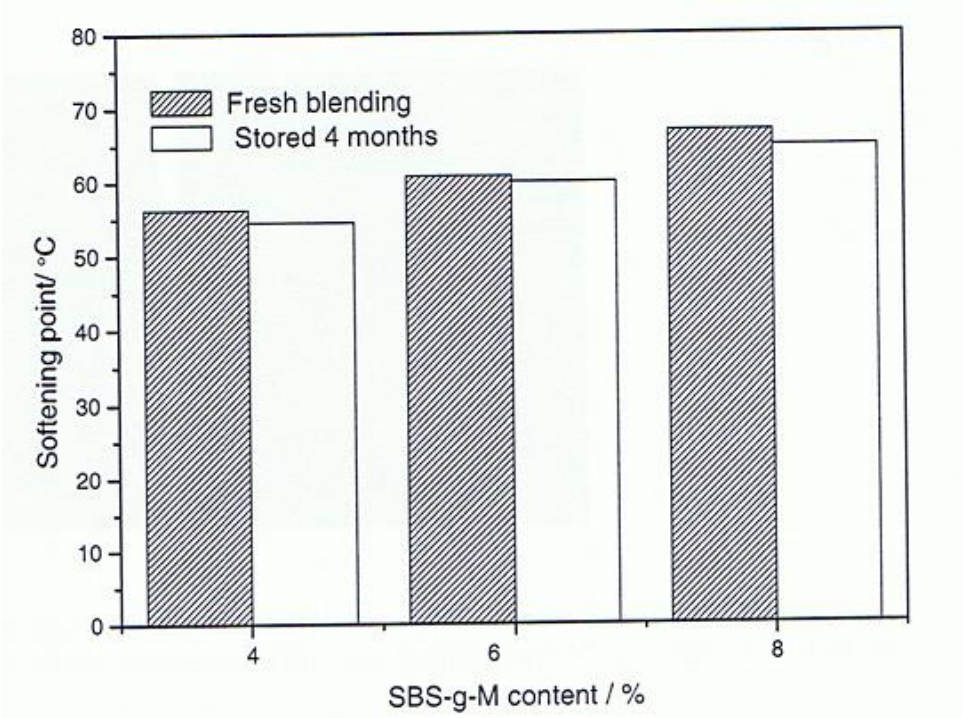

Figure 30. Effect of SBS-g-M content on softening point of modified asphalt binder [15]

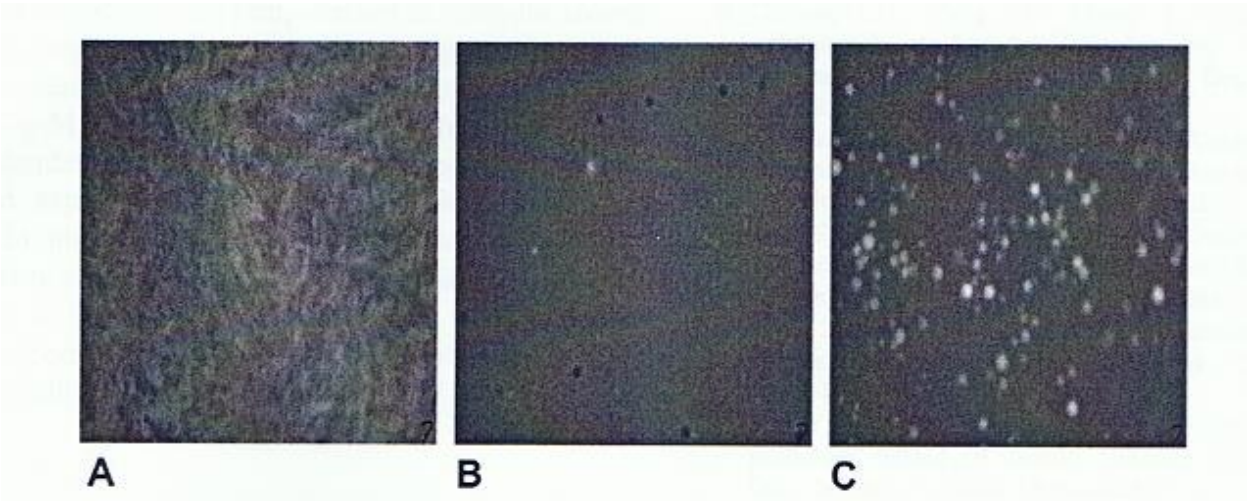

Figure 31. Phase structure of modified asphalt with 6% SBS-g-M before and after storage of 4 months observed by fluorescence microscope with a magnification of 100x at room temperature. (a) Fresh blending, (b) Bottom section of the tube after 4 months store at room temperature, (c) Top section of the tube after 4 months stored at room temperature. [15]

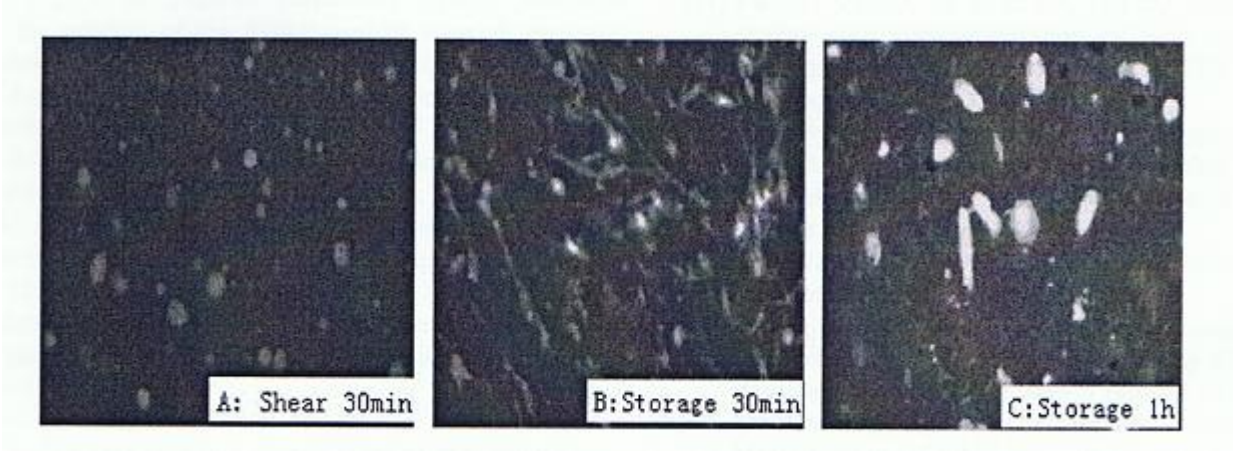

Figure 32. Fluorescence micrographs of modified asphalt binder with 6% SBS [15]

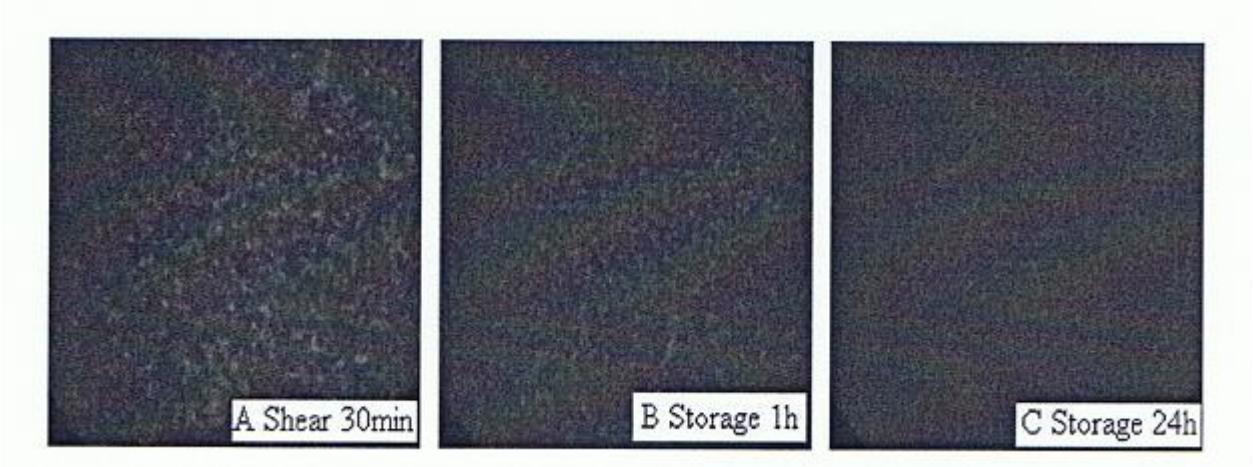

Figure 33. Fluorescence micrographs of modified asphalt binder with 6% SBS-g-M [15]

Zhang and Yu, 2009 studied the high temperature storage stabilities of the pure SBR modified asphalts, PPA/SBR modified asphalts and PPA/SBR/sulfur modified asphalts. They concluded that for the pure SBR-modified asphalt, the differences of the softening points (ΔS/°C) between the top and bottom sections of the samples were large which indicate a serious phase separation as seen in Figure 34 below. Storage stable SBR modified asphalt can be prepared by mixing PPA and sulfur at high temperatures under high shear mixing. They observed that the PPA/SBR modified asphalts with different SBR contents showed good storage stability. The stability of a PMA depends not only on the density and viscosity of the bitumen and polymer but also on the molecular weight and structure of the bitumen phase. As PPA shifts from sol to gel structure makes the asphalt similar to a solid material and affects the stability of PMA. Also, the storage stability of the PPA/SBR modified asphalt is improved by addition of sulfur. The addition of sulfur caused a decrease in the softening points of PPA/SBR/sulfur modified asphalt which indicate that sulfur improves the compatibility between the asphalt and SBR through a dynamic vulcanization process. [53]

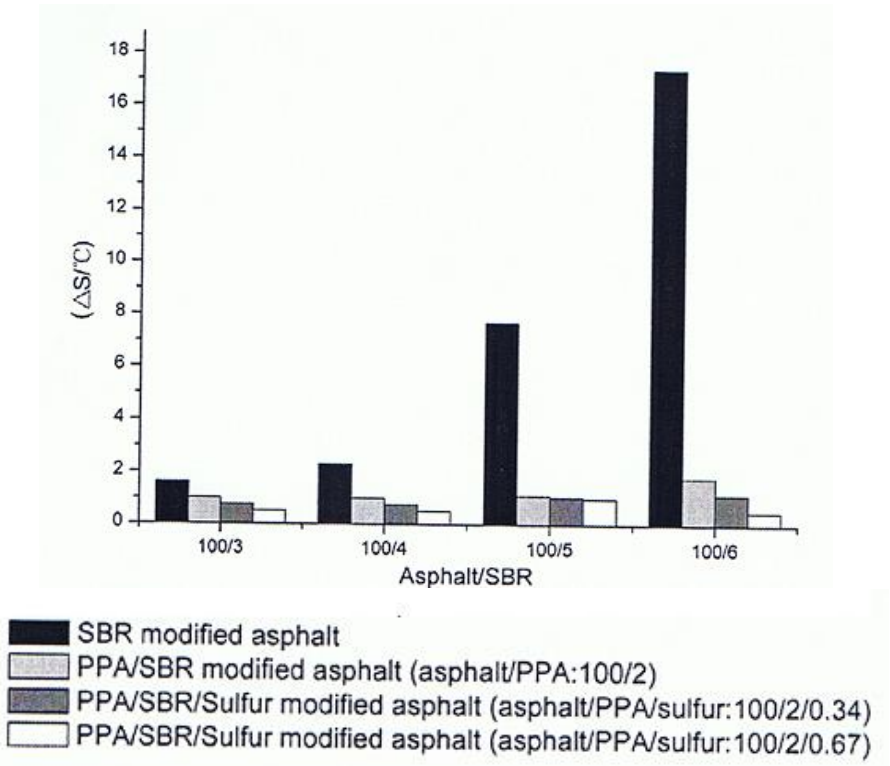

Figure 34. Storage stabilities of SBR compound modified asphalt [53]

According to a study by Haddadi et al, 2008, asphalt concrete specimens with EVA modified bitumen had the highest stability and smallest flow as shown in Figures 35 & 36 below. M_0, M_1 and M_2 are three types of bitumen concrete that were considered in their testing. M_0 is obtained by mixing the unmodified bitumen with aggregates and is called control mix. M_1 is obtained by mixing the polymer modified bitumen with aggregates. They used 3%, 5% and 7% of EVA contents by weight of optimum bitumen content to prepare the binders. M_2 is obtained by mixing the unmodified bitumen, EVA and the aggregates at the same time. The same contents of EVA were used for this mixture too. [19]

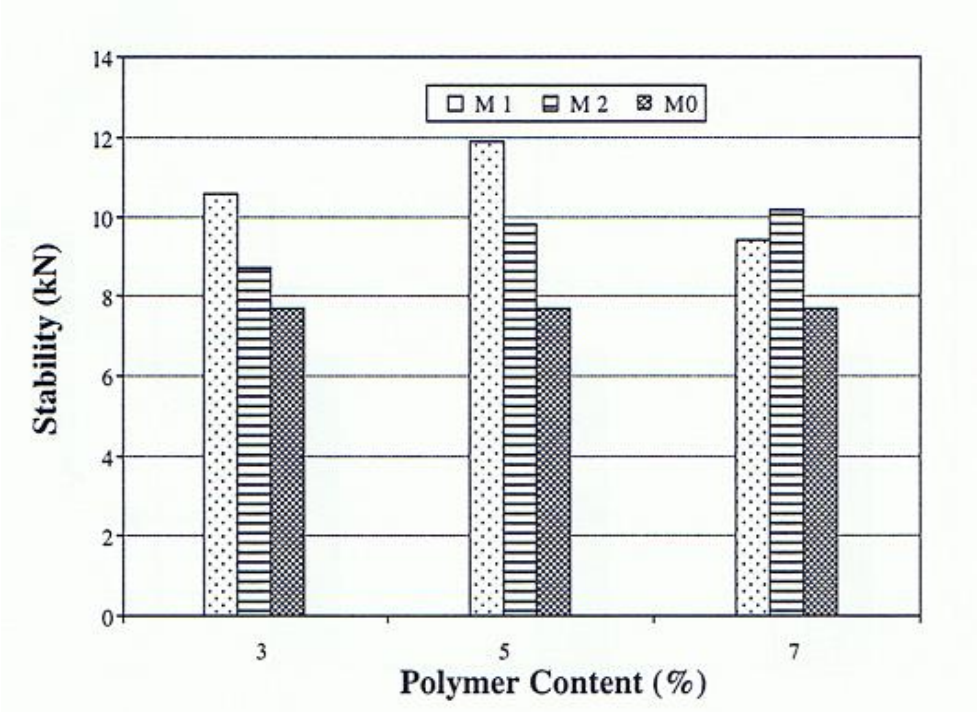

Figure 35. Stability of the different asphalt concrete mixtures versus the EVA content [19]

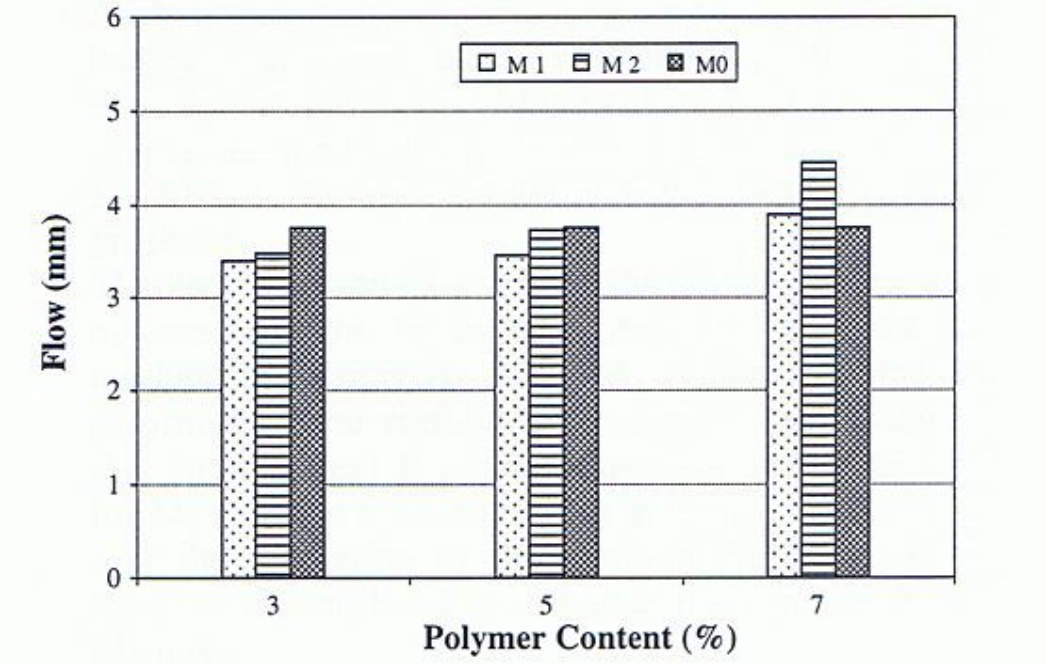

Figure 36. Flow of the different asphalt concrete mixtures versus the EVA content [19]

Table 7. PMA's content and softening point [2]

PMAs content and softening point

Mix	Polymer (6% by weight)	Temperature (°C)	Mixing time (min)	$T_{R\&B}$ (°C)	
				After mix	After cure
M1	Riblene®FF20	180	30	53.0	–
M2	Riblene®FC20	180	30	53.7	–
M3	Escor®5100	180	30	49.4	–
M4	Lotader®AX8930 (10%) Riblene®FC20 (90%)	180	30	52.6	66.0
M5	Lotader®AX8840 (7%) Riblene®FC20 (93%)	180	30	53.8	58.1
M6	PEGMA1	180	30	59.2	73.6
M7	PEGMA2	190	120	52.3	68.9
M8	Flexirene®FF25	190	120	120.5	–

In a study by Polacco et al, 2005, a 70/100 penetration grade asphalt obtained from vacuum distillation was modified with 6% by weight of different polyethylenes and polyethylene-based polymers. Different polymers used for the study are: Riblene FF20, Riblene FC20, Escor 5100, Lotader AX8930 (10%), Riblene FC20(90%), Lotader AX8840(7%), Riblene FC20 (93%), PEGMA1, PEGMA2 and Flexirene FF25. The morphological and storage stability analysis showed that the materials obtained were strongly biphasic and tended to separate into polymer rich and asphalt rich phases. No storage stability was achieved as there was a large difference $T_{R\&B}$ (Ring and Ball softening point) of the samples between the upper and lower parts of the tube for all the PE-based polymers as seen in Table 7. But a linear low density polyethylene (LLDPE) enhanced the mechanical properties. So mixes with different percentages such as 2%, 4% and 6% of this polymer were prepared and studied from a rheological point of view. The curves showing storage J' and loss J" compliance for the base asphalt (BA), PMA2, PMA4, and PMA6 can be seen in Figures 37 & 38 below. They analyzed that, though the polymer was insoluble, it spread continuously throughout the asphalt matrix by forming a very low extent of cross linking between the polymer chains as seen from loss tangent curves in Figure 39 below. [2]

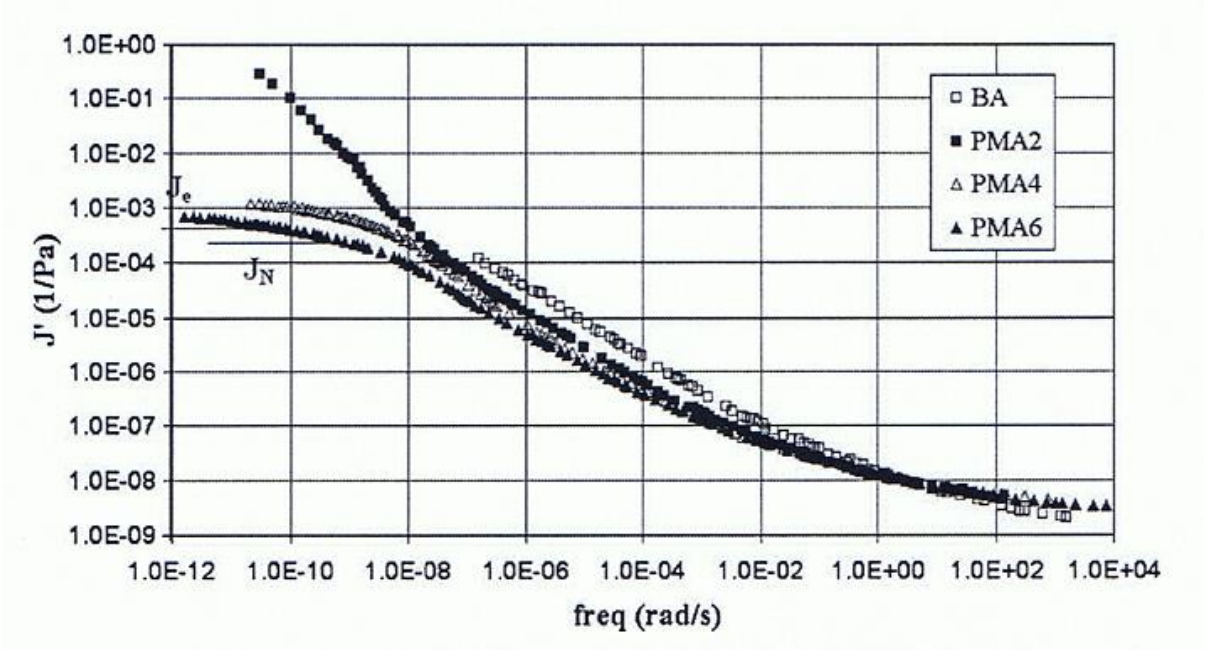

Figure 37. Storage compliance for BA, PMA2, PMA4 and PMA6 [2]

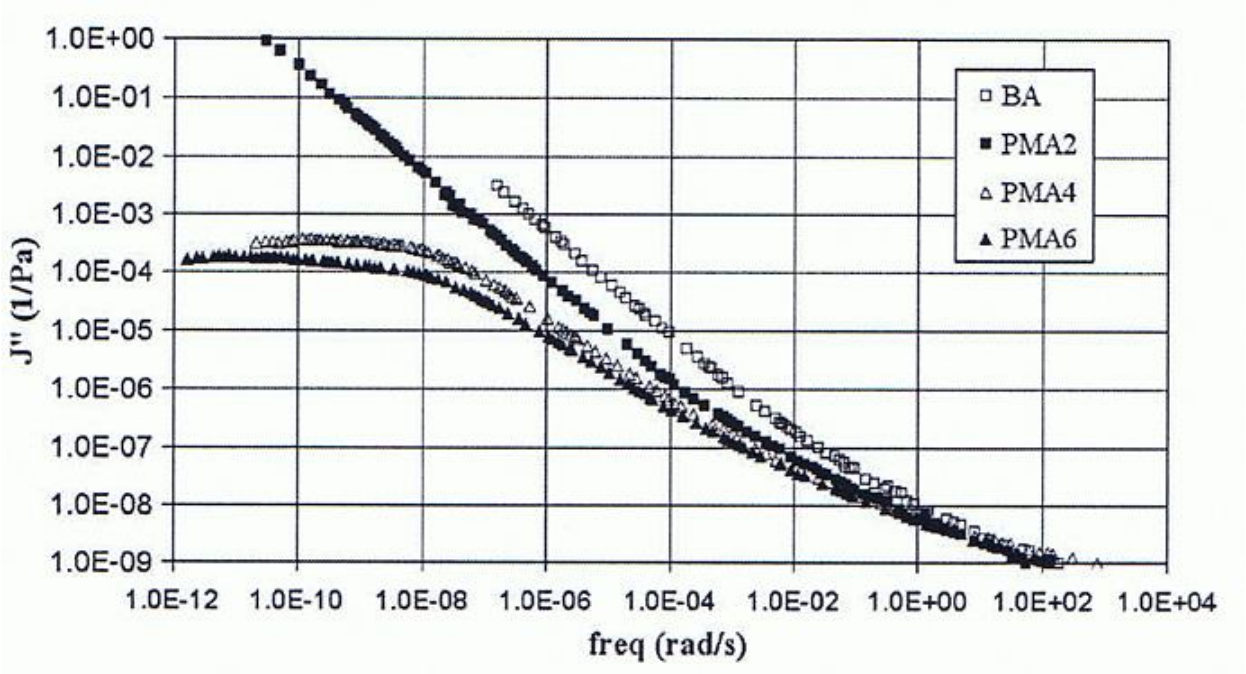

Figure 38. Loss compliance for BA, PMA2, PMA4 and PMA6 [2]

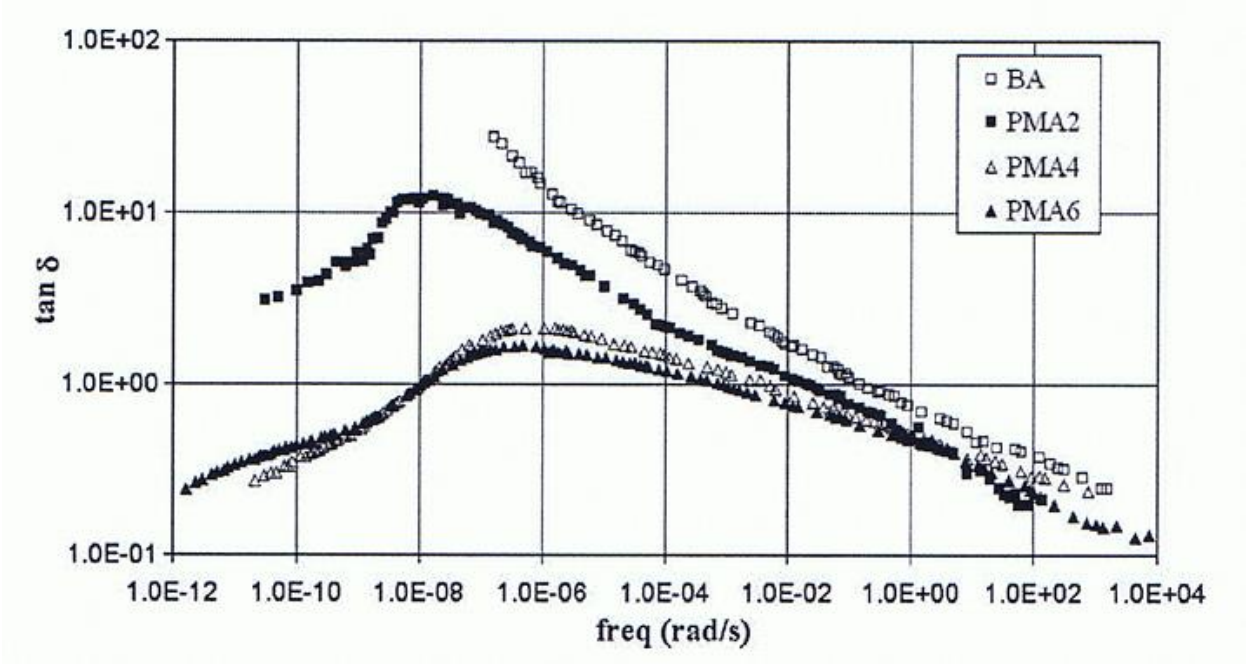

Figure 39. Tan(δ) for BA, PA2, PMA4 and PMA6 [2]

2.7 Field Performance of Modified Binders

In a study by Sirin et al, 2008, the researchers evaluated the rutting performance of a typical Superpave mixture, PG67-22 used in Florida and the same mixture modified with SBS polymer. FDOT's heavy vehicle simulator (HVS) was used to evaluate the long term performance of these Superpave mixtures and SBS modified Superpave mixtures with emphasis on rutting resistance. This HVS simulates 20 years of interstate traffic on a test pavement within a short period of time. There were a total of 15 test sections as shown in Figure 40. The testing program is divided into two phases. Phase I testing was conducted on five test sections, 1C-5C, at ambient conditions. Phase II was conducted on the other ten test sections with temperature control. In Phase II, lanes 1 & 2 have two 5 cm lifts of SBS modified Superpave mixture and were tested at controlled pavement temperatures of 50 and 65°C. All the other sections in Phase II were tested at only one temperature i.e., 50°C. The results from the Heavy Vehicle Simulator showed that the pavement sections with two 5-cm lifts of SBS modified mixture outperformed the two 5 cm lifts of unmodified mixture which had two to two and half times the rut rate. From the changes in thickness and density of the cores from the test sections they concluded that the rutting of the unmodified mixtures was due to combination of densification and shoving while the rutting of SBS modified mixtures is primarily due to densification. [54]

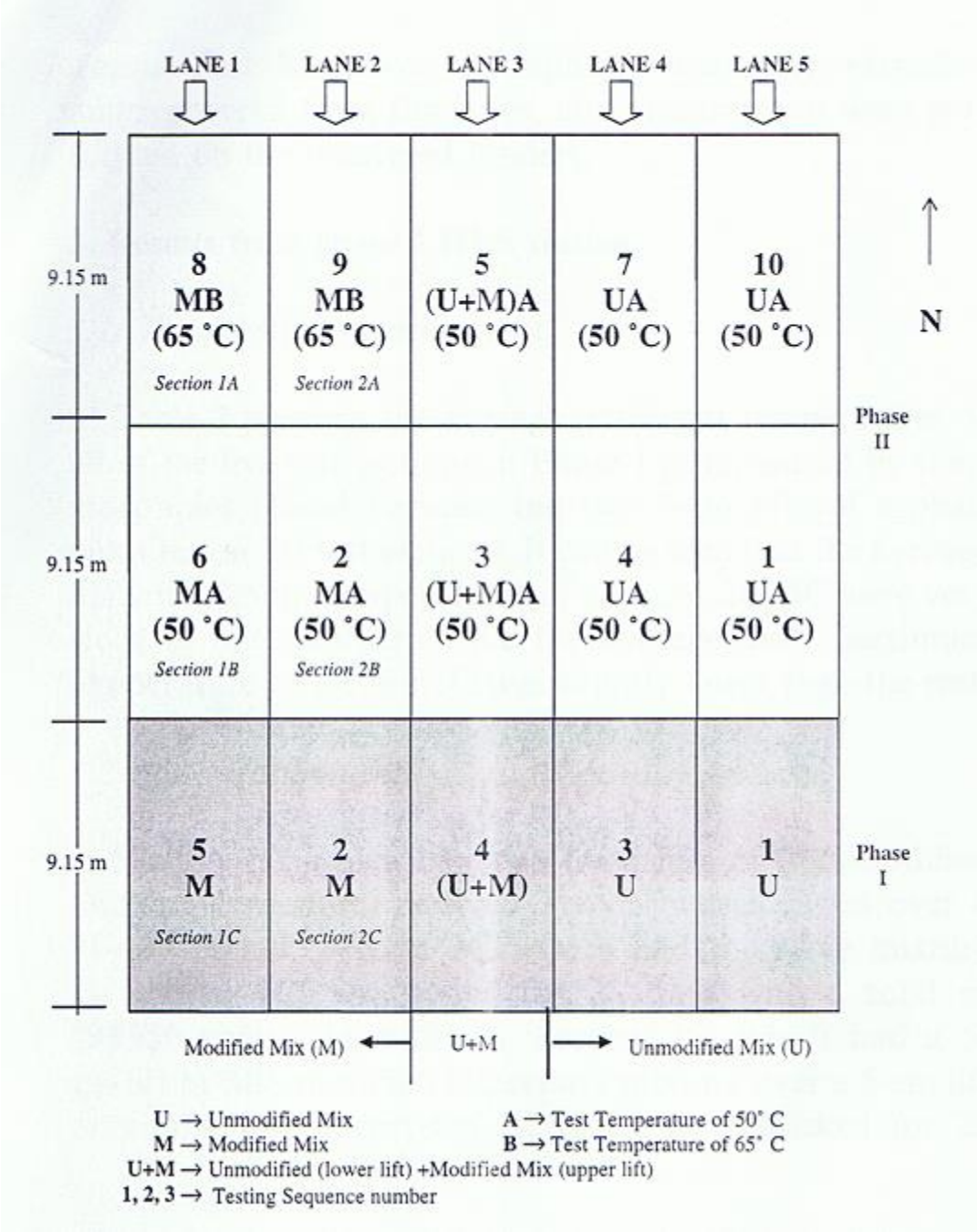

Figure 40. HVS testing sequence (Plan View) [54]

2.8 Summary of Literature Review

- Styrene Butadiene Rubber (SBR) improves the low-temperature ductility, increase viscosity and elastic recovery; as well as, improves adhesive and cohesive properties of the mixes.
- Styrene Butadiene Styrene (SBS) significantly increases strength at higher temperatures as well as flexibility at lower temperatures
- There are varieties of other modifiers that show improvements : Elvaloy, Ethylene Vinyl Acetate (EVA), Polyphosphoric Acid (PPA) and Crumb Rubber Modifiers (CRM).

- Superpave binder specifications are not sensitive enough to polymer modification
    - not adequately ensure that modified binders will perform well in intended applications
- New tests have been developed to be sensitive to polymer modification, including: Elastic Recovery (ER), Forced Ductility (FD) and Multiple Stress Creep Recovery (MSCR)
- MSCR testing is simpler and quicker to perform than its counterparts ER and FD.
    - Performed using the Dynamic Shear Rheometer (DSR) with 1 second of controlled shear stress and then 9 seconds of recovery.
    - The first 10 cycles (cycles 1-10) are run again at 0.1 kPa and represent the results for 0.1 kPa
    - The next 10 cycles (cycles 11-20) are run at 3.2 kPa
    - The test results are $J_{nr,}$ the non-recoverable creep compliance and average creep recovery for each stress condition
- Elastic Recovery measures the percentage recovery of a stretched asphalt sample
- Forced Ductility measures the load the resulting of the stretching of an asphalt at a constant rate, with the resulting parameters:
    - Peak Ratio- is the ratio from the first load peak to the second load peak
    - Area under the force displacement curve
- Gel Permeation Chromatography (GPC) measures molecular size distribution
    - Research shows it can be used to identify binder source and presence of modifiers
    - It can determine polymer concentration if polymer is known
- Fourier transform infrared spectroscopy (FTIR) can be used to determine polymer content
- Analysis of the chemical composition of can be performed by breaking asphalt down into saturates, aromatics, resins, and asphaltenes
- Dynamic Complex Modulus (DCM) testing is a performance test performed at a range of temperatures and frequencies that can be used to develop a master curve of the visco-elastic properties
    - The master curve can be extrapolated to determine properties outside the original testing
- The Mechanistic Empirical Pavement Design Guide(MEPDG) is a software that uses the results of DCM testing in conjunction with site and environmental conditions to predict pavement performance
- Flow Time testing is a lab performance test for rutting
    - The asphalt mix is compacted and tested under a constant load
    - “Flow Time” is achieved, after the primary and secondary phases, when the mix becomes unstable with significantly deformation occurring rapidly
- The morphology and storage stability of the modified binders were largely dependent on the polymer content and were influenced by the characteristics of the base bitumen and the polymers.
- The chemical modification that takes place during aging is the formation of oxidation products coming from the asphalt and from the degradation of the polymer which gives rise to insoluble cross-linking products
- Aging improves the temperature susceptibility of asphalt binders and damages the polymer network.

- Coarse graded asphalt mixtures have more resistance to permanent deformation than the dense graded mixture.
- The results from the Heavy Vehicle Simulator showed that the pavement sections with two 5-cm lifts of SBS modified mixture outperformed the two 5 cm lifts of unmodified mixture which had two to two and half times the rut rate.

Chapter 3 Experimental Design

The experimental design is categorized into three components: Mechanical Binder Testing, Chemical Binder Testing and Mix Performance Testing. Table 8 is the test matrix for the entire project, encompassing each component, it includes: specification followed, property measured, and the number of binders tested.

Table 8. Test Matrix

Test	Specification	Property	Number of binders and mixes tested
Superpave	AASHTO M320	High temperature true grade	39
Superpave	AASHTO M320	Low temperature true grade	16
Elastic Recovery	AASHTO T301	Percent Recovery (%)	31
Forced Ductility	AASHTO T300	Peak Ratio	20
MSCR	AASHTO TP 70	J_{nr} (kPa^{-1}) and Percent Recovery (%)	34
GPC		Molecular Weight (M_w)	23
SARA	D 4124 – 01	SARA Composition	5
DCM	T342	Dynamic Complex Modulus	3
Flow Time	TP79-11	Flow Time (sec)	10

3.1 Mechanical Binder Testing

A binder study was initiated to better understand the relationship between polymer, type and concentration amongst the Superpave, MSCR, Elastic Recovery (ER), and Forced Ductility (FD) testing. In-House modified binder was used to examine the impact of concentration of modification on testing; while plant produced modified binders were also examined for the impact of different modifiers on testing. The binders tested along with identifiers to be used throughout the paper are listed in Table 9. The table also includes the source, either a plant or in-house mix, and the PG grade of the binder.

Table 9. Binder Identifier

Binder Identifier	Binder	Source	PG High Temperature Grade
1	NS 82-22	NuStar	82
2	NS 82-22 Tank 73	NuStar	82
3	NS 76-22	NuStar	76
4	NS 76-22 Tank 1007	NuStar	76
5	Road Science 76-28	Road Science	76
6	76-28 Rat 295	NJDOT	76
7	CRM V=2900	NJDOT	94
8	CRM V=3200	NJDOT	94
9	Valero 937	Valero	64
10	NS 64-22	NuStar	64
11	Valero 937, 1.5% K	In-House	64
12	NS 64-22, 1.5% E, 0.8% PPA	In-House	64
13	NS 64-22, 1.5% E	In-House	70
14	NS 64-22, 2.5% E	In-House	70
15	NS 64-22, 1% K	In-House	70
16	NS 64-22, 1.5% K	In-House	70
17	NS 64-22, 2% K	In-House	70
18	NS 64-22, 3% K	In-House	76
19	NS 64-22, 4.5% K	In-House	82
20	NS 64-22, 5% K	In-House	82
21	NS 64-22, 7% K	In-House	82

*NS- Nu Star; *CRM – Crumb Rubber Modifier; *E – Elvaloy modified; *K – Kraton modified

The first step in evaluating modifier concentration was to determine an appropriate blending procedure. In order to minimize complexity, cross-linking agents were not evaluated. It was determined that along with the benefit of reduced complexity, the polymer could be evaluated without the contribution of the agent. It was thought that cross linking agents would also cloud the chemical analysis and possibly mask the molecular weight distribution of the polymer in question. The team adapted and adopted a procedure provided by NuStar Energy for blending SBS.

The asphalt was heated to a temperature of 190˚C and then polymer is added slowly while mixing. Mixing continued for two hours at temperature. These were both incorporated into our mixing process. Initially the asphalt was heated to a high temperature above 140˚C, and then moved from the oven to the heating mantle covered by fiberglass insulation. A thermocouple was used to monitor the temperature of the asphalt. A Ross high shear mixer was then used to mix the asphalt. This helps to ensure a uniform temperature throughout the asphalt and is necessary when mixing SBS. Once the asphalt is heated and being maintained at a temperature of 190˚C, the polymer is slowly added over a 30 minute period. Once the polymer is added, the mixture is mixed for 2 hours while frequently scraping the side of the can to move polymer towards the impellor of the mixer and ensure a uniformly mixed binder. After 2 hours, if the

binder exhibits the proper consistency, it is removed from heat and allowed to cool. The lab acknowledges the importance of the cross-linking the modifier and base binder, and although the in-house produced binders may not have fully developed the cross linking, the same procedure was followed for each mix, therefore comparison within in-houses mixes is reasonable.

3.2 Chemical Properties of Binders

The chemical properties of binders were tested using: FTIR, GPC, MSCR Curve, and SARA analysis. In-house binders were prepared under controlled conditions as outlined for the mechanical testing and again no additional cross linker or catalyst were used in the study.

3.2.1FTIR and GPC

It was desired to have a good range of polymer contents to test using FTIR and GPC. This was to have the most data points possible to be able to make accurate findings from data. Thus, a NS 64-22 Base binder was mixed to form 1-5 weight % mixes of two different polymers commonly used on roads today, Kraton D1101 and Elvaloy AM.

3.2.2 MSCR Curve

In addition to FTIR and GPC testing a study using ASTM D7405-10a MSCR testing is carried out on industry and in-house modified binders, as well as neat, or unmodified, binders, in the development of the MSCR curve. Industry has provided limited information on the type of polymers used in polymer modification. In-house binders were prepared under controlled conditions as outlined for the mechanical testing and again no additional cross linker or catalyzes were used in the study. The details of industry and in-house binders are given in Table 10.

Table 10. Binders used in MSCR Curve testing

Industry prepared binder		**In-house prepared binder**		
Sr. No.	**Type of polymer in the binder**	**Sr. No.**	**Type of binder**	**Type of polymer in the binder**
IN_1	Unknown	RO_1	Source 1 (PG64-22)	1.5% SBS
IN_2	Unknown	RO_2	Source 1 (PG64-22)	3% SBS
IN_3	Crumb rubber	RO_3	Source 1 (PG64-22)	4.5% SBS
IN_4	Unknown	RO_4	Source 1 (PG64-22)	Elvaloy 1.5%
IN_5	SBS	RO_5	Source 1 (PG64-22)	Elvaloy 2.5%
IN_6	SBS	RO_6	Source 1 (PG64-22)	Elvaloy 1.5% and 0.8% PPA
		RO_7	Source 2 (PG64-YY)	1.5% SBS
		RO_8	Source 1 (PG64-22)	5% SBS

MSCR testing was conducted on in-house and industry binder at 64^{o}C and then the creep and recovery curve was analyzed to determine linear viscoelastic parameters, non-linear viscoelastic parameters, and PS components. The linear viscoelastic parameters were determined by evaluating the creep and recovery curve at a low stress of 0.1 kPa. The strain data of 10 cycles were similar at 0.1 kPa, therefore, only the first cycle was used to determine linear viscoelastic parameters. The non-linear viscoelastic parameters were determined by analyzing the creep and recovery curve of 1, 6 and 10 cycles at 3.2 kPa. Finally, the permanent strain component was determined by analyzing the non-recoverable strain at the end of 10 seconds of

each cycle. The linear viscoelastic, non-linear viscoelastic, and PS parameters define the entire curve of creep and recovery. The effect of different PMB on creep and recovery could be better understood by analyzing the parameters that define all three components (linear viscoelastic, non-linear viscoelastic, and PS). The methodology to determine linear viscoelastic parameters, non-linear viscoelastic parameters, and PS is as follows, along with a sample calculation and results for industry binder 5 (IN_5) is shown below.

Step 1: Conduct the MSCR testing on asphalt binder as per AASHTO TP 70-08 or (ASTM D7405-10a).
Step 2: Analyze recovery data – Start each cycle with zero, this could be done by subtracting the strain value of a given cycle by the last strain value of the previous cycle. In the subsequent steps, the recovery data that are analyzed were all zeroed as explained above.
Step 3: Calculate the creep compliance for each cycle using equation 1.
Step 4: Determine the linear viscoelastic parameters.
The authors tried both the Generalized Burger model and the Kelvin model, however, the latter model fit the data better. A two-mode Prony series linear viscoelastic Kelvin-Voigt model (equation 17) was assumed for the creep compliance.

Equation 17 $$\boldsymbol{J(t) = A + B\left(1 - e^{\frac{-t}{C}}\right) + D\left(1 - e^{\frac{-t}{E}}\right)}$$

A recovery curve for cycle number 6 at a lower stress level of 0.1 kPa (equation 18) was fit to the measured data. The concept was derived from equation 2 and the linear viscoelastic parameters A, B, C, D, and E were calculated. The elastic component A was almost zero and was neglected in subsequent analysis.

Equation 18 $$\varepsilon(t) = 0.1\left[A + B\left(1 - e^{\frac{-t}{C}}\right) + D\left(1 - e^{\frac{-t}{E}}\right)\right] - 0.1[A + B\left(1.e^{\frac{-(t-1)}{C}}\right) + D\left(1 - e^{\frac{-(t-1)}{E}}\right)]$$

Figure 41 shows the comparison of measured and calculated strains plotted using linear viscoelastic parameters B, C, D, and E.

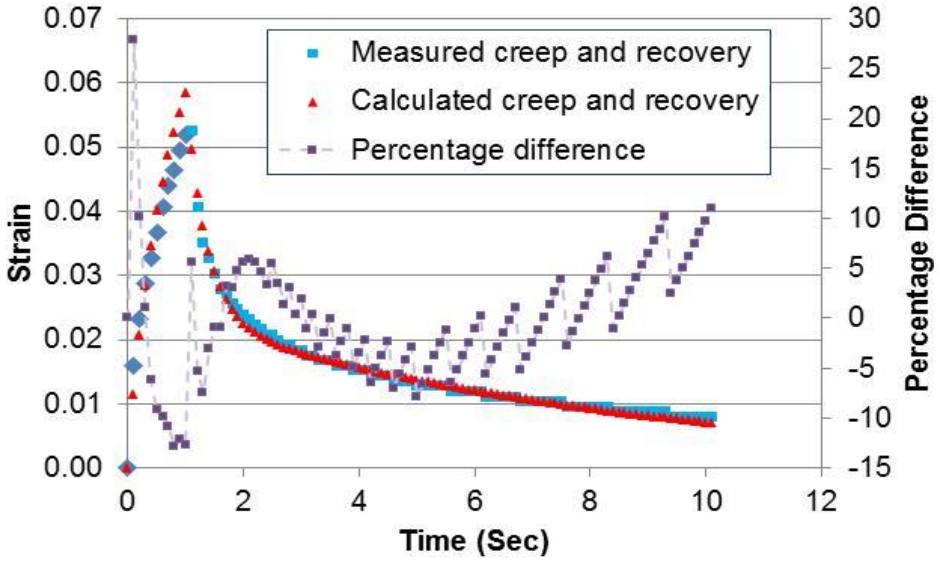

Figure 41. Comparison of measured and calculated strain for binder IN_5 by fitting linear viscoelastic parameters at a stress level of 0.1 kPa and a cycle of 6 seconds.

Step 5: Determine the non-linear viscoelastic parameters.
The parameter G_1 is determined by fitting the model (equation 19) to the first 10 data points of the measured recovery curve (recovery time from 1 second to 2 seconds) for cycles 1, 6, and 10 at a stress level of 3.2 kPa.

Equation 19 $\varepsilon(t)_{NLVE-G1} = G_1\{[B\left(1-e^{-\frac{t}{C}}\right)+D\left(1-e^{-\frac{t}{E}}\right)]-[B(1-e^{\frac{-(t-1)}{C}})+D\left(1+e^{-\frac{(t-1)}{E}}\right)]\}$

Parameters G_2 and G_3 are determined by fitting the remaining 80 data points of the measured recovery curve with equation 8.

Equation 20: $\boldsymbol{\varepsilon(t)_{NLVE-G2-G3} = G_2\{3.2[J_{LVE(t=2)}-J_{LVE(t=1)}]\}+G_3\{3.2\left[B\left(1-e^{-\frac{t}{C}}\right)+D\left(1-e^{-\frac{t}{E}}\right)\right]-\left[B\left(1-e^{-\frac{t-1}{C}}\right)+D\left(1-e^{-\frac{t-1}{E}}\right)\right]\}}$

Where:

Equation 21: $J_{LVE(t=1)} = B\left(1-e^{-\frac{1}{C}}\right)+D(1-e^{-\frac{1}{E}})$

Equation 22: $J_{LVE(t=2)} = B\left(1-e^{-\frac{2}{C}}\right)+D(1-e^{-\frac{2}{E}})$

Figure 42 shows the comparison of a measured compliance curve and calculated compliance curve plotted using non-linear viscoelastic parameters G_1, G_2, and G_3. The percentage difference at 0.1 s and 0.2 s of creep curve were within 35-40% and 15-20%, respectively. The remaining data points of the creep curve were within 15%. The data points of recovery were within 10%. The first two data points are subject to the effects of ramp-up time of the shear stress. It is well known that to minimize effects of the ramp on the analysis, data points should be considered at approximately 10 times the ramp-up time it takes to achieve the creep stress.

Step 6: Calculated values – Calculated values of each cycle are determined by using linear and non-linear viscoelastic parameters.

Step 7: Permanent strain – Calculate permanent strain using following equation.

Equation 23:

$$Permanent\ strain, \% = 100\{(Measured\ Strain)-(Calculated\ Strain)\}_{@\ end\ of\ cycle}$$

The viscoelastic parameters B, C, D, and E determined for IN_5 at cycle 6 are 0.37, 0.365, 1.855, and 7.77 respectively. The non-viscoelastic parameters G_1, G_2, and G_3 determined for IN_5 at cycle 6 are 1.105, 0.105, and 1.005, respectively. The PS is 30.91%

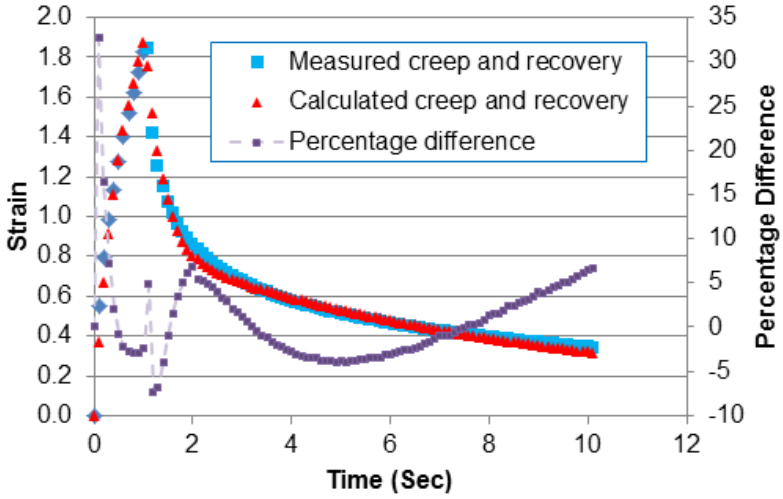

Figure 42. Comparison of measured and calculated strain for binder IN_5 by fitting non-linear viscoelastic parameters at a stress level of 3.2 kPa and a cycle of 1second.

3.2.3 SARA Analysis

The ASTM Designation: D 4124 – 01 a standard test method for separation of asphalt into four fractions' was used to obtain SARAs fractions. This test method was used to separate the petroleum asphalts into four different fractions: Saturates, naphthalene Aromatics, polar aromatics or Resins and Asphaltenes (SARAs). There are two methods in the specification called method A and method B for separation of the asphalt into these four fractions. Method B was adopted. The length of the chromatogram is 1000 mm for procedure A as against 510 mm for procedure B and needs further equipment for testing. The height of the hood in the lab is not tall enough to accommodate the full test equipment with 1000mm column, and the chemicals are very hazardous to work with outside the hood. Procedure A is very lengthy and expensive compared to procedure B and as both the procedures could be adopted to get the same results, to avoid expense and shorten the length of time, test method B was adopted.

3.3 Mix Performance Testing

Performance testing is the crucial step necessary to link binder testing to performance. Dynamic Complex Modulus (DCM) testing and subsequent analysis using the Mechanistic Empirical Pavement Design Guide (MEPDG) was initially selected as the performance test; however, after initial testing Flow Time testing was selected. The higher strains of Flow Time testing, which leads to failure of the test samples, was selected in favor of the low, nondestructive, stresses in which DCM testing is conducted under.

3.3.1. Dynamic Complex Modulus /Mechanistic Empirical Pavement Design Guide

The Mechanistic Empirical Pavement Design Guide was used for analysis of three mixes using the results of dynamic complex modulus (DCM), to determine a correlation between pavement predicted performance to J_{nr} values. The traffic used was a 4 lane highway (2 each direction) with AADTT of 4740, 50% of trucks in design direction and 95% of trucks in the design lane. Table 11 shows the pavement structure. Table 11 shows the level 1 analysis inputs for binder data. Table 12 shows all of the mix data including the second level 1 analysis input, the stiffness data, E* along with the binder content for each mix and the gradation of the mixes.

To compare the effects of the binder the gradation of each mix were kept consistent. MEPDG uses Fahrenheit instead of Celsius for temperature inputs.

Table 11. Pavement Structure

Layer Material	Thickness (inches)	Modulus (psi)
HMA DCM Layer	6.2	Level 1 Analysis
A-1-a Gravel	7.5	40000
A-1-b Subgrade	Semi-infinite	26500

Table 12. MEPDG Binder Data for the surface layer

	NS 70-22	
Temperature, °F	**G***	**Phase Angle**
147	5.285	76.89
158	3.553	79.37
169	1.823	81.85
	NS 76-22	
Temperature, °F	**G***	**Phase Angle**
158	5.431	66.69
169	3.747	69.14
180	2.065	71.59
	NS 82-22 Tank 73	
Temperature, °F	**G***	**Phase Angle**
158	4.087	66.34
169	2.283	67.8
180	1.307	69.71

Three binders were preliminarily selected: NuStar 70-22, 76-22 and 82-22. The binders were selected as each binder had a different high grade while all shared the same low grade and the varied J_{nr}. By selecting different binders with similar PG grades and different J_{nr} the interaction between J_{nr} and PG grade can be compared, in addition to J_{nr}'s interaction to DCM and MEPDG.

3.3.2 Flow Time

Flow time testing was conducted to determine the high temperature laboratory performance in regards to permanent rutting deformation and determine its relationship to the multiple stress creep recovery (MSCR) parameter J_{nr}. Ultimately the objective is to make a case for or against the use of J_{nr} as a valid test parameter for polymer modified binder.

During this uniaxial static creep test, the specimen is subjected to a constant compressive load of 600 KPa (30 psi) at a test temperature of 52.5^{o}C (130^{o}F). The test may be conducted with or without confining pressure (NCHRP 2008). For this study, the test was performed without confining pressure. While MSCR testing uses standard values during testing the temperature of 52.5^{o}C (130^{o}F) for flow time testing was selected to match conditions in New Jersey.

A total of ten different mixtures including conventional and unconventional mixtures were obtained for this study. The conventional mixtures consist of hot mix asphalt (HMA) with

different performance-graded (PG) binders as follows: PG 64-22, PG70-22, PG76-22, and PG82-22. The mixes with PG 70-22, PG 76-22 and PG82-22 binder were mixed in house and shared the same gradation. The plant-produced unconventional mixtures analyzed in this study were Warm Mix Asphalt (WMA) and Reclaimed Asphalt Pavement (RAP), Stone Matrix Asphalt (SMA), Binder Rich Intermediate Course (BRIC), and Bridge deck asphalt. WMA is the generic name of technologies that allow lower production temperatures, leading to several benefits, including: cutting fuel consumption and decreasing the production of greenhouse gases. According to the National Asphalt Pavement Association (NAPA), engineering and construction benefits include better compaction of pavements; the ability to pave at lower temperatures, extending the paving season; and the potential to be able to recycle at higher rates, as well. WMA is also comprised of 25% reclaimed asphalt pavement (RAP). RAP is the end product of old roads that have milled for replacement. SMA is a gap-graded HMA that is designed to maximize rutting resistance and durability by using a structural basis of stone-on-stone contact. Because the aggregates are all in contact, rutting resistance relies on aggregate properties rather than asphalt binder properties. Since aggregates do not deform as much as asphalt binder under load, this stone-on-stone contact greatly reduces rutting [55]. BRIC is specifically designed to help mitigate reflective cracking. Bridge deck asphalt employs a highly modified binder to allow for thin overlays on bridge decks. An additional dense graded aggregate sample was provided by the Rhode Island Department of Transportation. Table 13 summarizes the materials used in this project including mixtures characteristics, while Figure 43 is plot of the aggregate gradation for each mix.

Table 13. Mix properties

	Mixtures									
	HMA PG82-22	**HMA PG76-22**	**HMA PG70-22**	**HMA PG64-22A**	**HMA PG64-22B**	**WMA-RAP**	**SMA**	**BRIC**	**Dense Graded Aggregate**	**Bridge Deck**
PG grade	82-22	76-22	70-22	64-22	64-22	64-22	76-22	70-22	70-28	76-28
RAP (%)	0	0	0	0	0	35	0	0	0	0
AC Content (%)	5.41	5.02	4.83	5.69	6.42	5.25	4.87	8.4	6.42	7.5

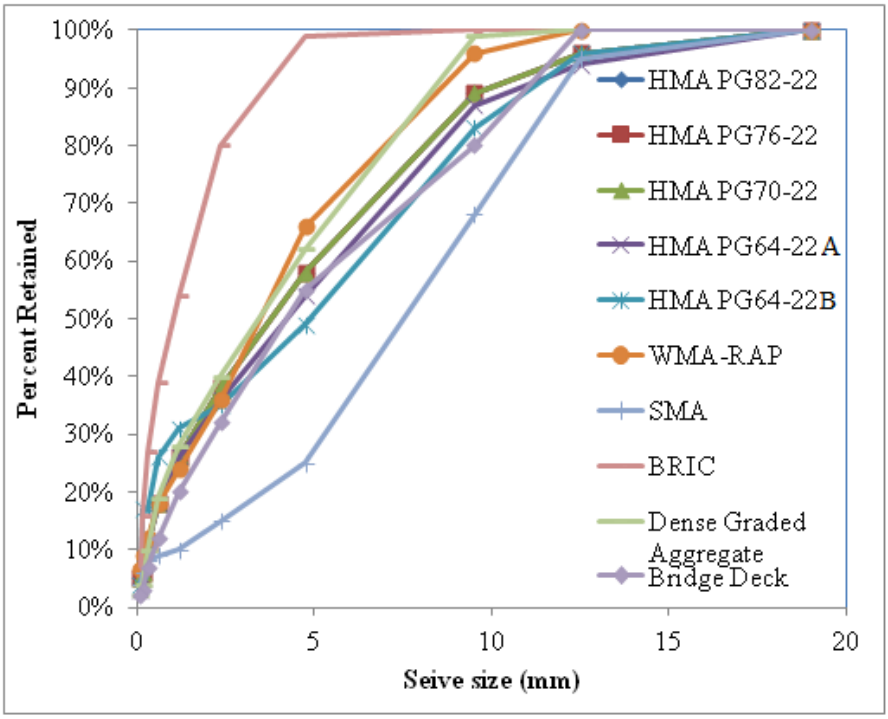

Figure 43. Aggregate gradation of each asphalt mix

Chapter 4 Results

The results of testing are presented within this chapter, raw tabular binder data is available in the Access database that is explained in chapter 6.

4.1 Mechanical Binder testing Results

The results of tradition Superpave testing conducted using the Dynamic Shear Rheometer (DSR) are presented in Figures 44, 45 and 46 for the following parameters: phase angle (δ), G* and G*/sin(δ), respectively. Table 9 list the binders with their identifiers, source and PG grade, mixes 11 through 21 were modified in-house.

The largest phase angle was recorded in binder 9, Valero 93, while the smallest phase angle was recorded by binder 5, Road Science 76-22. Of the in-house modified binders binder 12, Ns 64-22 with 1.5% Elvaloy and 0.8% PPA, recorded the smallest phase angle, while binder 15, NS 64-22, 1% K had the largest phase angle. Within the modified binders their phase angle does decrease as the binder becomes more modified, as is the case with binders 15 to 21, however it does not appear to be significant. Nebraska, Wisconsin, Michigan, Arizona, South Carolina, Utah, Ohio, Georgia, and Florida require the phase angle of the original DSR to be 75° or less.

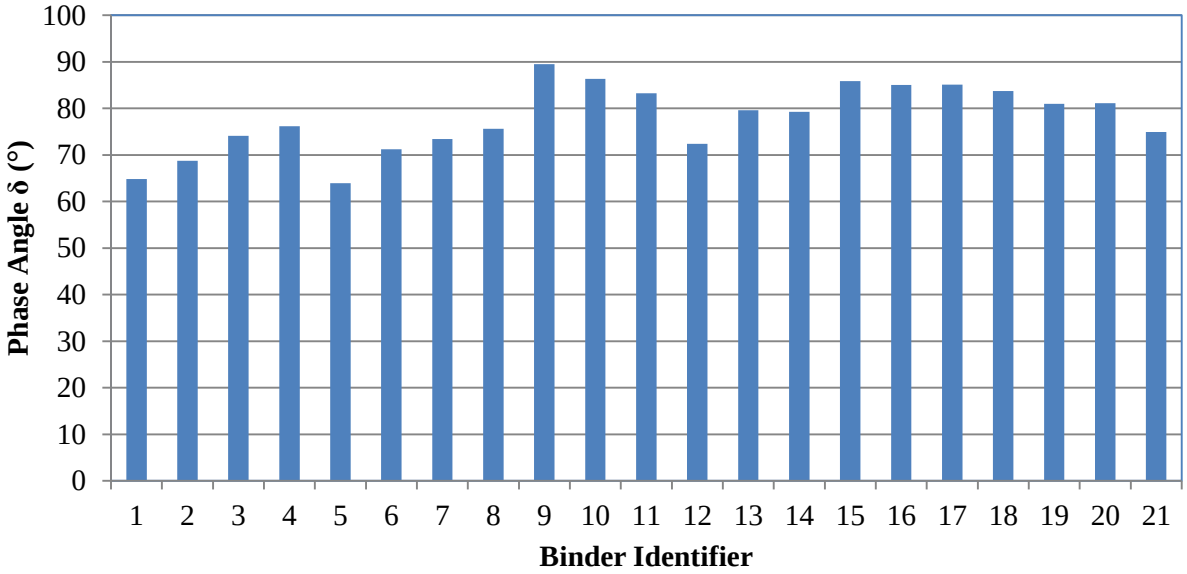

Figure 44. Phase Angle (δ) from ODSR at PG Grade

The largest complex modulus, G*, is binder 11, Valero 937 modified with 1.5% Kraton, however this appears to be a false result as it is outside the expected values. Binder 2, NS76-22, has the largest complex modulus amongst plant modified binders while binder 21, NS 64-22 with 7% Kraton, has the largest amongst in-house modified binders. The in-house modified binders have shown an increasing trend as modification increases, from binders 18 to 21.

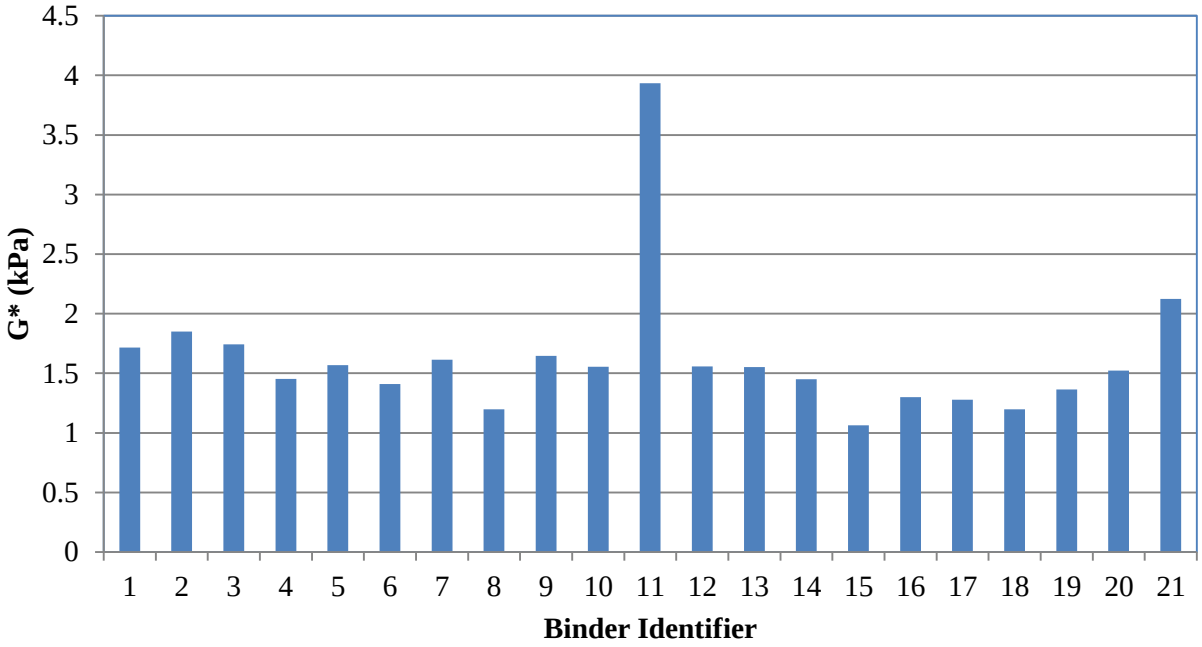

Figure 45. Complex Shear Modulus from ODSR at PG Grade (Please add axis label with units)

The G*/sin(δ) results of Figure 45 closely follows the results of Figure 42's G*, which is reasonable because the phase angles from Figure 43 were fairly close to each other for most of the binders, therefore, the number dividing G* (sin(δ)) was fairly close from sample to sample. Again Binder 11 appears to be a false result.

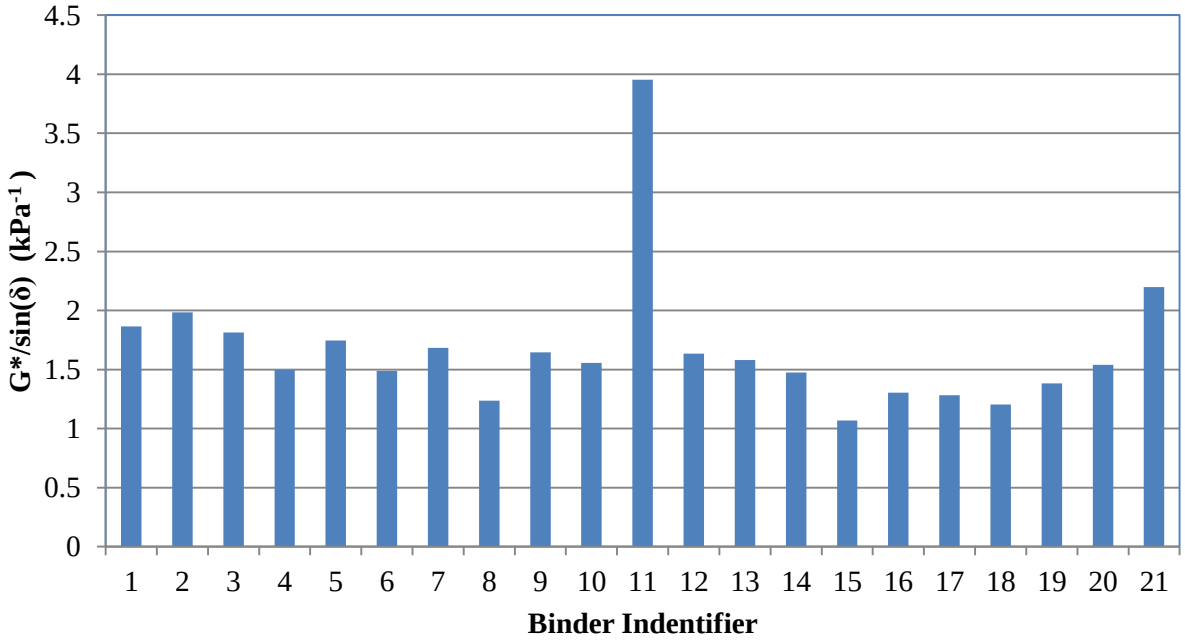

Figure 46. G*/sin(δ) of ODSR at High temperature PG Grade

The results of elastic recovery testing are presented in Figure 47 and are categorized according to their high performance. It is evident that as the performance grade increased, the elastic recovery also increased. However, at the higher performance grades, the binders did not varying greatly regardless of the base binder or polymer percentage. The addition of a polymer, at different percentages, had an effect on the elastic recovery of the binder. As seen with NS 64-22, with the addition of Kraton polymer from zero to 3%, there was a steady increase in elastic recovery.

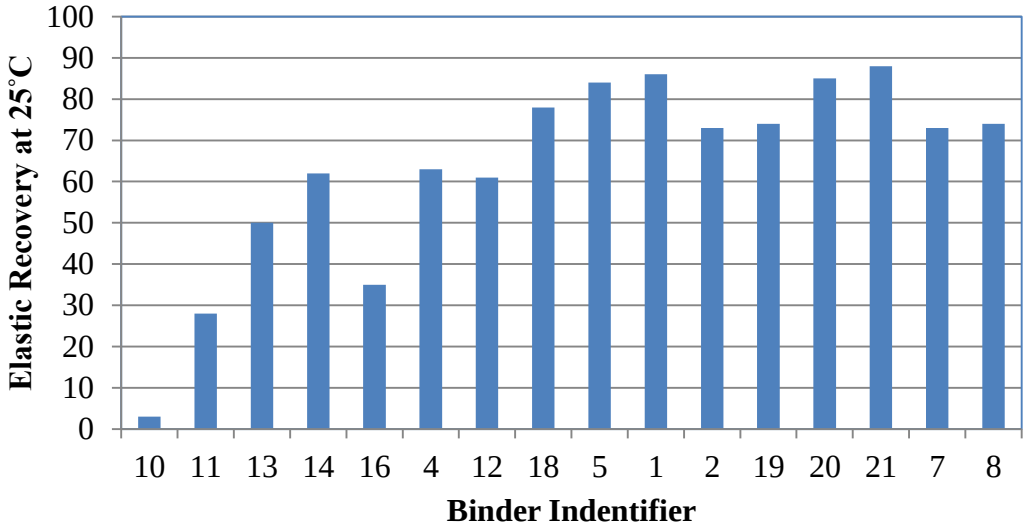

Figure 47. Elastic Recovery (%) at 25˚C with identifiers

The peak ratio and area under the load displacement curve as measured by the forced ductility test are presented in Figures 48 and 49. Once again, Figure 48 displayed the incremental effects of polymer modification were observed in the area under the load displacement curve. The area increased with the addition of higher polymer percentages. Similar to peak ratios, area under the load displacement curve did not show sensitivity to performance grade. The area does show sensitivity to changes in base binder with respect to a particular polymer. It appeared that Force Ductility may verify the presence of polymer. However, conclusive evidence has not been found to suggest that Force Ductility can: (1) be used to identify or quantify the specific polymers within mixes without the aid of test statistics data, or (2) exhibit sensitivity to performance grades.

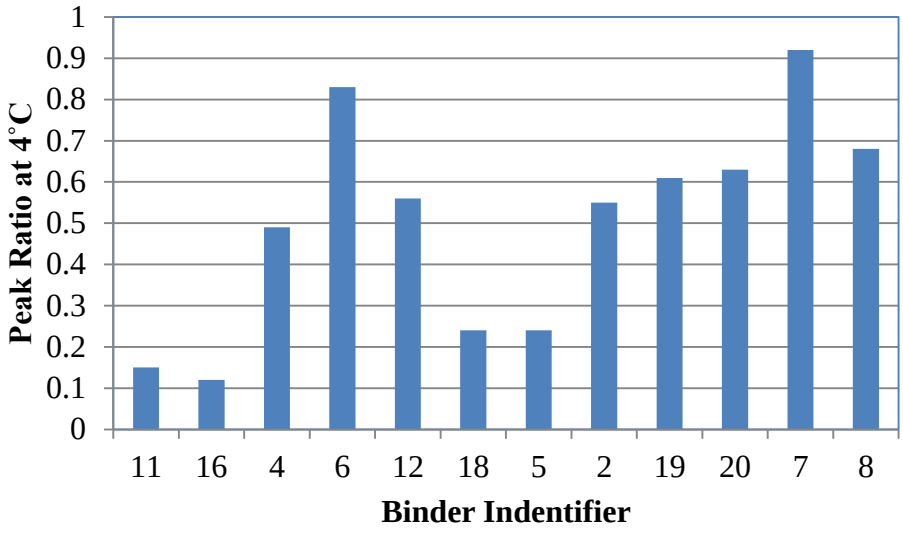

Figure 48. Peak Ratio at 4˚C

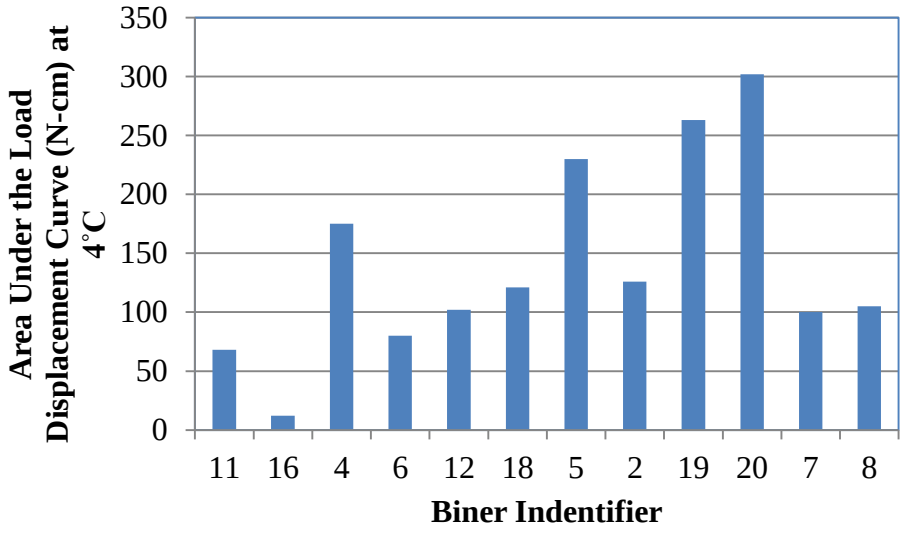

Figure 49. Forced Ductility Area Under the Load Displacement Curve 4˚C

The results of MSCR testing of J_{nr} and Recovery are presented in Figures 50 and 51 both test were conducted at 64˚C and at both stress 0.1 and 3.2 kPa. Table 9 should again be used to discern the identifiers used, please note that data is not available for some binders, however, they remain to hold their place.

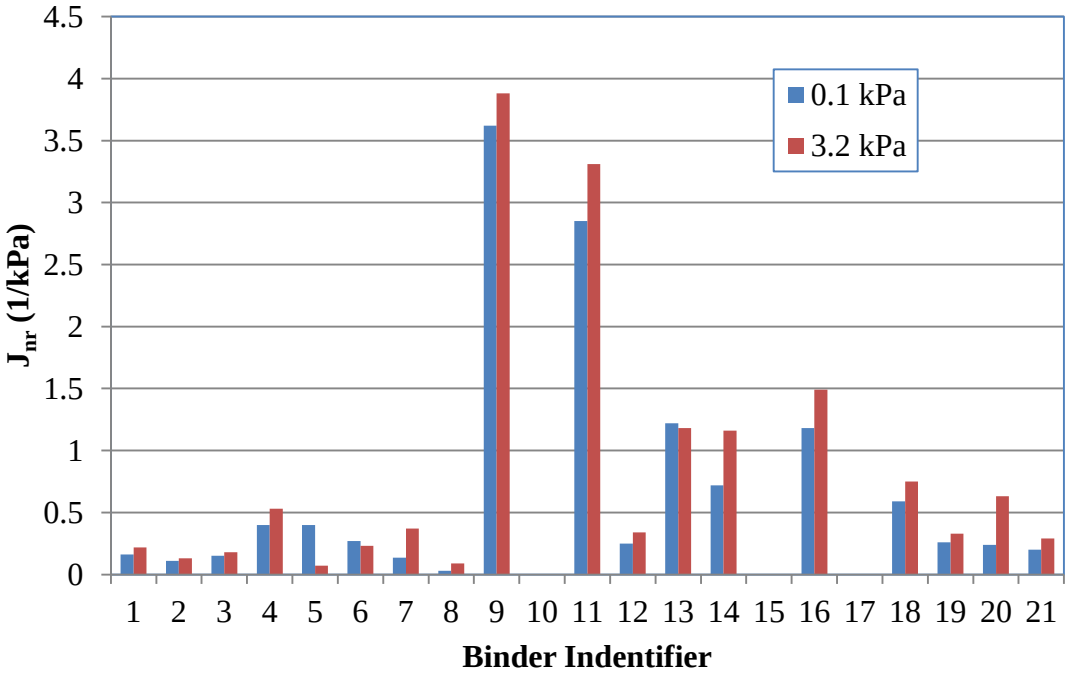

Figure 50. MSCR J_{nr} results at 64˚C

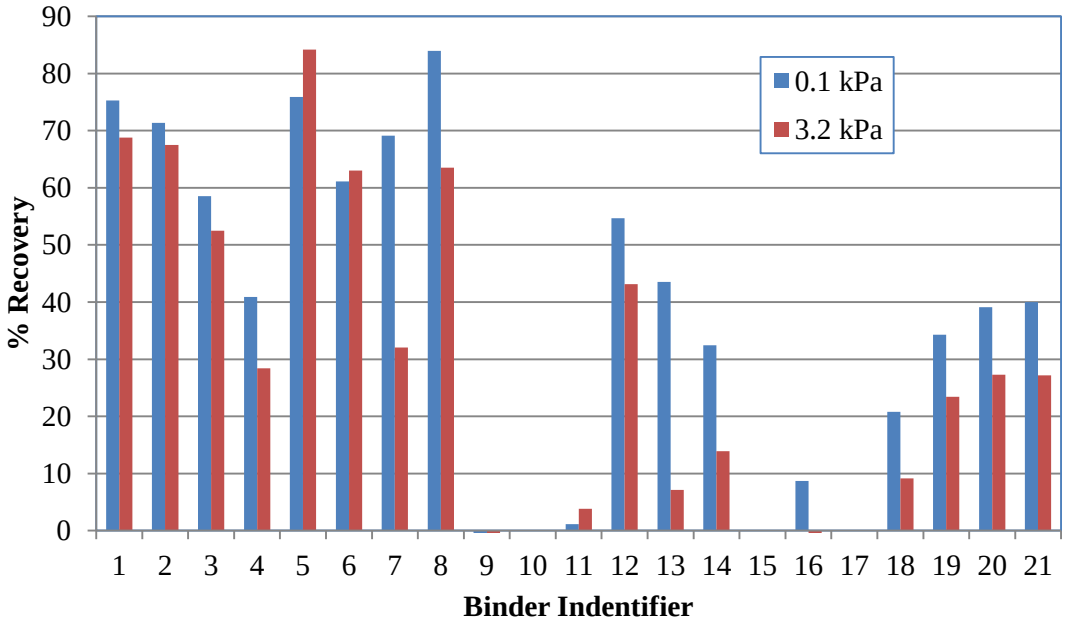

Figure 51. MSCR Recovery results at 64˚C

4.1.1. Impact of Modification on Binder Grade based on AASHTO MP-19.

The results have shown that PG 76-22, PG 76-28, PG 82-22, and PG 64-28, all could be graded as PG 64E. Extreme traffic indicates more than 30 million ESALs or standing traffic. The last binder PG 64-28 would be graded as PG 64E due to the modification to provide better low

temperature performance. Therefore, there could be a case, where a binder graded as PG 64E may not actually be able to withstand Extreme traffic and may perform poorly at high temperatures. One way to resolve this issue is by closely looking at the ODSR result of binders. For example, at 64˚C, if the G*/sin(δ) is below 2.0 kPa, it is unlikely to pass a higher grade and withstand heavy traffic.

4.2 Chemical Properties of Binders

The SARA test results of nine binders are shown in Table 14. The results include a NuStar 64-22 binder base binder and eight modified variation of it and one modified Valero 64-22.

Table 14. SARA Analysis Testing Results

Binder	Modifier	SARA Analysis (wt.%)			
		Saturates	Asphaltenes	Resins	Aromatics
PG 64-22 (NS)	Base binder	26.39	26.39	9.72	30.00
PG 64-22 (NS)	1.5% Elvaloy	4.17	72.92	4.17	18.75
PG 64-22 (NS)	2.5% Elvaloy	9.72	43.06	13.89	25.00
PG 64-22 (NS)	1.5% Elvaloy+0.8%PPA	28.00	36.00	16.00	16.00
PG 64-22 (Valero)	1.5% Kraton	21.33	41.33	9.33	12.00
PG 64-22 (NS)	1.5% Kraton	18.67	42.67	10.67	20.00
PG 64-22 (NS)	3.0 % Kraton	20.83	37.50	16.67	25.00
PG 64-22 (NS)	4.5% Kraton	8.33	58.33	8.33	22.92
PG 64-22 (NS)	5 5 Kraton	4.86	82.78	11.11	31.25

4.3 Mechanical Properties of Mix

4.3.1 DCM

The results of the three binders preliminarily selected for performance testing by means of Dynamic Complex Modulus testing: NuStar 70-22, 76-22 and 82-22, are presented in table 15.

4.3.2 Flow time

Figure 51 illustrates the results of the flow time testing conducted, with each sample reaching the primary, secondary and tertiary phases with the exception of the SMA, Bridge Deck and the PG 64-22A. The SMA and PG 64-22A samples reached each phase in testing but is not entirely shown in Figure 52 because it did not fit the scale of the graph, while the Bridge Deck sample did not reach the tertiary phase after 10,000 seconds. In addition to a high flow time, a shallow slope during the secondary region is desired; the Bridge Deck mix had the lowest rate of increase during the secondary phase.

Table 15. Dynamic Complex Modulus testing results

Binder	Binder Content, %	Dynamic Complex Modulus, E*, ksi					Gradation	
			Frequencies				Sieve Size	CPP, %
		Temp, °F	10 Hz	5 Hz	1 Hz	0.5 Hz		
NS 70-22	4.65	10	5000	4048	4071	4101	3/4"	100
		39.5	2444	2263	1831	1653	1/2"	92.33
		68	1022	860	557	451	3/8"	88.53
		104	232	182	93	68	No. 4	58.72
		130	97	75	30	23	No. 8	40.01
NS 76-22	5.00	10	4996	4226	4208	3214	No. 16	30.2
		39.5	2418	2255	1885	1719	No. 30	20.71
		68	1141	992	681	557	No. 50	13.62
		104	268	211	115	869	No. 100	8.97
		130	66	58	34	22	No. 200	6.86
NS 82-22 Tank 73	5.20	10	3010	2902	2613	2472	Pan	4.74
		39.5	2221	2035	1615	1444		
		68	1098	928	615	506		
		104	218	169	89	68		
		130	51	39	21	17		

4.3.2 Flow time

Figure 51 illustrates the results of the flow time testing conducted, with each sample reaching the primary, secondary and tertiary phases with the exception of the SMA, Bridge Deck and the PG 64-22A. The SMA and PG 64-22A samples reached each phase in testing but is not entirely shown in Figure 52 because it did not fit the scale of the graph, while the Bridge Deck sample did not reach the tertiary phase after 10,000 seconds. In addition to a high flow time, a shallow slope during the secondary region is desired; the Bridge Deck mix had the lowest rate of increase during the secondary phase.

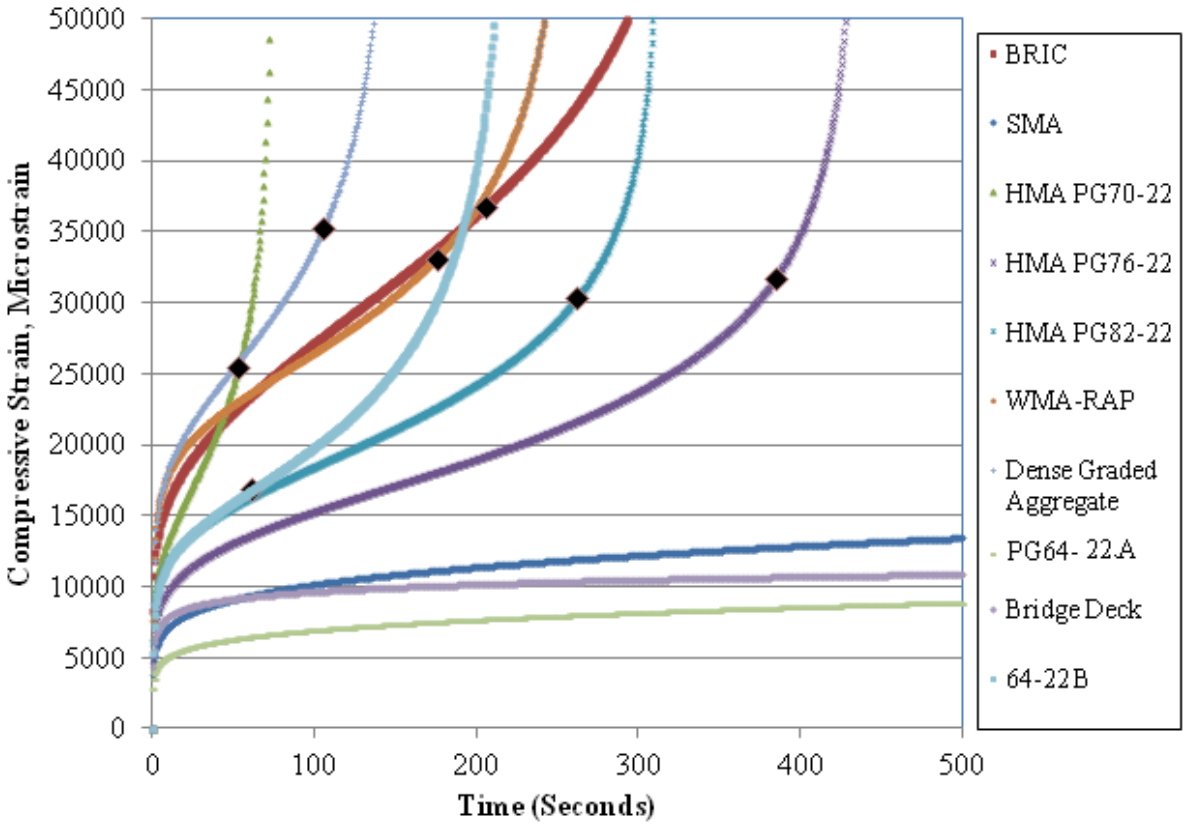

Figure 52. Flow Time Results

Table 15 shows the binder testing results of each binder as well as the flow time results for each binder. Each binder has three sets of data for flow time testing: the time in seconds and micro strains between: the primary to secondary, secondary to tertiary (flow time) and the differences between the two. The time and microstrains accumulated from the primary to secondary region was considered as this phase is typically a result of a densification of the aggregate matrix. While the flow time is the time at which the mixture transitions from the secondary to tertiary, micro cracks become macro cracks and ultimately leads to the failure of the sample. When the flow time is subtracted the flow time by the transition point from primary to secondary, the secondary phase is captured. By capturing the secondary phase, the response of the binder during testing is captured. The highlighted results in Table 15 are test results from extracted and recovered binder and are, therefore, aged samples compared to the remaining samples.

The Bridge Deck mix did not reach the tertiary phase and thus a flow time was not reached, this was after 10,000 seconds of testing so it is safe to say that the mix would have the highest flow time and is rut resistant. As shown in both Figure 52 and Table 15, the SMA mix registered the highest flow time value for reaching the tertiary flow stage as compared to the remaining mixtures. The lowest flow time value was reached by the HMA PG70-22 mixture. Results from flow time testing indicate that among all the mixtures tested SMA, Bridge Deck and 64-22A are the most rut resistant. SMA is designed to rely on aggregate to aggregate interlock making it more resist rutting. Bridge Deck mixes are highly modified and should be expected to perform well in rutting conditions.

Table 16. Flow time and Corresponding Binder Results

	MSCR results	Flow time results							Binder results	
Mix	J_{nr}	Primary to secondary (I)		Secondary to Tertiary (II)		(II)- (I)		Slope (IV)/(II)	G*/sin (δ) (KPa) @64C	G*/sin (δ) (KPa) @70C
		Time (sec.)	Micro Strain	Flow time (sec.)	Micro Strain	Time (sec.) (III)	Micro Strain (IV)			
WMA RAP	1.68	83.5	25379	175.5	33119	92	7740	84.13	14.46	8.026
PG 76-22 SMA PG	1.26	892	15136	4001 1	39661	39119	24525	0.626	1.258	0.5829
PG 70-22	1.09	23	16671	53	25424	30	8753	291.76	1.793	0.9702
70-28 BRIC	0.58	121	29068	206	36808	85	7740	91.05	1.281	0.6703
PG 76-22	0.18	170.5	17913	384.5	31721	214	13808	64.52	1.812	0.9746
Dense Graded Aggregate	0.16	50	25540	105.5	35243	55.5	9703	174.82	5.362	2.533
PG 82-22	0.13	110.5	19055	262	30302	151.5	11247	74.24	1.385	0.7616
Bridge Deck	0.35	68.5	9382	-	-	-	-	-		
Rat 71 PG 64-22A	3.425	23	8558	2064	13686	2041	5128	2.51	1.6585	0.759
PG 64-22B	3.11	15.5	12612	61	16818	45.5	4206	92.43	3.514	1.696
Note: Extraction and recovered binder										

Chapter 5 Analysis

5.1 Binder Correlations

New Jersey, along with several other states, specifies Elastic Recovery (ER) to be greater than 60%. Figure 53 is a plot of ER and J_{nr} with the 60% recovery criteria, the ER decreases as Jnr increases.

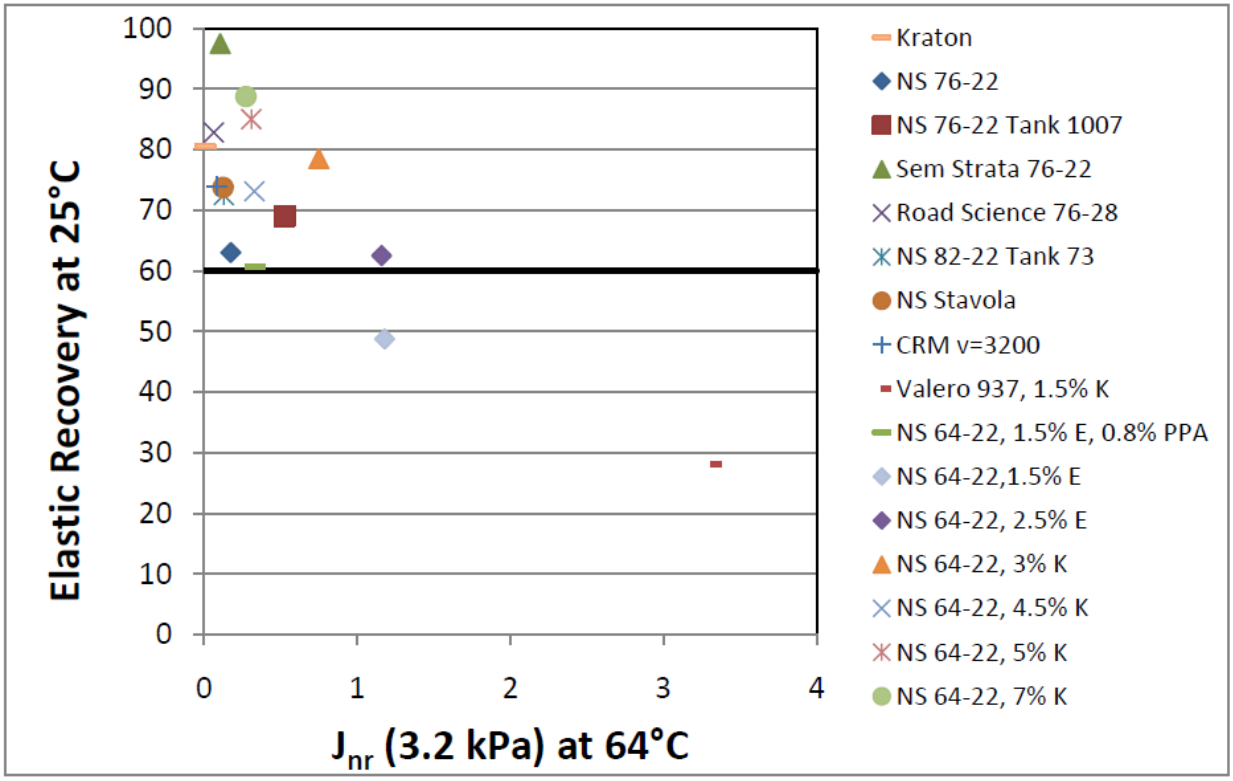

Figure 53. Elastic Recovery at 25°C vs. J_{nr} (3.2 kPa) at 64°C

According to New Jerseys ER specification, only two binders failed Valero 937 with 1.5% Kraton and NS 64 with 1.5% Elvaloy. Although the NS 64-22 with 1.5% Elvaloy does not meet specification, the addition of 0.8% PPA improved the recovery enough to be greater than 60%. Valero 937 with 1.5% Kraton is an extreme outlier, proving that polymers can react differently with different base binders. For percentage recovery (%Re) versus Jnr, there is no longer a 60% standard. However, binders must fall above the line with equation, $\%Re=29.371*J_{nr}-0.2633$, to be considered up to specification as shown in Figure 54.

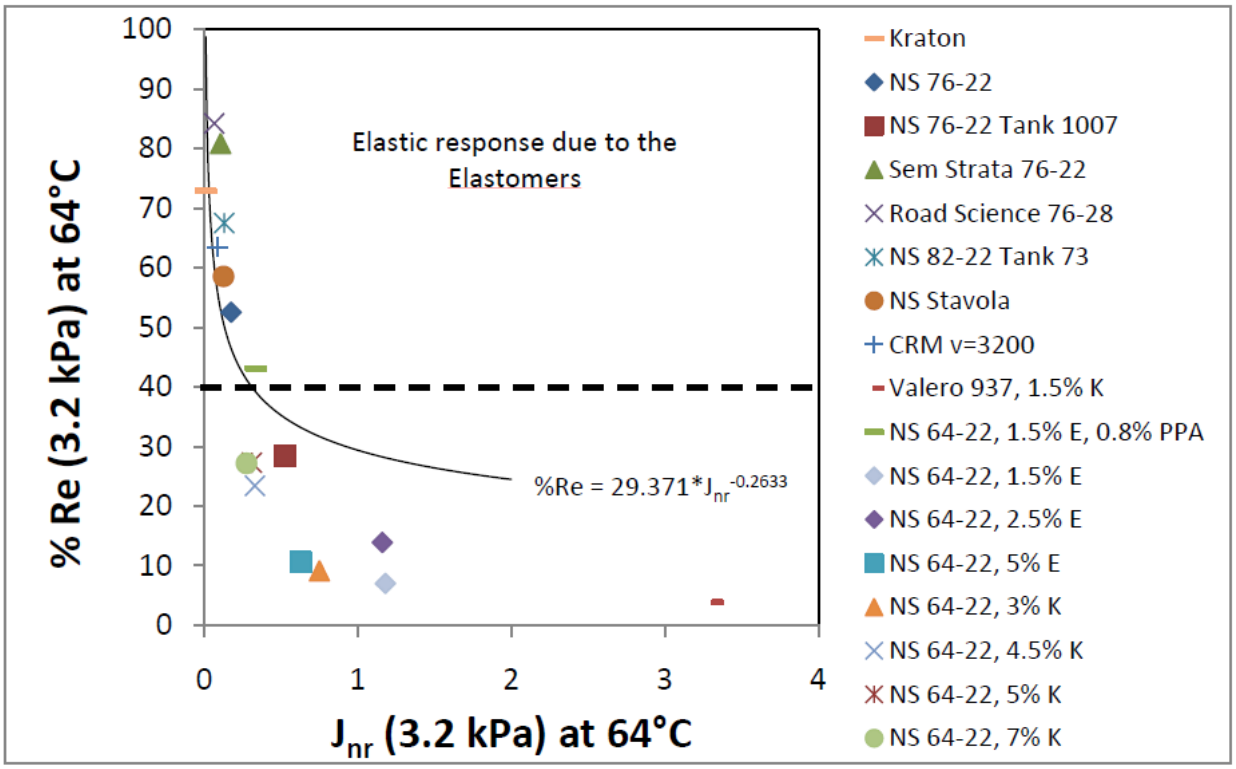

Figure 54. Percentage Recovery (3.2 kPa) at 64°C vs. J_{nr} (3.2 kPa) at 6°4C

The same binders that did not meet the ER specification, (NS 64-22 with 1.5% Kraton and Valero 937 with 1.5% Kraton), are not meeting the standard set for percent recovery. Once again, the Valero 937 with 1.5% Kraton acted as an extreme outlier in comparison to the rest of the binders. The %Re specification accepted much fewer binders. Of the 9 binders that it did not accept, 7 of them were mixed in house with various percentages of Elvaloy and Kraton using a NuStar base binder. Since the binders were mixed in house, additional equipment would be necessary to determine when the binder is completely networked, hence completing the mixing process. For the binders that are above the curve, it shows that the elastic response is due to the elastomers. Of the binders that showed elastic response due to elastomers, all of them fell above the dotted line in Figure 54 at 40% recovery from MSCR.

5.1.1 Temperature Dependency

In order to test the temperature dependency of percent recovery (%Re), four binders were tested at the high temperatures of 64, 70, and 76°C. The four binders tested were Kraton NS BD, NS 76-22, NS 76-22 Tank 1007, and NS 64-22 with 1.5% Elvaloy. As shown in Figure 55, NS 64-22 with 1.5% Elvaloy starts with a very low recovery when tested at 64°C.

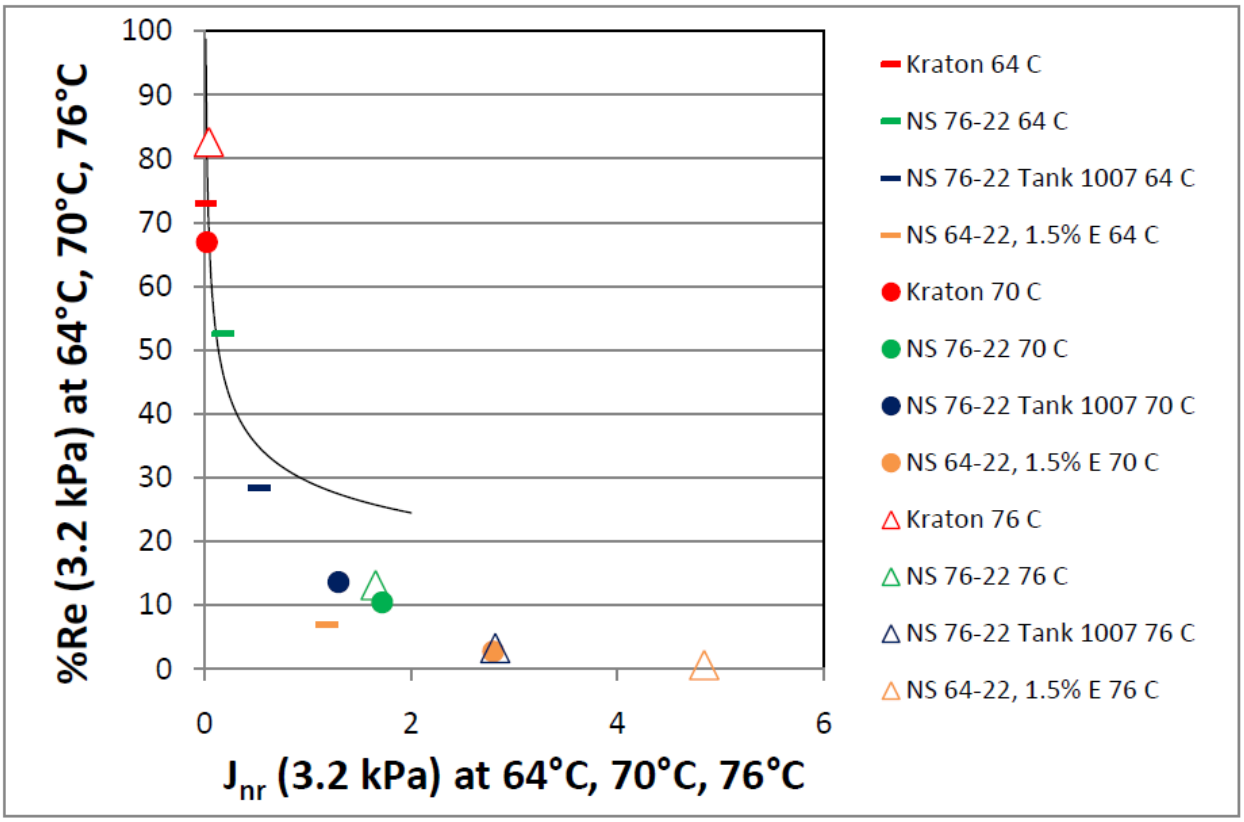

Figure 55. Percentage Recovery (3.2 kPa) at 64°C vs. J_{nr} (3.2 kPa) conducted at 64°C, 70°C and 76°C

When the temperature was raised to 70 and 76°C, the %Re decreased as the Jnr dramatically increased. The same trend is seen with the NS 76-22 Tank 1007. There was a high percentage recovery at the low temperature, and Jnr increase as the percent recovery increased decreased. The NS 76-22 and Kraton NS BD started with a much higher %Re for the 64°C testing temperature. The NS 76-22 once again followed the aforementioned trend when tested at 64 and 70°C; however at 76°C, Jnr decreased, and %Re increased. This is seen more profoundly with the Kraton NS BD. When the testing temperature increased from 70 to 76°C, the Jnr remained relatively constant, and the %Re increased dramatically. Therefore, there does seem to be a temperature dependency for binders that exhibit high %Re values. Binders, however, that have low %Re at the 64°C temperature, will have decreasing recoveries in relation to an increasing J_{nr}.

5.1.2 Correlation between properties measured on Original DSR

Many states including Georgia, Florida, and Arizona require phase angles to be 75° or less to ensure elasticity in binders. Most of the binders in Figure 56 did not meet this requirement. The binders that had phase angles less than 75° included 2 received binders NS 76-22, NS 82-22 Tank 73, and 2 In-House mixes NS 64-22 with 1.5% Elvaloy and 0.8% PPA, and NS 64-22 with 7% Kraton. It is interesting to observe that NS 64-22 with 2.5% Elvaloy had greater phase angle and Jnr values than NS 64-22 with 1.5% Elvaloy and 0.8% PPA. Although there is 1% more Elvaloy and 0.2% more net polymer in the NS 64-22 with 2.5% Elvaloy mix, this was not shown through performance testing. This seems to support indications that certain polymers behave differently with base binders.

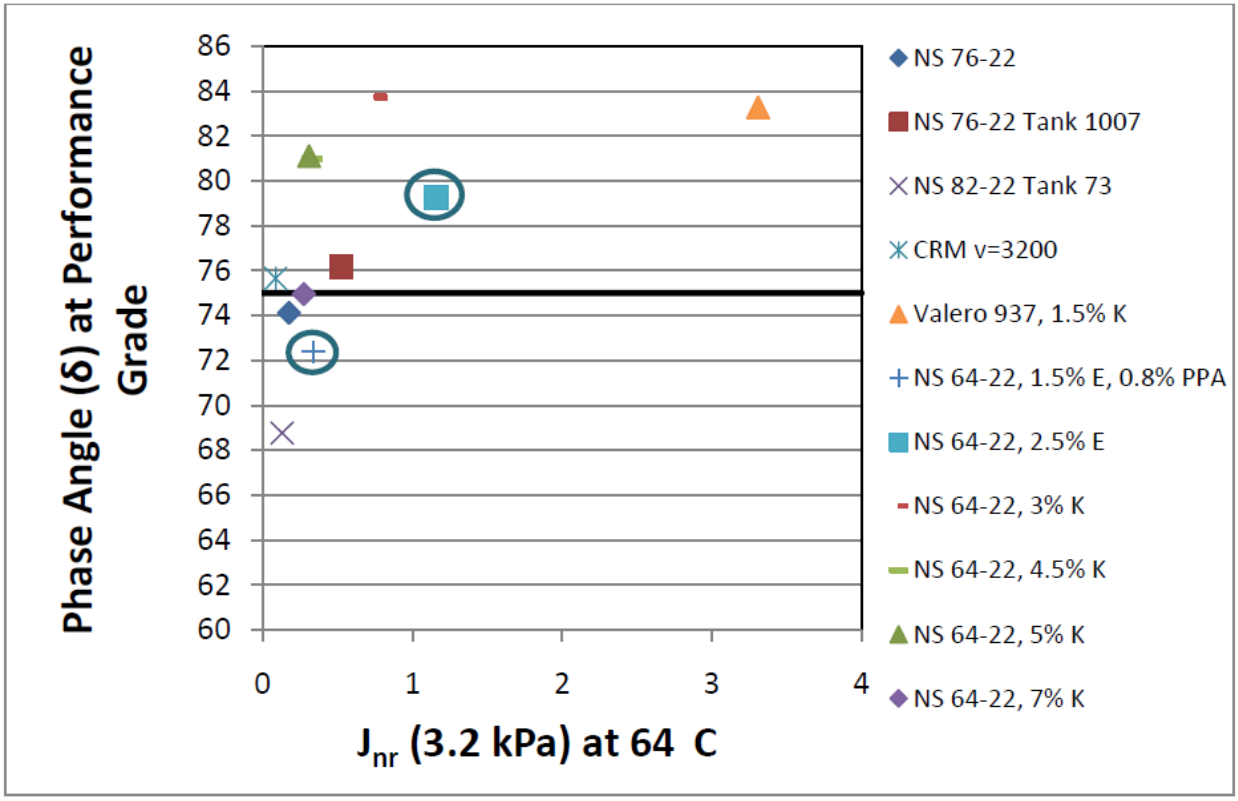

Figure 56. Phase Angle from ODSR at PG grade vs. J_{nr} (3.2 kPa) at 64°C

New Jersey requires binders to exhibit at least 60% recovery from ER testing at 25°C. To compare this specification to the phase angle specification used in other states, boundary lines for both are shown in Figure 57. It appears that most binders, both received and In-House mixes, had recoveries greater than 60%. However, of the 13 binders with recoveries greater than 60%, 6 binders had phase angles greater than 75°, seven binders had phase angles less than 75°. Therefore, Figure 57 suggests that the phase angle specification is stricter than the ER specification.

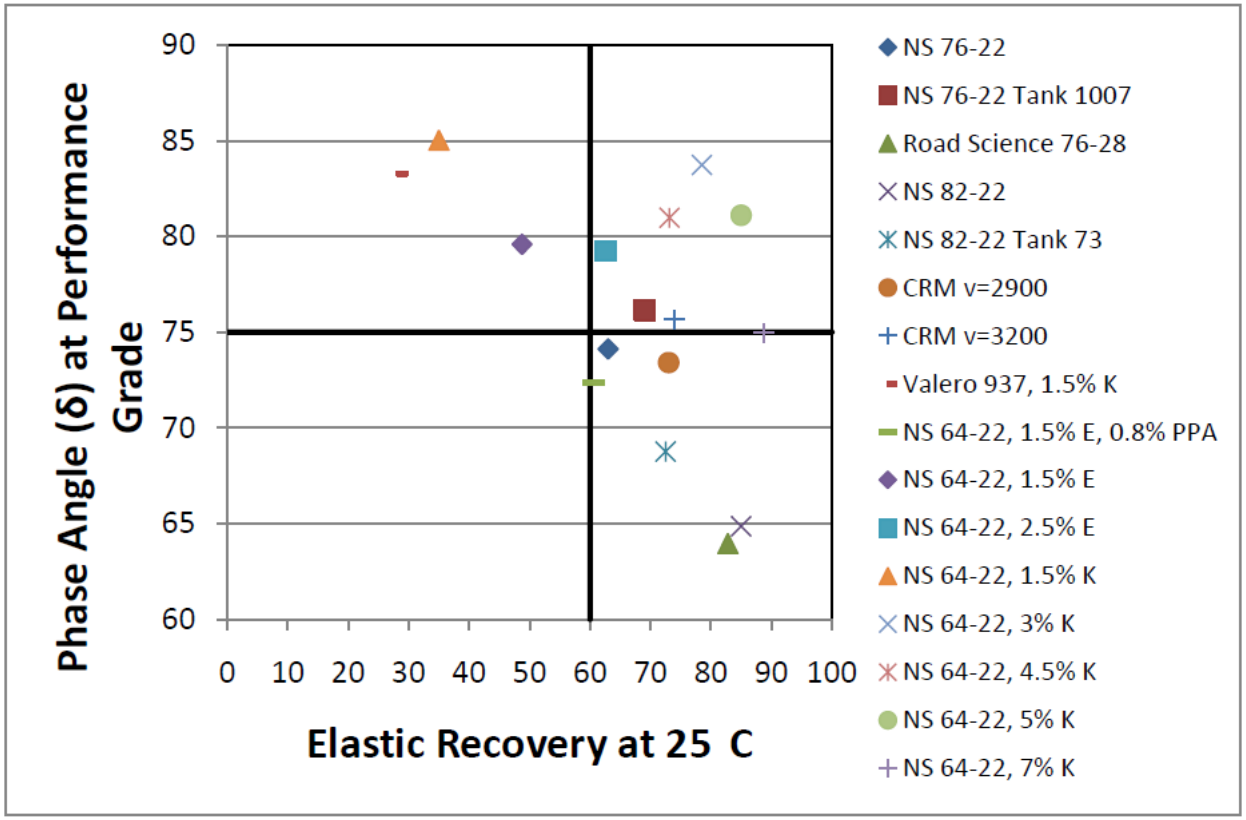

Figure 57. Phase angle from ODSR at PG grade vs. Elastic Recovery at 25°C

Phase angles from DSR run on original binders at PG temperature were compared to %Re from MSCR. MSCR testing characterizes binders in the nonlinear visco-elastic region. Therefore, in Figure 58, the phase angle specification was correlated to the effects of polymers within the binder. As mentioned previously, results showed that when binders have 40% or greater recovery from MSCR the elastic response is most likely due to the presence of elastomers. From Figure 57, with the exception of CRM v=3200, %Re of 40% appears consistent with the phase angle specification. CRM v=3200 may have behaved as an outlier in this comparison as it is often more difficult to test these types of binder. More binder testing is needed to converge on a specific level of recovery from MSCR to agree with the phase angle specification. If consistency from MSCR with ER and phase angle is achieved, it may be possible to retrieve the necessary data from MSCR alone.

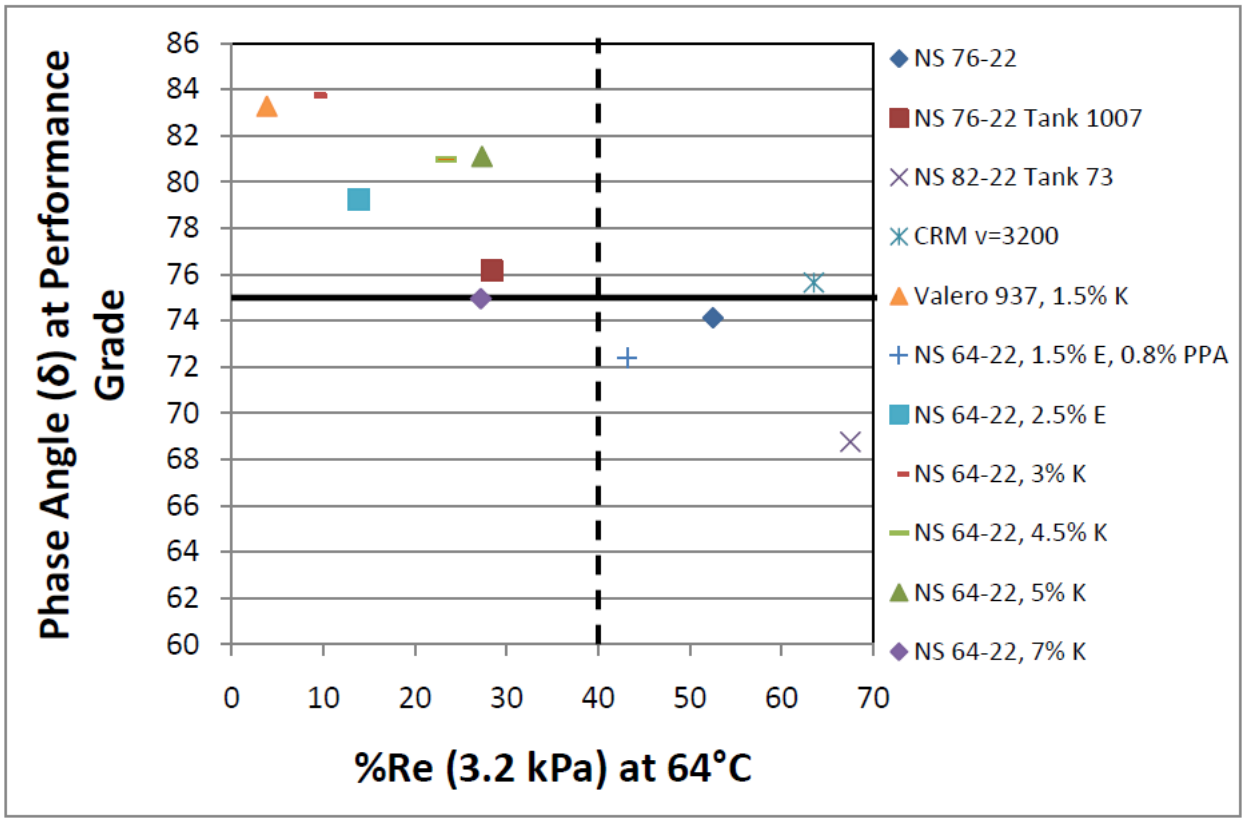

Figure 58. Phase Angle (δ) from ODSR at PG grade vs. Percentage Recovery (3.2 kPa) at 64°C

The binders circled in Figure 59 were In-House mixes of NS 64-22 with Kraton. The PG high temperate of those binders has been noted on the graph. As the PG high temperatures of the binders increased from 70°C, to 76°C, to 82°C, significant changes in Jnr were observed. It was also observed that the PG high temperatures did not increase in grade level from 4.5% K to 7%K. This showed that the effects of polymer additions on Jnr were converging to a plateau. Although the 4.5%, 5%, and 7% mixes did not decrease significantly with Jnr, the G*/sin(δ) values increased considerably. Binders appeared to be stiffer, having high G*/sin(δ), at low strains. A similar effect was not observed in J_{nr}. From these results, it is evident that at high strains performance properties of binders become strain dependent.

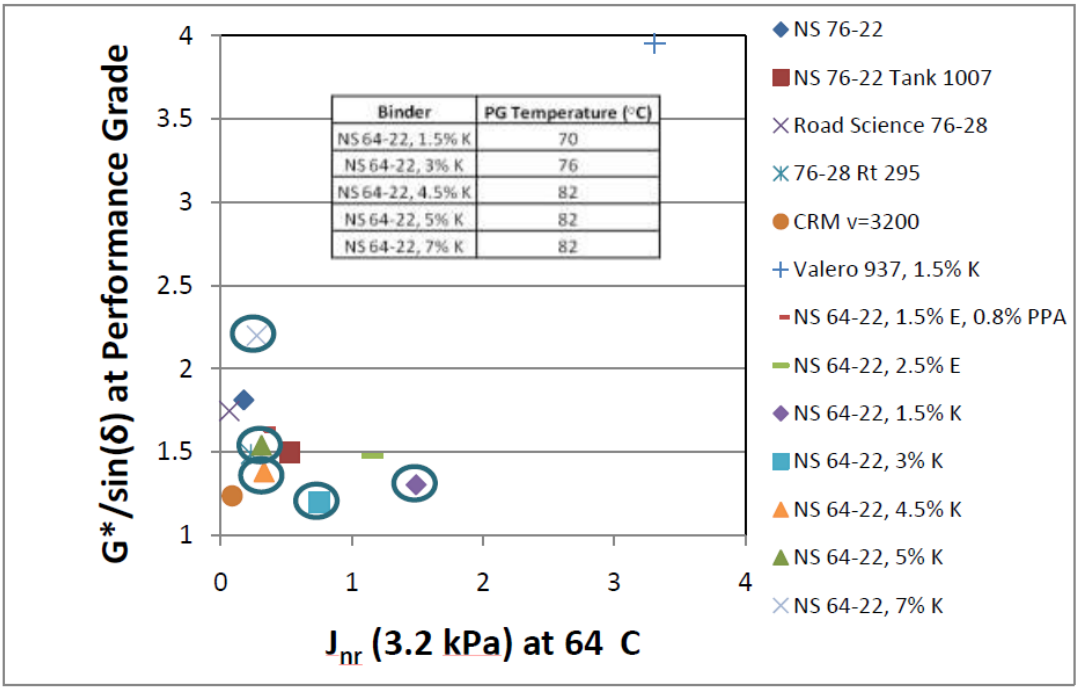

Figure 59. G*/sin(δ) from ODSR at PG grade vs. J_{nr} (3.2 kPa) at 64°C

5.1.3 Force Ductility

Peak ratios displayed a linear trend against phase angles at 64°C, Figure 60. The linear trend would make sense if keeping in mind that with greater modification, peak ratios increased and phase angles decreased. It appeared that phase angles would steadily reduce with greater response from the second Force Ductility peak. In turn, that would indicate greater networking at high peak ratios. However, 64°C is not the specified temperature to check phase angles. As the phase angle temperature was raised to PG temperature in Figure 61, the phase angle values increased, but the linearity was not preserved. Due to polymer activations at different temperatures, peak ratios do not seem to make any strong indications towards polymer networking. From Figures 60 and 61, Force Ductility did not provide any correlation to performance at high temperatures.

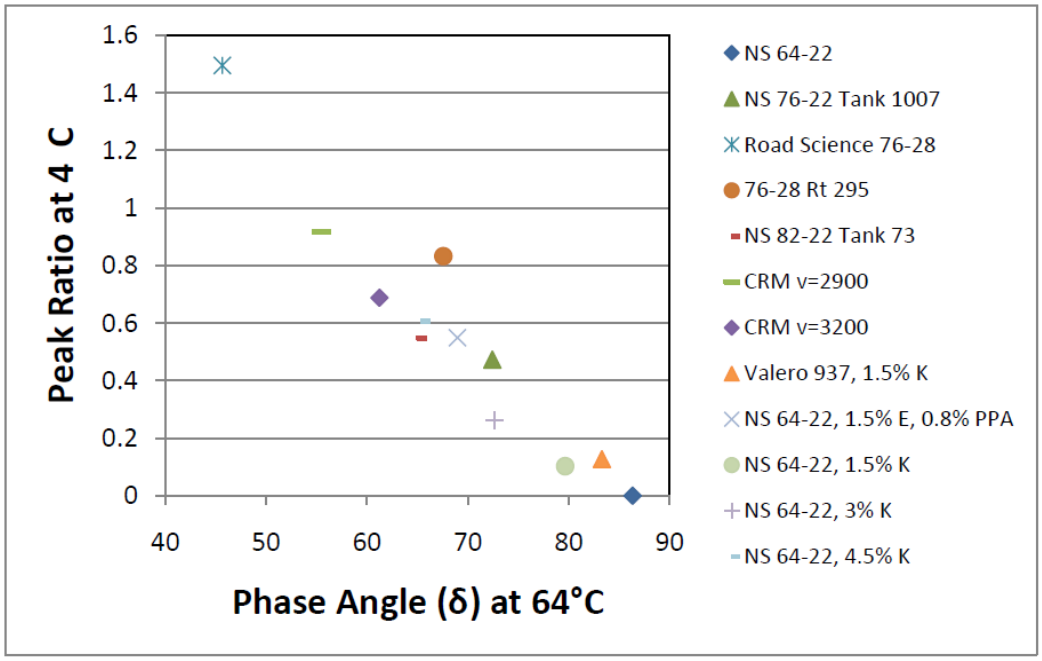

Figure 60. Peak Ratio at 4°C vs. Phase Angle (δ) from ODSR at 64°C

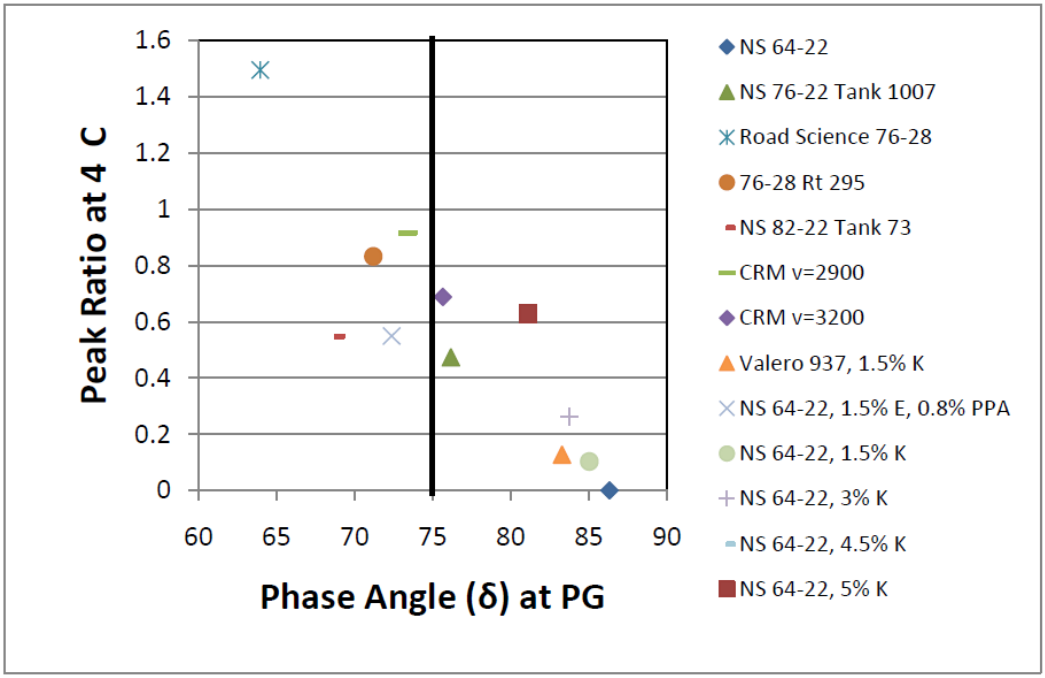

Figure 61. Peak Ratio at 4°C vs. Phase Angle (δ) from ODSR at PG grade

5.2 MSCR Curve Analysis

The authors observed that the linear viscoelastic parameters were statistically similar between the three cycles. Then the non-linear viscoelastic parameters G1, G2, and G3, and PS component were determined using cycles 1, 6, and 10 at a 3.2 kPa stress level. The J_{nr} at 10 sec was determined using the following equation for the 1st, 6th, and 10th cycle and considering an average for all 10 cycles for 3.2 kPa applied stress. Tables 16 and 17 show the results for six industrial binders (IN_*x*) and seven in-house (RO_*x*) binders. The linear viscoelastic parameters

(B, C, D, and E), non-viscoelastic parameters (G1, G2, and G3), and PS are averaged for the two replicates. Due to the space constraint results of non-viscoelastic parameters for cycle 1 and 10 only are shown in Tables 16 and 17.

Table 17. Linear viscoelastic, non-linear viscoelastic and PS for Industry binders

Parameters	**IN_1**	**IN_2**	**IN_3**	**IN_4**	**IN_5**	**IN_6**
Cycle 6 (Applied Stress 0.1 kPa)						
B	0.33	0.29	0.16	0.21	0.37	0.18
C	0.71	0.91	0.50	0.33	0.37	0.80
D	5.11	18.33	1.38	1.12	1.86	3.84
E	12.83	35.88	8.73	7.10	7.77	17.56
Cycle 1 (Applied Stress 3.2 kPa)						
G1	1.07	1.11	1.185	1.12	1.11	1.07
G2	0.39	0.44	0.575	0.39	0.31	0.35
G3	0.69	0.69	0.69	0.76	0.8	0.73
PS, %	25.09	18.69	11.29	10.22	32.84	13.19
$J_{nr@cycle1}$ (kPa^{-1})	0.30	0.52	0.13	0.09	0.13	0.18
Cycle 10 (Applied Stress 3.2 kPa)						
G1	1.06	1.13	1.25	1.12	1.11	1.05
G2	0.22	0.49	0.58	0.07	0.08	0.18
G3	0.87	0.67	0.76	1.05	1.04	0.89
PS, %	23.01	20.04	10.93	9.08	30.40	10.99
$J_{nr@cycle10}$ (kPa^{-1})	0.26	0.54	0.13	0.06	0.10	0.16
Average non-recoverable compliance for all cycles as reported in AASHTO TP70-08						
J_{nr} (kPa^{-1})	0.26	0.525	0.125	0.065	0.105	0.16

Table 18. Linear viscoelastic, non-linear viscoelastic and PS for in-house mixed binders

Parameters	RO_1	RO_2	RO_3	RO_4	RO_5	RO_6	RO_7
Cycle 6 (Applied Creep Stress 0.1 kPa)							
B	0.25	0.16	0.19	0.38	0.34	0.30	0.21
C	0.92	0.73	1.22	0.95	0.89	0.77	1.58
D	921.74	56.92	24.71	55.68	38.99	8.34	1687.96
E	784.80	86.46	83.41	60.14	44.04	22.57	577.36
Cycle 1 (Applied Creep Stress 3.2 kPa)							
G1	4.56	1.14	1.10	1.21	1.24	1.08	1.09
G2	6.14	0.78	0.58	0.78	0.80	0.42	0.93
G3	0.23	0.40	0.53	0.47	0.47	0.70	0.17
PS, %	0.82	8.92	1.25	12.63	21.42	19.33	2.98
J_{nr_cycle1} (kPa^{-1})	1.46	0.76	0.34	1.15	1.09	0.34	3.24
Cycle 10 (Applied Creep Stress 3.2 kPa)							
G1	1.19	1.13	1.08	1.24	1.33	1.11	1.12
G2	0.97	0.65	0.48	0.86	0.92	0.33	0.90
G3	0.24	0.51	0.61	0.42	0.44	0.81	0.23
PS, %	4.55	12.55	9.95	13.32	25.45	19.24	1.49
$J_{nr\_cycle10}$ (kPa^{-1})	1.52	0.75	0.33	1.19	1.18	0.34	3.32
Average non-recoverable compliance for all cycles as reported in AASHTO TP-70							
J_{nr} (kPa^{-1})	1.49	0.75	0.33	1.18	1.16	0.34	3.31

The calculated J_{nr}_cycle for 3.2 kPa is determined using linear and non-linear viscoelastic parameters. The percentage difference between measured and calculated was within 15 percent for creep and within 10 percent for recovery curve of all the industry and in-house binders. The first data point of creep curve is zeroed for all the binders.

Figures 62 to 64 show the effect of non-viscoelastic parameters G_1, G_2, and G_3 on the recovery curve. Increases in the values of G_1 shift the first part of the curve vertically. Parameters G_2 shift the second part of the curve vertically and G_3 controls the slope of the second part of the recovery curve. Statistical analysis is carried out to determine the effect of non-recoverable compliance on non-linear viscoelastic parameters and PS.

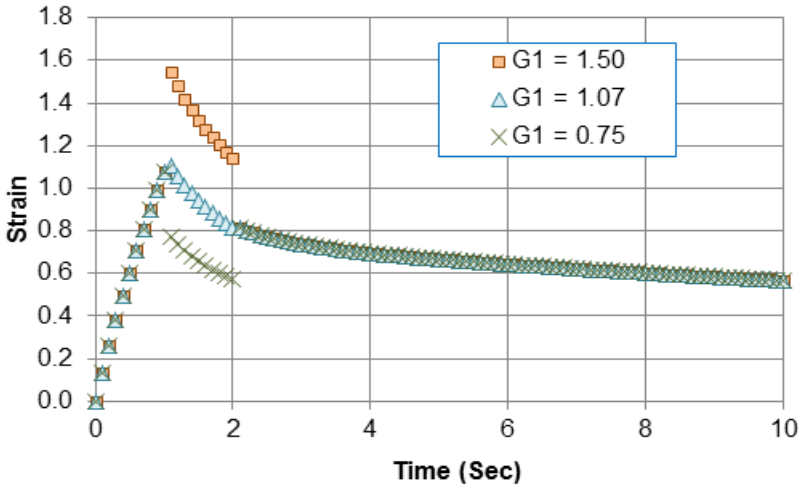

Figure 62. Effect of non-linear viscoelastic parameter G_1.

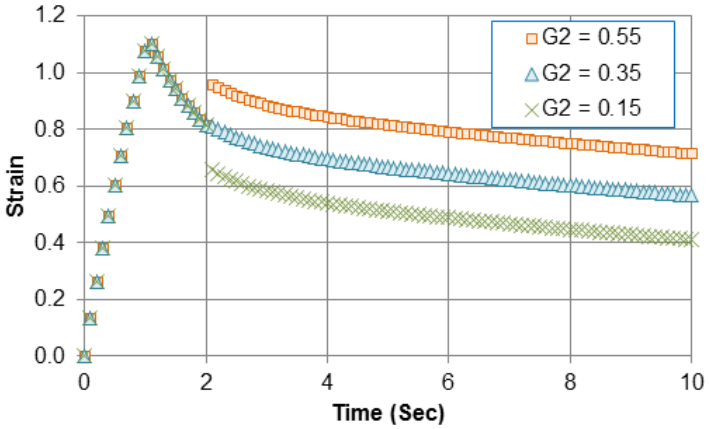

Figure 63. Effect of non-linear viscoelastic parameter G_2

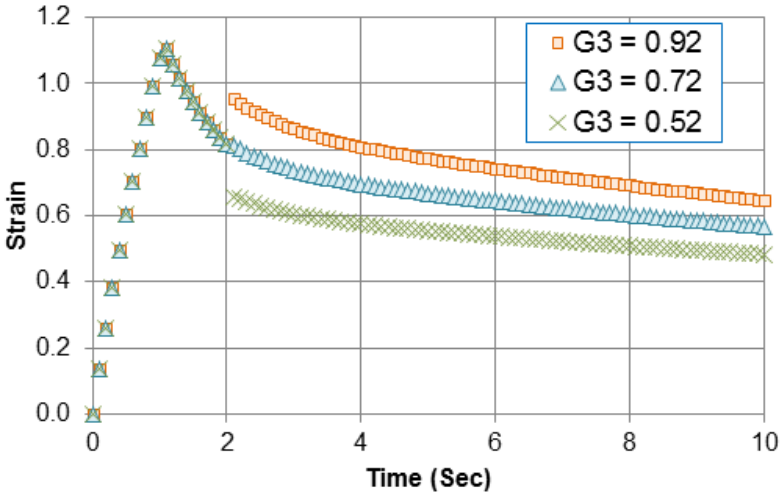

Figure 64. Effect of non-linear viscoelastic parameter G_3.

The purpose of the statistical analysis was the following:

A. To determine the effect of J_{nr}_cycle on non-linear viscoelastic parameters and PS.

B. To study the effect of cycle, and type and quantity of polymer on J_{nr}, linear and non-linear viscoelastic parameters, and PS.

C. To study how polymer loading of SBS, Elvaloy and PPA affect J_{nr}, linear viscoelastic parameters, non-linear viscoelastic parameters, and PS. Each of the above will be discussed in detail below.

5.2.1 To Determine the Effect of J_{nr} on Non-linear Viscoelastic Parameters and PS

Factorial regression analysis is carried out to determine the relationship between J_{nr} and independent variables such as non-linear viscoelastic parameters G_1, G_2, and G_3, and PS. In this case, a separate analysis of variance (ANOVA) test may not be appropriate, because the J_{nr} is dependent on all of the independent variables. Therefore, the continuous variables G_1, G_2, G_3, and PS were categorized into discrete levels depending on how the values clustered together. After the independent variables G_1, G_2, and G_3 were grouped into different levels, a factorial analysis was conducted.

5.2.2 Null Hypothesis

The dependent variable J_{nr} at each cycle is not statistically affected by the independent variables G_1, G_2, G_3, and PS.

5.2.3 Results and Discussion

The significance values for the non-linear viscoelastic parameters G_1, G_2, G_3, and PS are 0.087, 0.228, 0.000, and 0.043, respectively. In this analysis, the parameters are considered to have a significance effect if they are less than 0.050. The independent variables G_1 and G_2 have significance values higher than 0.05. The parameters G_3 and PS have values less than 0.05 and have a significant effect on J_{nr}. This indicates that the J_{nr} value is more influenced by the latter part of the strain recovery curve.

5.2.4 To Study the Effect of Cycle, Type and Quantity of Polymer on J_{nr}, Linear and Non-linear Viscoelastic Parameters, and PS.

The performance of PMB depends upon the stiffness of the base binder, cross linking between base binder and polymer, type of polymer, and quantity of polymer (*5*). A statistical analysis to study the effect of different cycles, base binders and type and quantity of polymer on: J_{nr}_cycle; the non-linear viscoelastic parameters G_1, G_2, and G_3,; the linear viscoelastic parameters B, C, D, and E; and PS was conducted. Table 19 shows group coding used for type of base binders, quantity of polymers, and stress cycles to conduct the statistical analysis.

Table 19. Test matrix for statistical analysis

Factors	Number of levels	Unit	Level	Code
Cycle	3	Cycle number	1, 6, 10	1, 2, 3
Base binder	2	Grade of binder	Base binder 1 and base binder 2	1, 2
Elvaloy	2	Quantity (by % of total weight)	1.5, 2.5	1, 2
PPA	2	Quantity (by % of total weight)	0, 0.8	1, 2
SBS	3	Quantity (by % of total weight)	1.5, 3.0, 4.5	1, 2, 3

5.2.5 Null Hypothesis

The null hypothesis is that the J_{nr} value or the non-linear viscoelastic parameters G_1, G_2, G_3, and PS or the linear viscoelastic parameters B, C, D, and E are similar for different level of cycles, types of base binder, and quantity of Elvaloy, PPA, and SBS.

Null hypothesis: H_0: $(J_{nr\_cycle})_1 = (J_{nr\_cycle})_2 = (J_{nr\_cycle})_3$

$(G_1)_1 = (G_1)_2 = (G_1)_3$

$(G_2)_1 = (G_2)_2 = (G_2)_3$

$(G_3)_1 = (G_3)_2 = (G_3)_3$

$(PS)_1 = (PS)_2 = (PS)_3$

Subscript 1, 2, and 3 represent level code 1, 2, and 3 (wherever applicable).

The analysis of variance (ANOVA) test is best suited to compare the mean of one or more groups. In this analysis, the groups are created based on either sequence of cycle or type of base binder or quantity of polymers, hence they are considered as independent variables. Dependent variables are J_{nr}_cycle, G_1, G_2, G_3, and PS. A significance criterion is considered as 5% (0.05 or 1 in 20). True null hypothesis would be accepted with the tolerance of p-value of 0.05.

5.2.6 Results of Statistical Analysis

Table 20 gives the p-values of a one way ANOVA test. If the p-value is greater than 0.05, it implies that the mean of the independent variable is influenced by the dependent variables. If the significance of homogeneity of variance is greater than 0.05, this implies that the condition of homogeneity of variance is reasonably satisfied. The results of the homogeneity test are not presented here; however, if condition of homogeneity was not satisfied, statistical test of Dunnett's T3 for non-homogeneity was conducted. Following is the interpretation of the results;

i) **Cycle**: The mean of J_{nr}_cycle, G_1, G_2, G_3, and PS are statistically similar for the three cycles (cycle 1, 6, and 10).

ii) **Base binders**: The mean of G_1 and G_2 are statistically similar for two different base binders. Therefore, the base binders selected in this study influence: J_{nr}; PS; linear viscoelastic parameters B, C, D, and E; and non-linear viscoelastic parameter G_3.

iii) **Elvaloy**: The mean of all the parameters except non-linear viscoelastic parameters G_2, G_3 and J_{nr} are statistically similar for different samples with 1.5% and 2.5% Elvaloy. Therefore, the quantity of Elvaloy does statistically influence J_{nr}_cycle and non-linear viscoelastic parameters G_2, and G_3.

iv) **PPA:** The mean of all parameters are statistically different for different samples with 0% and 0.8% PPA. Therefore, the quantity of PPA influences all linear and non-linear viscoelastic parameters, and PS.

v) **SBS:** The mean of C and PS are statistically similar for different samples with 1.5%, 3%, and 4.5% SBS. Therefore, the quantity of SBS influences: J_{nr}_cycle; linear viscoelastic parameters B, D, and E; and non-linear viscoelastic parameters G_1, G_2, and G_3.

Table 20. Curve Parameters

	Parameters								
Factors	Linear viscoelastic parameters				Non-linear viscoelastic parameters			J_{nr}_cycle	PS
	B	C	D	E	G_1	G_2	G_3		
Cycle					0.988	0.999	0.383	0.999	0.810
Base binders	0.000	0.000	0.000	0.000	0.099	0.150	0.000	0.000	0.010
Elvaloy	0.011	0.016	0.000	0.000	0.010	0.195	0.409	0.485	0.004
PPA	0.000	0.000	0.000	0.000	0.000	0.000	0.000	0.000	0.001
SBS	0.008	0.183	0.014	0.024	0.009	0.006	0.000	0.000	0.064

Note: The grey colored cell indicates significance at 95% confidence level.

5.2.7 Effect of Polymer Loading of SBS, Elvaloy and PPA affect J_{nr}, Linear Viscoelastic Parameters, Non-linear Viscoelastic Parameters, and PS

The effect of quantity of polymer (SBS), Elvaloy, PPA on non-linear viscoelastic parameters, PS, and J_{nr} was evaluated. This analysis includes four different quantities of SBS, two different quantities of Elvaloy and PPA. MSCR tests were carried out on these binders with two replicates. Figure 65 shows the average values of G_1, G_2, G_3, and J_{nr} for different proportions of SBS. Table 21 shows the average values of G_1, G_2, G_3, and J_{nr}_cycle for different proportions of Elvaloy and PPA. The authors observed that the values of G_1, G_2, G_3, and J_{nr}_cycle were statistically similar between the three cycles and between two replicates.

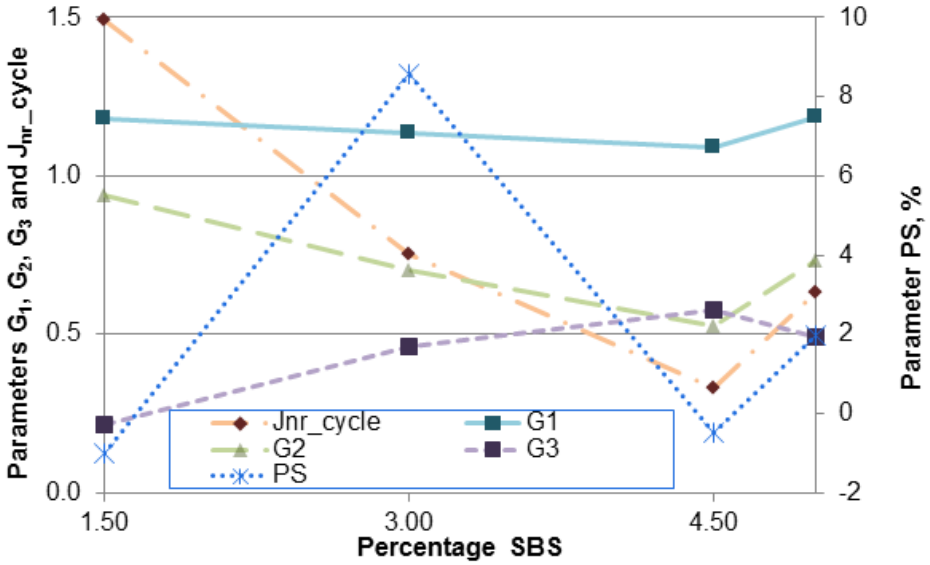

Figure 65. Variation of different parameters with percentage of SBS.

Table 21 Percentage difference for Elvaloy and PPA

Parameters	Elvaloy (%)			PPA (%)		
	1.5	2.5	% diff.	0.00	0.80	% diff.
Sample	RO_4	RO_5		RO_4	RO_6	
G_1	1.24	1.30	4.76	1.24	1.10	10.80
G_2	0.84	0.88	4.92	0.84	0.36	57.17
G_3	0.44	0.45	2.95	0.44	0.78	-77.57
J_{nr}_cycle	1.18	1.15	-2.77	1.18	0.34	70.96
PS	12.89	20.99	38.57	12.89	19.08	-47.96

Note: % diff. – Percentage Difference

The value of J_{nr}_cycle and G_2 decreases until around 4.5 percent SBS and then increases. The reduction in J_{nr}_cycle appears to be primarily influenced by the reduction in G_2. On the other hand, G_1 and G_3 remain constant or decrease until 4.5 percent SBS and then increase. These trends appear to indicate optimum performance of the PMB could be obtained at around 4.5 percent of SBS. This could be because in-house blending may be subject to error, especially

at the higher polymer percentages. This may be due to the fact that we did not have a direct method to verify the level of cross linking of the polymer.

The percentage difference in the values of parameters G_1, G_2, G_3 and J_{nr}_cycle were within 5% for 1.5% and 2.5% Elvaloy. The PPA content significantly influenced the non-linear viscoelastic parameters and J_{nr}. The parameters G_3 and PS decrease with increase in PPA content, on the other hand, G_1, G_2, and J_{nr}_cycle increase with increase in PPA content.

5.3 Gel Permeation Chromatography and FTIR

GPC results are gathered from the software and each of the peaks represents a component within the sample being tested. Figure 66 below shows a GPC chromatogram for the NS 64-22 sample with 3% Kraton. The bottom portion of the plot is the detector response versus the Elution volume (in µL). However, this elution is at a rate of 1 µL per minute through the 12 minute test, therefore the plot can be directly translated to detector response vs. time.

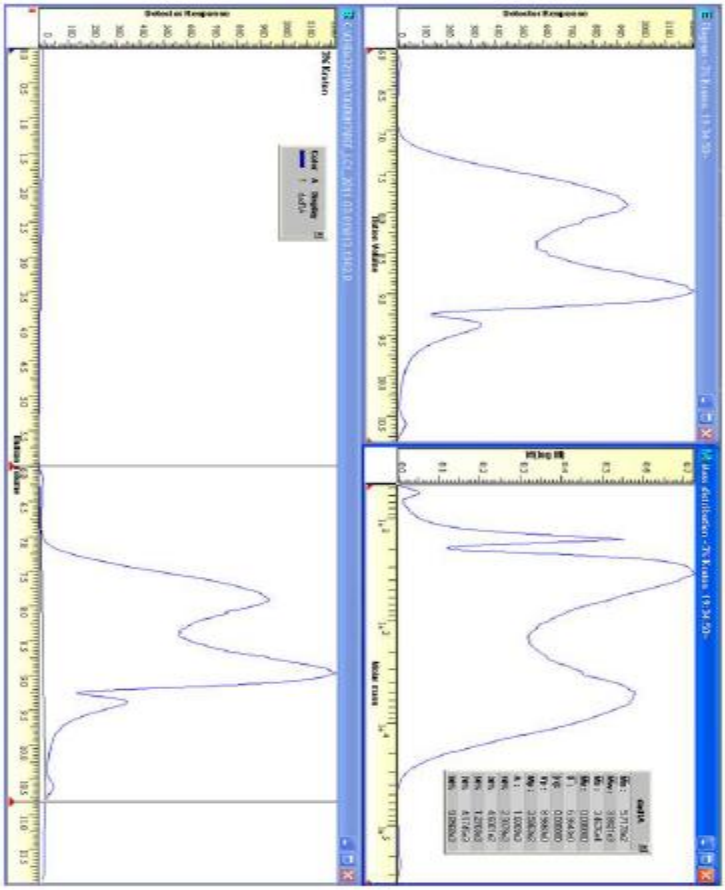

Figure 66. GPC Chromatogram from NS 64-22 with 3% Kraton

A larger peak within a chromatogram means that the component within that peak has a high weight percentage within the mixture. Since the binder itself makes up such a large percentage of the sample, its peaks are much larger than the polymer peaks. In fact, sometimes the polymer peaks can be difficult to locate within the chromatogram. However, the polymer molecules themselves are many times larger than the binder molecules, and thus are the first ones reported in the chromatogram. The top left portion of the plot is the same as the bottom, however it is a zoomed in version of the isolated region between the two sliders. The top right part of the

plot is a graph on a logarithmic scale which shows the molecular weight distribution. The computer software is able to find the molecular mass of the components of the sample using the elution volume of the sample. It is able to use the elution volume to find the intrinsic viscosity of the sample. After this, the Mark-Houwink equation is used to find the molecular weights. The Mark Houwink Equation is shown in Figure 66. [η] is the intrinsic viscosity of the sample, while M is the molecular weight. K and *a* are the Mark-Houwink parameters, which are determined graphically through the software. Once the other 3 variables are known, molecular weight can be solved for and reported in the plot vs. elution volume. This is how molecular weights are reported through the software.

Equation 24 $[\eta] = KMa$

This part of the plot is the most important. The data table in the top right is where the data is gathered from to be analyzed. Figures 66 show the data tables for the base binder peak region and the polymer peak region of NS 64-22 with 3% Kraton. Figure 67 is a screen view of the software output with the table to the left showing the binder peak region, and the table to the right is the polymer peak region. There are many different variables within this table that need to be explained. The two main numbers to focus on in this table are the M_n and A. M_n is the number average molecular weight and is the mean of molecular weights within the selected region. A is the area under the curve for the selected region. M_w is the weight average molecular weight, while M_z is the z average molecular weight. P is the polydispersity of the region (M_w/M_n) and M_p is the peak molecular weight.

dad1A	
$\overline{Mn}$:	5.7178e2
$\overline{Mw}$:	3.9821e3
$\overline{Mz}$:	3.4676e4
$\overline{Mv}$:	0.000000
$\overline{D}$:	6.9643e0
[n]:	0.000000
Vp :	8.9660e0
Mp :	3.5863e2
A :	1.6009e3
10%	2.3079e2
30%	4.6001e2
50%	1.2703e3
70%	4.1745e3
90%	9.8568e3

dad1A	
$\overline{Mn}$:	2.4024e5
$\overline{Mw}$:	2.4503e5
$\overline{Mz}$:	2.4987e5
$\overline{Mv}$:	0.000000
$\overline{D}$:	1.0199e0
[n]:	0.000000
Vp :	6.1793e0
Mp :	2.4417e5
A :	1.5908e0
10%	2.0159e5
30%	2.2463e5
50%	2.4296e5
70%	2.6240e5
90%	2.9171e5

Figure 67. Data Tables for the Binder Peak and Polymer Peak regions of NS 64-22 with 3% Kraton

As the data shows, the average molecular weight of the binder within the sample is several orders of magnitude smaller than the polymer's average molecular weight. Conversely, the Area under the curve for the polymer peak is far smaller than the binder peak. Because the binder makes up roughly 97% of the sample and the polymer only 3%, this is what the data should look like. Besides the average molecular weight, the Area under the curve can also be used to further

analyze samples. As the amount of polymer within a sample increases, so does the size of the peak. The amount of polymer in a sample is directly related to the area under the curve for a polymer peak. Thus, if the same polymer is used, a plot of the area under the curve vs. polymer content will be linear and can be used to make a calibration curve for a certain polymer. Figure 68 below shows a calibration curve for Kraton made by plotting the area under the curve versus the amount of polymer in the sample.

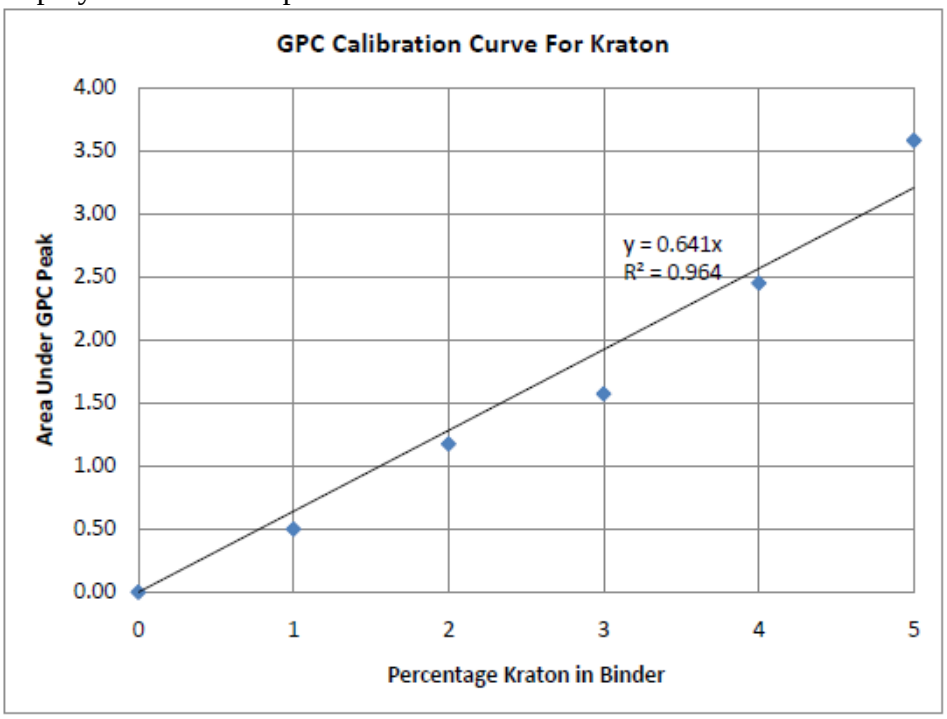

Figure 68. GPC calibration curve for Kraton

The line is a relatively good fit to the data, and thus the equation of the line can be used to find the amount of polymer in an unknown sample so long as it is known that Kraton is used. While this may be true, there is some margin for error in these findings, as the polymer peaks are very small from GPC and therefore it is easy to slightly skew data by not putting the sliders in the proper place within the program. Therefore, for the purpose of finding the mass fraction of polymer within a sample, it is better to use FTIR.

The software used to run an FTIR test supplies a plot of Absorbance vs. the wavelength of light which can be used as well as the data points in a comma separated file (.csv) which can be opened in Microsoft Excel to plot the data as well. The Excel plot is better to use in the case of data analysis because it can be manipulated to find the information needed to make a calibration curve for each polymer used. There were no issues in testing to find the peaks to analyze. Figure 70 below shows an FTIR plot made in Excel showing three different samples: NS 64-22 Base Binder, NS 64-22 with 5% Kraton, and NS 64-22 with 5% Elvaloy. All hydrocarbons have a signature absorbance peak within what is known as the "fingerprint region" of wavelengths of light. So long as it is known where the polymer has its signature peak, then the test can be used to find the composition of a mixture. Thanks to AASHTO Spec. T-302 it was known that the base binder signature absorbance peak would always be at 1375 wavenumbers (cm-1) and that the Kraton signature peak and all other Styrene-Butadiene polymers would be at 965 wavenumbers. However, it was not known at which wavelength of light that Elvaloy would have a signature absorbance peak. Through testing it was determined that this peak would occur

around 1735 wavenumbers. As with GPC, a larger peak indicates more polymers present within the binder.

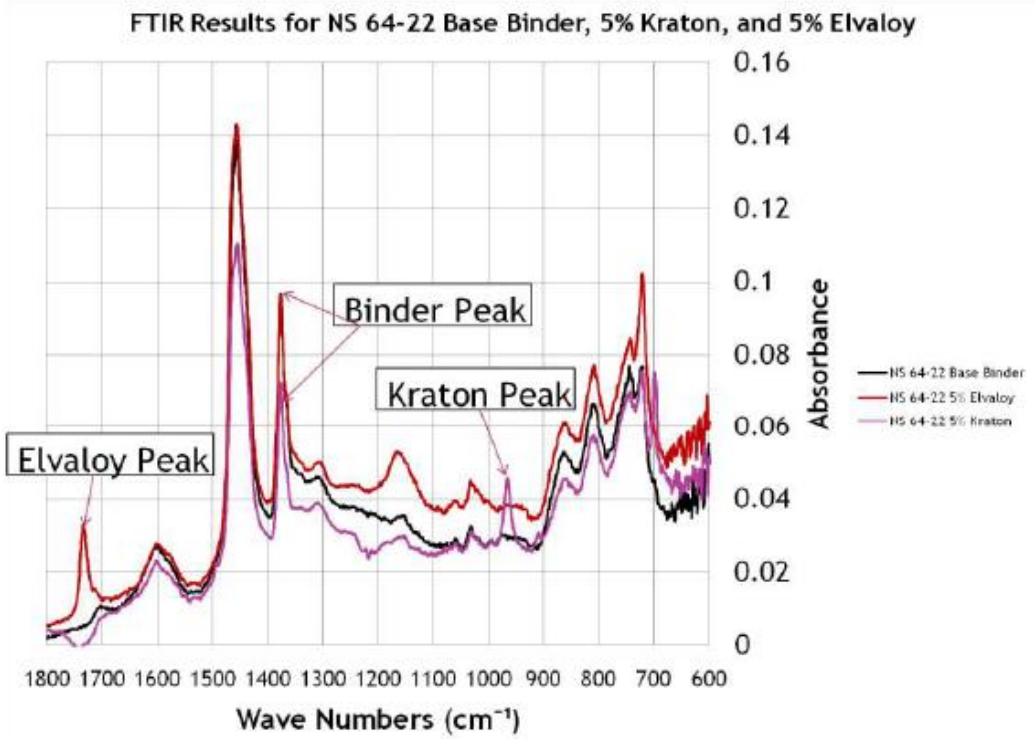

Figure 69. FTIR plot for NS 64-22 based binder, 5% Elvaloy an 5% Kraton mixes

The area under the curve can be found using a numerical integration method for each polymer peak for the samples tested. Then, plotting this area vs. the percentage of polymer gives a linear trend that can be used to find calibration curves for both Kraton and Elvaloy. Figures 70 and 71 below show the calibration curves that have been generated.

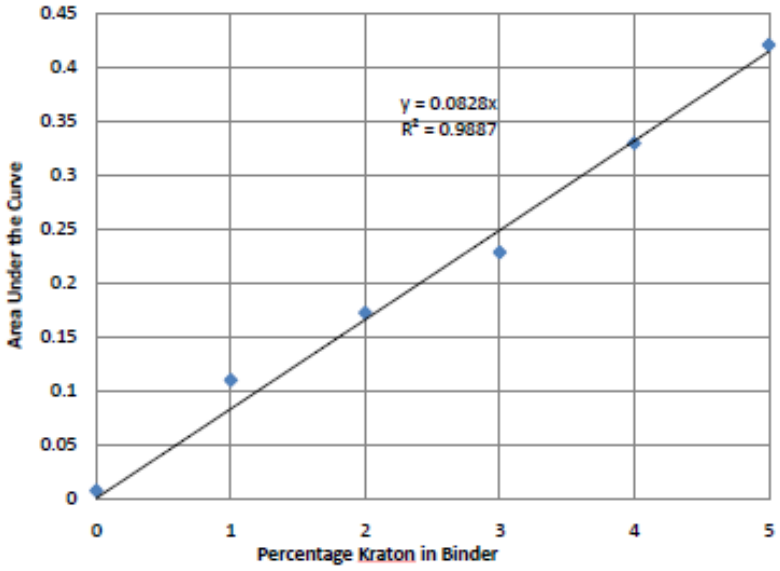

Figure 70. Calibration curve for Kraton

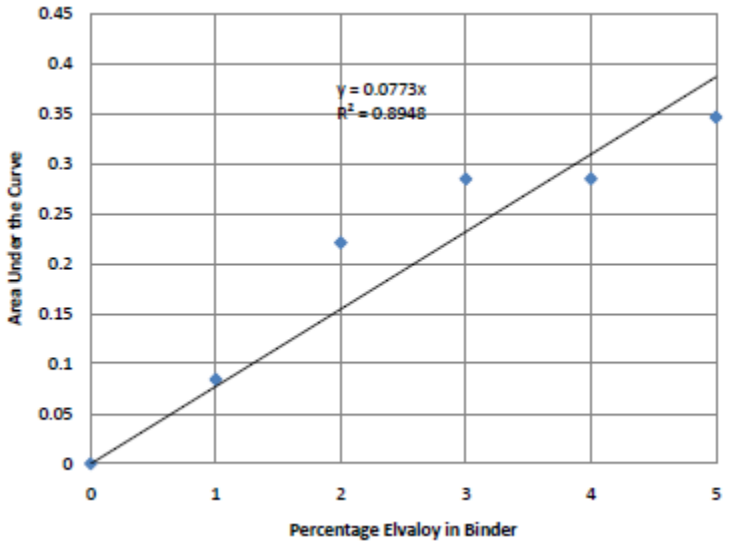

Figure 71. Calibration curve for Elvaloy

The line was a much better fit for the Kraton test runs than it was for the Elvaloy ones, but it still should be possible to make a reasonably good approximation to the amount of polymer within an unknown sample so long as it contains one of these two polymers. Seeing as how these are two of the most popular polymers in use today, there is probably a good chance that an unknown sample would contain one of these two polymers and the polymer content can be mapped out.

5.3 Correlating MSCR Parameters to Predicted Performance in MEPDG

The results of MEPDG analysis are presented in Table 18, with the following predicated parameters: terminal IRI, longitudinal cracking, alligator cracking, transverse cracking, and permanent deformation. The final row of the table is the J_{nr} of each binder used for the mix. The MEPDG analysis follows the same pattern of the dynamic complex modulus results. All of the predicted parameters increased as the mixes binder J_{nr} decreased, or in other words, cracking increased as the binder became stiffer. However, the difference between mixes could be considered negligible and does not correlate well with the large difference in J_{nr} between the mixes with NS 70-22 and NS 76-22 and the small difference between NS 76-22 and NS 82-22 Tank 73. The small strains of DCM testing may not capture the full effects of polymer modification. Flow Time testing was chosen for further testing to expose the mixes to higher strains.

Table 22. MEPDG evaluation analysis

Performance Criteria	Distress Target	Reliability Target	NS 70-22		NS 76-22		NS 82-22 Tank 73	
			Distress Predicted	Reliability Predicted	Distress Predicted	Reliability Predicted	Distress Predicted	Reliability Predicted
Terminal IRI (in/mi)	172	90	107.5	98.34	109.2	97.93	113.3	96.8
AC Surface Down Cracking (Long. Cracking) (ft./mile):	2000	90	2880	35.39	4050	19.52	6330	3.76
AC Bottom Up Cracking (Alligator Cracking) (%):	25	90	2.6	97.29	3.3	94.64	5.5	91.71
AC Thermal Fracture (Transverse Cracking) (ft./mi):	1000	90	0.2	99.999	1	99.999	1	99.999
Permanent Deformation (AC Only) (in):	0.25	90	0.15	97.51	0.17	90.18	0.23	59.99
Permanent Deformation (Total Pavement) (in):	0.75	90	0.38	99.999	0.41	99.999	0.49	99.69
Jnr(3.2kPa) at 64°C	--		1.09		0.18		0.13	

5.4 Correlating MSCR with Flow time

The results of the Flow time testing and respective J_{nr} of each binder are plotted in Figures 72, 73, and 74. The SMA, Bridge Deck and Rt71 PG 64-22A results were excluded because their flow time was magnitudes greater than the other results. In Figure 72 Flow time increasing as J_{nr} decreases from 1 kPa^{-1} and is generally low beyond 1 kPa^{-1}. The same trend is present in figure 73, which isolates the time during the secondary phase; by subtracted the flow time by the transition point from the primary to secondary phases. The secondary phase was isolated to study the response of the binder of each mix. The trend is more consistent throughout Figure 74, when the compressive strains accumulated during the secondary phase are graphed, microstrains increase as J_{nr} decreases. All three figures show better performance as the J_{nr} values decrease from 1 kPa^{-1} while the best performance are clustered as J_{nr} approach 0.5 kPa^{-1} or lower. Of the three mixes not included in the figures, the Bridge Deck supports the trend with a high

flow time and low J_{nr}, while the SMA and PG 64-22A have larger J_{nr} and higher flow times. The high flow time results of SMA may not be consistent with high J_{nr} values because the gradation and aggregate structure is significantly different than the rest. It is unclear why the flow time results of the mix with PG 64-22A was not consistent with the large non-recoverable compliance values.

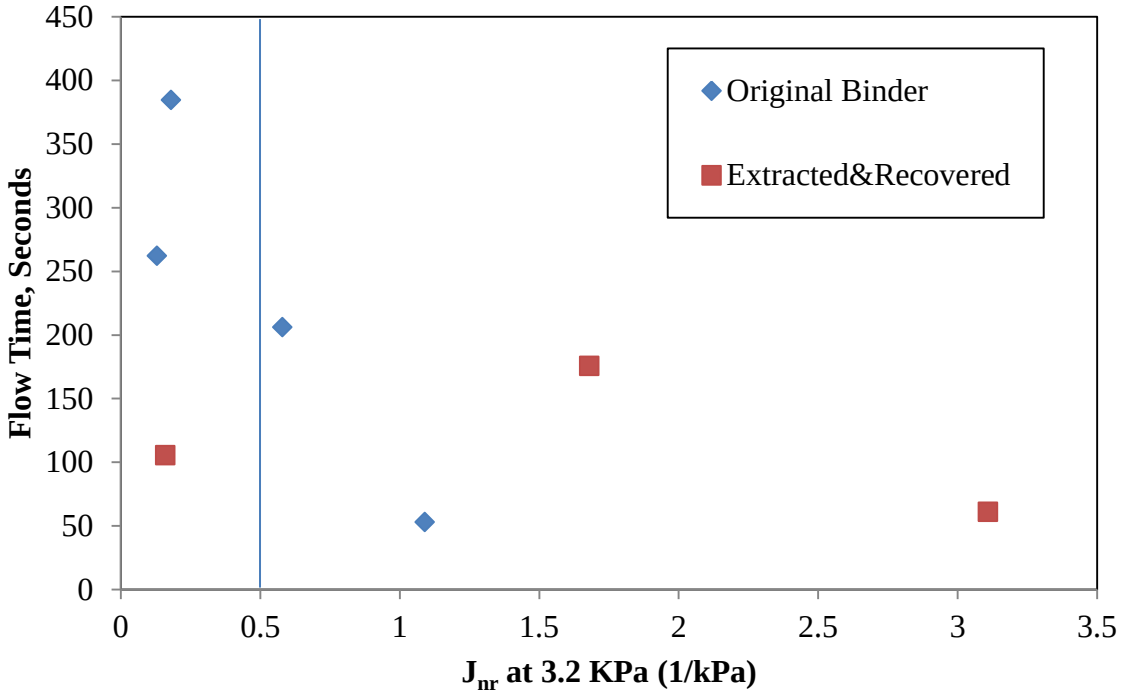

Figure 72. J_{nr} test results plotted versus the Flow Time results

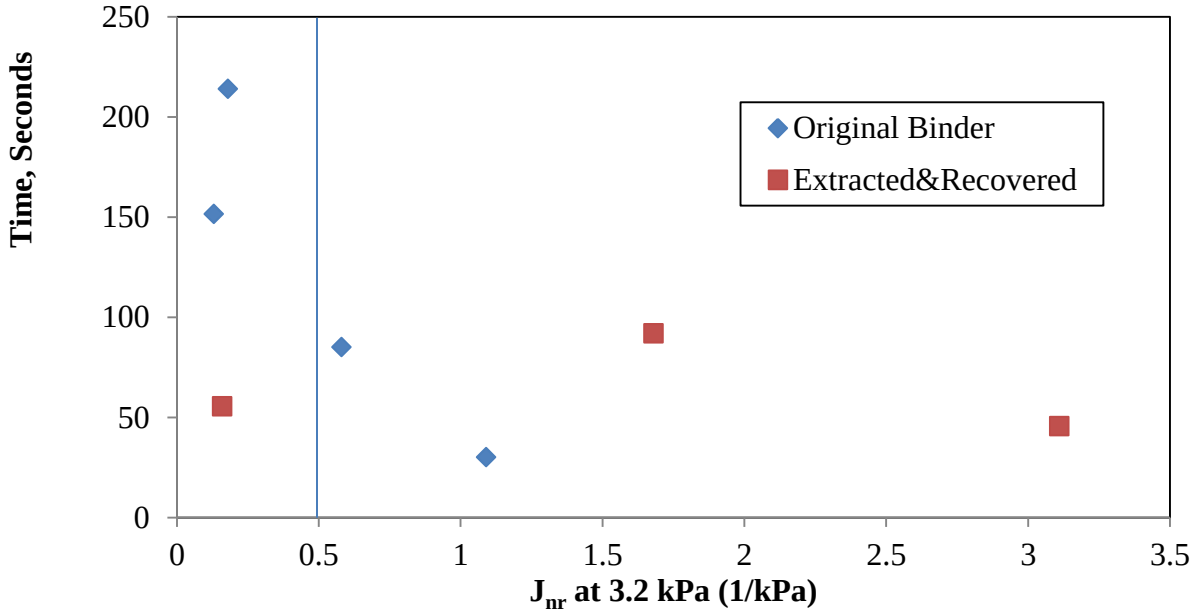

Figure 73. J_{nr} plotted versus the time of secondary region

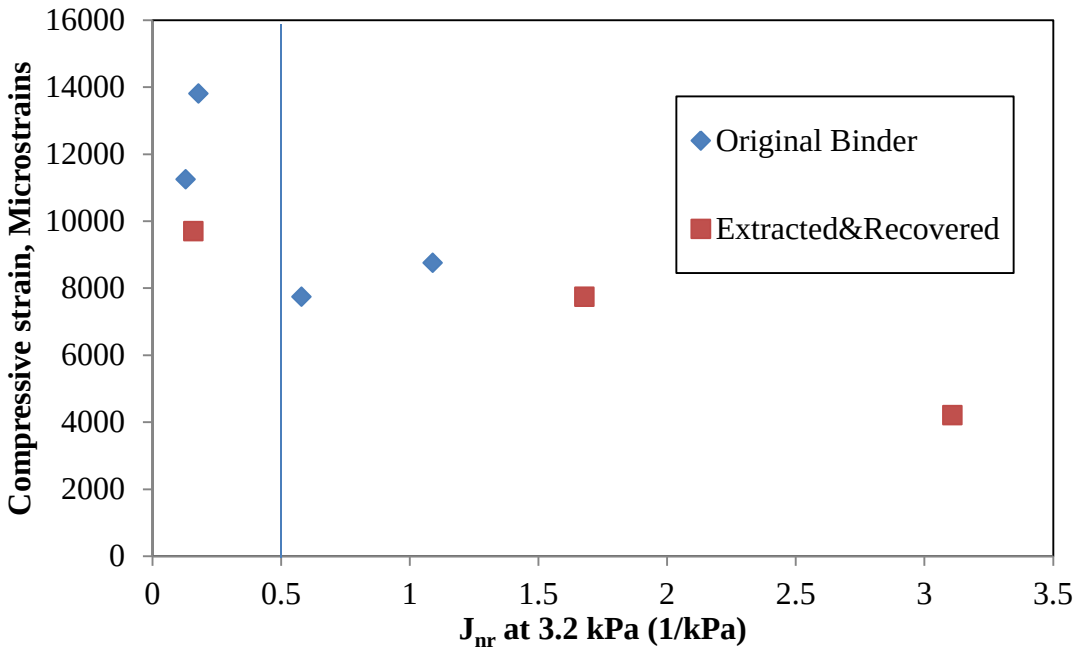

Figure 74. J_{nr} plotted versus the difference in micro strains between primary to secondary and secondary to tertiary

There is no correlation between G*/sin(δ) and Flow time (Figure 75). This may be primarily due to the difference in the strain regimes of the two tests. There is also no correlation observed between recovery from MSCR and flow-time results as shown in Figure 76. The three mixes not included in the graph, due to their large flow that didn't fit the scale of the plotted results, would have added to the scatter.

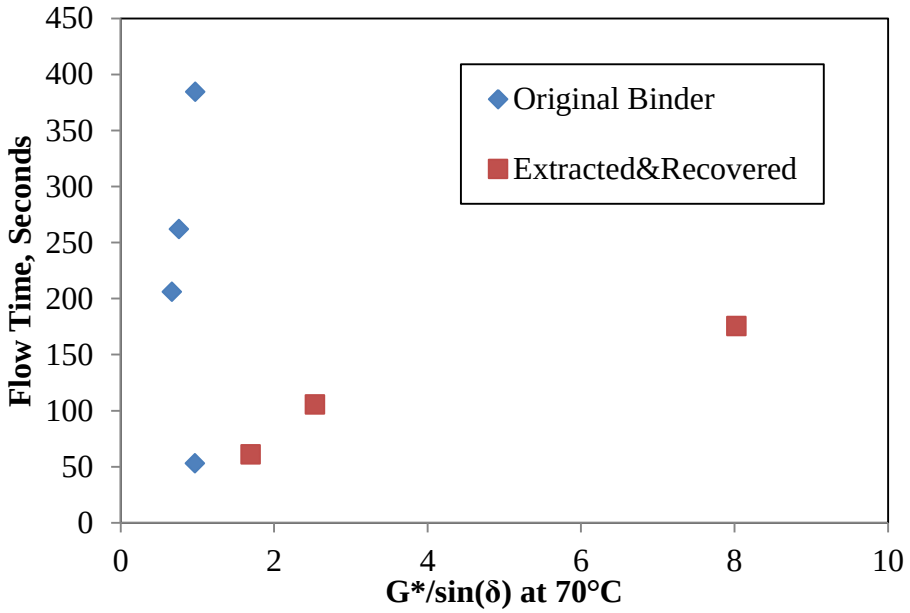

Figure 75. G*/sin(δ) (kPa) at 70C versus Flow Time Results

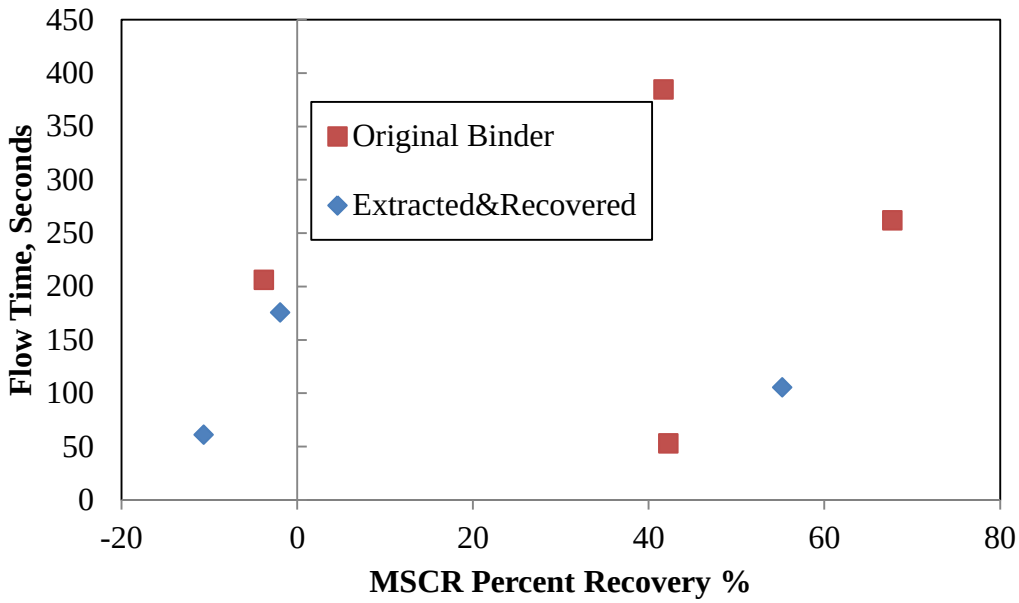

Figure 76. MSCR Percent Recovery versus Flow Time Results

The non-recoverable compliance J_{nr} has been demonstrated to correlate with rutting performance, as measured by flow time testing, with rutting resistance improving as J_{nr} decreased. Generally as J_{nr} increases from 0.5 1/kPa rutting resistance drops off. The Superpave parameter G*/sin(δ) and the MSCR recovery didn't correlate well with the flow time results.

In terms of rutting resistance, J_{nr} correlates well and should be consider as a simpler and more affordable alternative to elastic recovery and forced ductility testing for polymer modified binders. Mixes with a J_{nr} approaching 0.5 1/kPa, or lower can be expected perform well from a binder perspective, making it a reasonable criteria when selecting polymer modified binders.

5.5 Cost –benefit Analysis of Eliminating Elastic Recovery and Using MSCR

MSCR testing poses savings in the test process as compared to the current PG Plus specification elastic recovery. The cost per test is slightly less with MSCR testing typically costing $150 while elastic recovery is $250 for three tests and with an additional cost of $250 to RTFO the greater material needed to operate the test, for a grand total of $167 per test. The greatest savings are in equipment and time. MSCR testing uses the DSR and would not typically incur additional equipment cost while elastic recovery requires the purchase of approximately $15,000 in large equipment to be bought. The number of test that can be conducted per day per apparatus is limited for elastic recovery, typically its take approximately 4 hours per sample. MSCR testing requires approximately fifteen minutes; allow many test to be run in a single day. In all the MSCR procedure requires less upfront cost, is less per sample and can be performed much faster.

Chapter 6. Binder and Mix Database

The objective of this database is to provide the capability to the state to query for binder and mix data based on different criteria such as:

- Binder Name
- Traffic Classification
- PG Grade
- Type of binder used
- Flow time

Start Screen: Summarizes the use of the database and includes two buttons to get to the binder and mix database respectively (Figure 77).

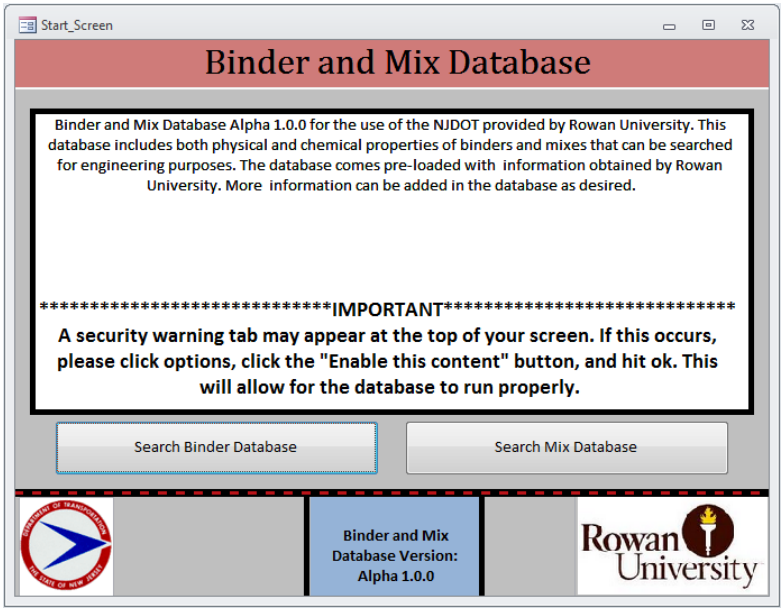

Figure 77. Start Screen for the Binder and Mix Database

Binder Database Main Menu: Describes the three sections of the database, search, add, and modify binder data. Each has a button to go to their next individual screens. The modify binder data has a drop down list of all the binders in the database that you can select and modify (Figure 78).

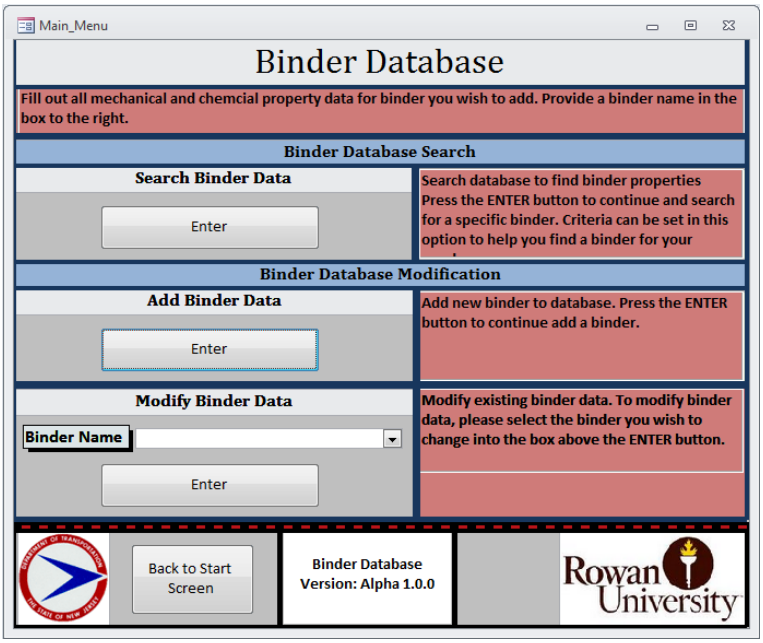

Figure 78. Binder Database Main Menu

Search Binder Menu: Searching by name is similar to the modify binder drop down list where it has a comprehensive list of the binders in the database (Figure 79). The classification search uses the MSCR traffic classifications based on J_nr at 3.2kPa values. Only binders with MSCR data have the classification values. Below the search is the traffic grading ranges in ESALs and J_{nr} values. Final search is for searching for binders with specific binder grade temperature requirements.

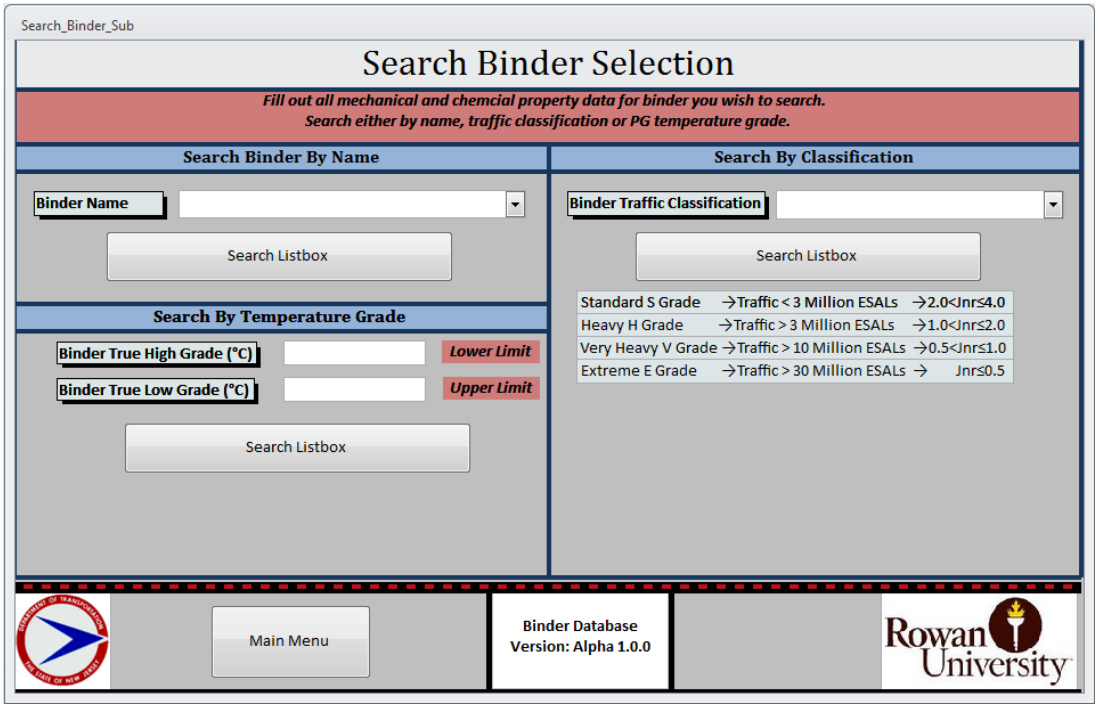

Figure 79. Binder Database Search Submenu

Search Binder Sub sheet: This screen would come up with a list of binders that follow the search parameters you provide either traffic classification or temperature grade (Figure 80). Then a binder can be selected and then using the search binder button brings you to the data sheet with all the binder information. The previous screen button brings you to the previous screen if you want to change your search parameters.

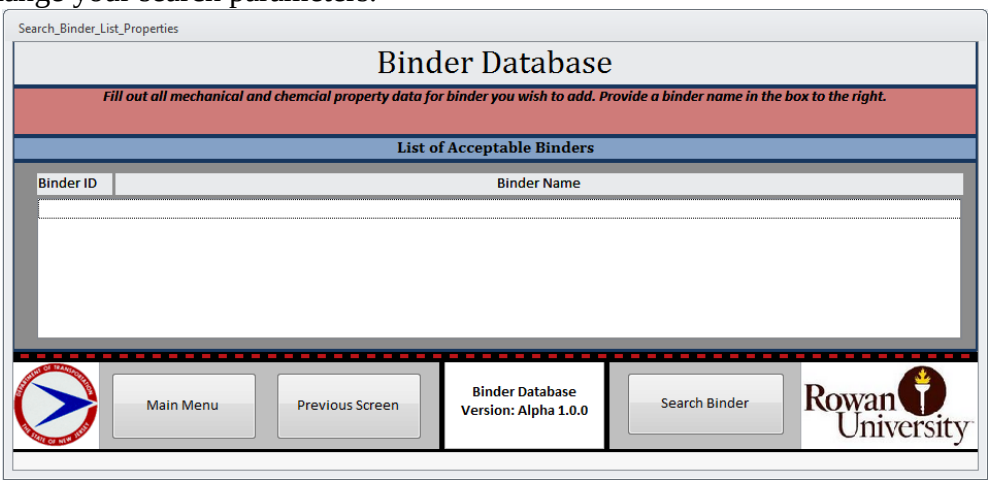

Figure 80. Binder Database Search Results Menu

Example Data Sheet: This datasheet is for the search, add or modify binder sections of the database. To modify and search sections, the fields will be filled in with the field's data if there is data for that field. For the add section of the database the user would fill in the fields. The only difference between the sections are the add and modify section will have a button at the bottom of the sheet stating about adding or modifying the binder while the search section will have a print binder report button instead. Buttons on the sheet are used to calculate different values based on parameters entered on the sheet (Figure 81).

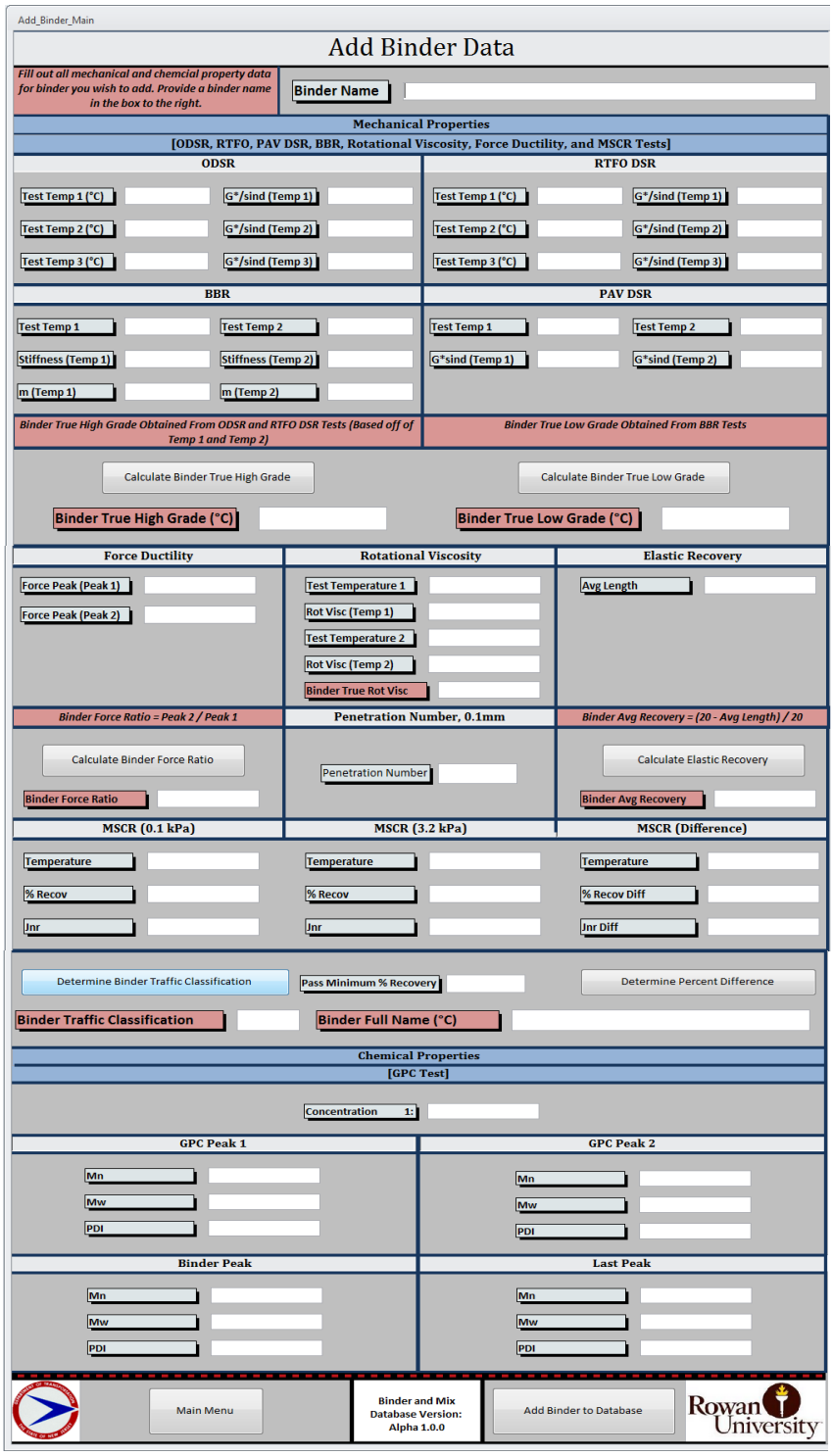

Figure 81. Binder Database Data Sheet

Mix Database Main Menu: The same setup as the binder database. The search function includes searches for mix name, binder name, and flow time (screen shot is in Figure 82). Then add and modify sections follow the same setup as the binder database.

Mix Search Main Menu: It has a simple interface with the three searches I mentioned previously (Figure 83). Once you fill in the criteria you want for the search you click the corresponding search button. Table 23 shows the description of all the fields.

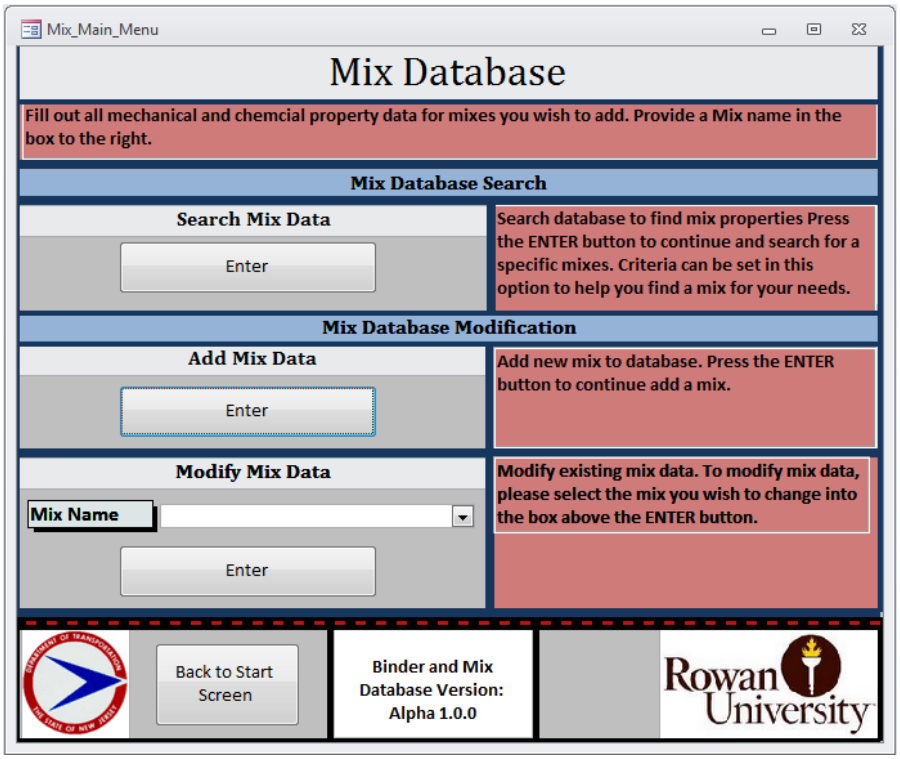

Figure 82. Mix Database Main Menu

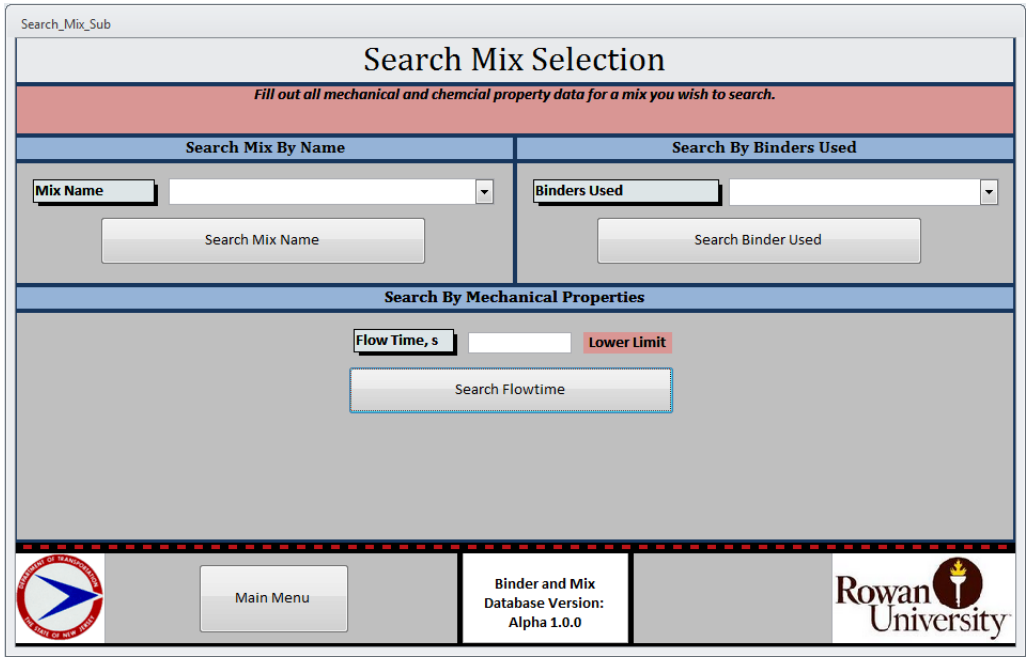

Figure 83. Mix Database Search Submenu

Search Mix List: The top title varies depending on which search was performed. The list box will have all the mixes that follow the given criteria. To look at a certain mixes data you MUST click one of the mixes. Once there you can click the search mix button and the data will come up as requested (Figure 84).

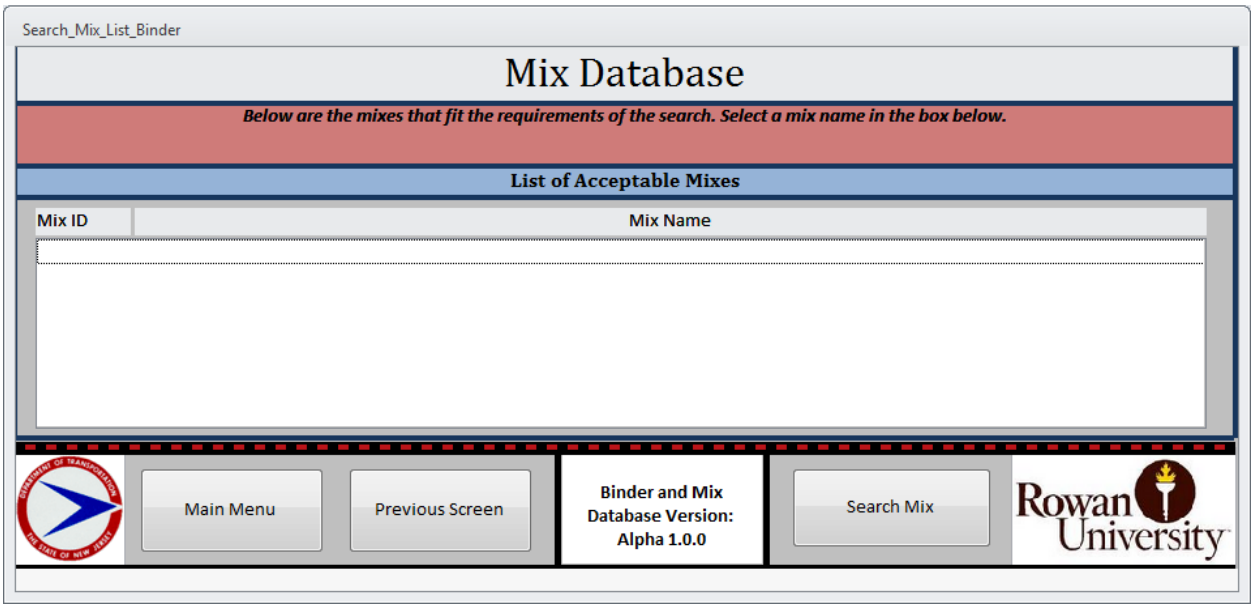

Figure 84. Mix Database Search Results Menu

Example Mix Datasheet: Similar to the binder database the add mix, modify mix, and search mix datasheet are the same except the titles and the button on the bottom of the sheet. The data sheet includes all of the basic mix information you may need along with binder selection. If the binder used is in the database it can be selected and some basic binder properties are included when the binder is selected. The binder data could also just be entered by the user themselves. If added via this datasheet the binder would not be added to the binder database. User will still need to add it into the binder database. In the search mix datasheet (Figure 85) it says Print Mix Data. The report follows the same format just without the buttons as they are unneeded for the printed report.

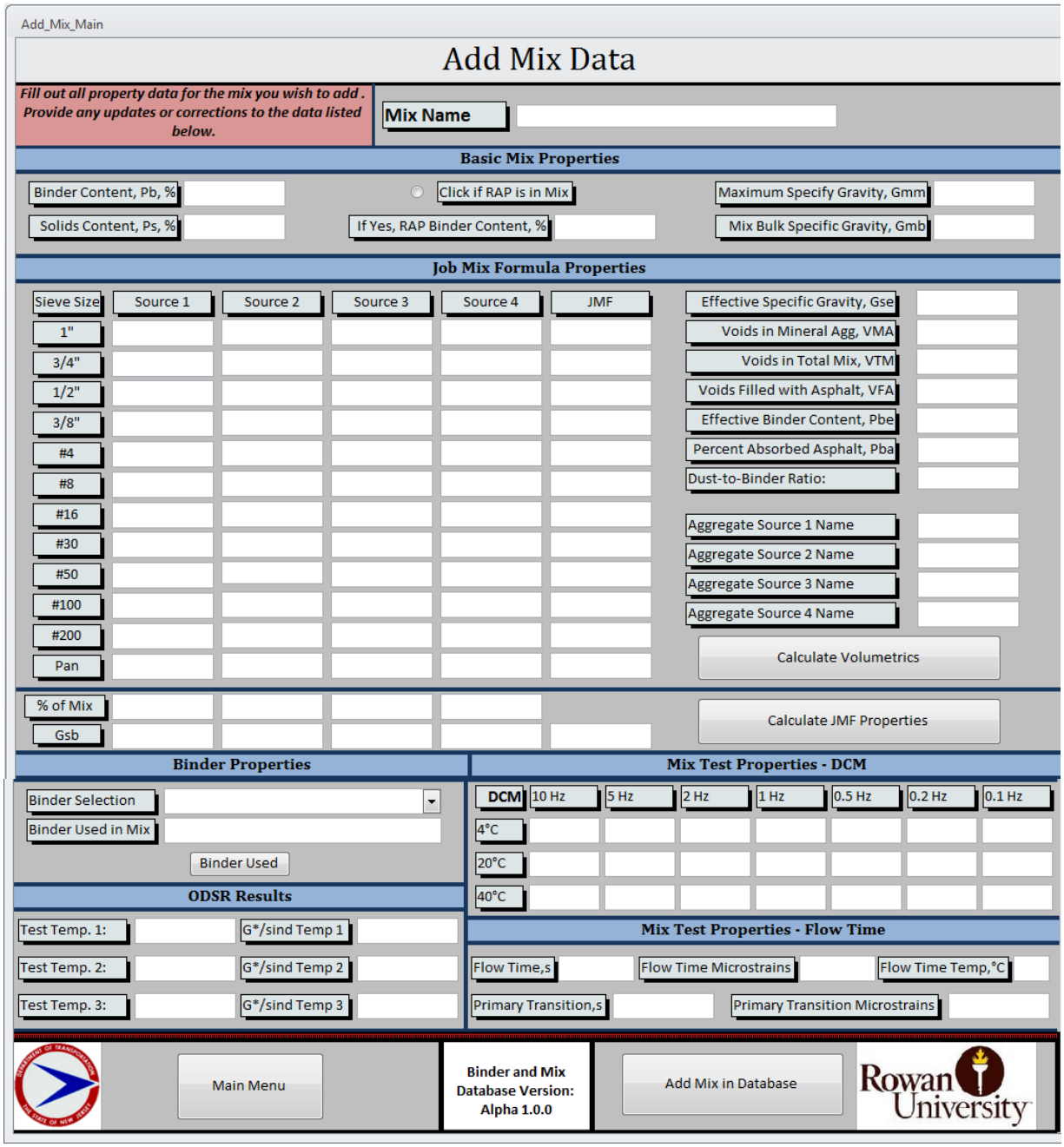

Figure 85. Mix Database Data Sheet

Table 23. Database field description

Field	Purpose
ID	Reference number for the database
Binder_Name	Identifier for User
OSDR_Test_Temp1	Unaged Binder DSR Test fields with space for up to 3 tests of data.
OSDR_Gsind_Temp1	
OSDR_Test_Temp2	
OSDR_Gsind_Temp2	
OSDR_Test_Temp3	
OSDR_Gsind_Temp3	
RTFO_Test_Temp1	RTFO Aged Binder DSR Test fields with space for up to 3 tests of data.
RTFO_Gsind_Temp1	
RTFO_Test_Temp2	
RTFO_Gsind_Temp2	
RTFO_Test_Temp3	
RTFO_Gsind_Temp3	
Binder_True_High_Grade	Actual high temperature grade field based on ODSR and/or RTFO results instead of PG High Temp Grade
BBR_Test_Temp1	BBR Stiffness Test fields with space for up to 3 tests of data.
BBR_Stiffness_Temp1	
BBR_m_Temp1	
BBR_Test_Temp2	
BBR_Stiffness_Temp2	
BBR_m_Temp2	
PAVDSR_Test_Temp1	PAV Aged Binder DSR Test with space for up to 2 tests of data.
PAVDSR_Gsind_Temp1	
PAVDSR_Test_Temp2	
PAVDSR_Gsind_Temp2	
Binder_True_Low_Grade	Actual low temperature grade based on BBR and/or PAV results instead of PG High Temp Grade
Force_Peak1	Force Ductility test results for the binder
Force_Peak2	
Binder_Force_Ratio	
Rot_Test_Temp1	Binder Viscosity test with space for up to 2 tests of data.
Rot_Visc_Temp1	
Rot_Test_Temp2	
Rot_Visc_Temp2	
Binder_True_Rot_Visc	
Avg_Length	Elastic Recovery test result fields.

Binder_Avg_Recovery	
MSCR_01kPa_Temp	MSCR data fields for both 0.1kPa and 3.2kPa and then difference of the 2 pressures.
MSCR_01kPa_Recov	
MSCR_01kPa_Jnr	
MSCR_32kPa_Temp	
MSCR_32kPa_Recov	
MSCR_32kPa_Jnr	
MSCR_Diff_Temp	
MSCR_Diff_Recov	
MSCR_Diff_Jnr	
Binder_Traffic_Classification	Based on value ranges of the 3.2 kPa J_{nr}.
Binder_Full_Name	Another field for the name or a more descriptive name based on the data calculated in the database
GPC_Concentration	Chemical properties of the binder component make up.
GPC_Peak1_Mn	
GPC_Peak1_Mw	
GPC_Peak1_PDI	
GPC_Peak2_Mn	
GPC_Peak2_Mw	
GPC_Peak2_PDI	
GPC_BinderPeak_Mn	
GPC_BinderPeak_Mw	
GPC_BinderPeak_PDI	
GPC_LastPeak_Mn	
GPC_LastPeak_Mw	
GPC_LastPeak_PDI	
Binder_GPC_Linear_Regression_Line_Equation	Linear regression based on the GPC values above

Chapter 7 Summary, Conclusions and Recommendations

7.1 Summary of Findings

- The percent recoveries of polymer modified binders at 3.2kPa measured in MSCR vary significantly (as much as six to seven times) within the same performance grade.
- The percent Elastic recoveries at 25C of polymer modified binders vary significantly (as much as three to four times) within the same performance grade.
- The addition of PPA in the 1.5% Elvaloy in NuStar 64-22 quadrupled the recovery measured in the MSCR test. However, such a dramatic improvement was not observed when Elastic Recovery was tested at 25°C.
- All received binders and the binder modified with PPA had recovery values greater than 60% while binders that graded at 64 and 70°C fell below the 60% recovery.
- All binders with a J_{nr} at 3.2kPa at 64 °C less than 0.6 kPa^{-1} exhibited elastic recovery more than 60%.
- All binders that had the MSCR recovery at 3.2 kPa greater than 40% was above the MSCR elastic recovery curve.
- All binders that were above the MSCR elastic recovery curve passed the elastic recovery requirement of 60%.
- There was no correlation observed between continuous grade of the binder and the non-recoverable creep compliance.
- Under AASHTO MP19 some PG 64-28 binders could grade similar to PG 82-22 at PG 64E. However, they may not actually be able to withstand Extreme traffic and may perform poorly at high temperatures. One way to address this issue is by analyzing the ODSR result of binders at 64C. AASHTO MP19 calls for a DSR on original material at the environmental grade. If $G^*/\sin(\delta)$ is below 2.0 kPa at the environmental grade it is unlikely it would pass the DSR requirement at next PG temperature.
- Based on the polymer modified binders tested in this study, more pass the elastic recovery requirement of 60% at 25C and the phase angle requirement of 75 degrees at high PG grade established by various states. On the other hand, very few (Sem Strata, Road Science and NuStar 82-22) are above the proposed MSCR elastic curve.
- Phase angle slightly increases with J_{nr}, and decrease with percentage of recovery.
- The peak ratio decreased with increase in non-recoverable compliance.
- Peak ratios and areas under the load displacement curve did not show sensitivity to performance grades
- The areas under the load-displacement curve have not provided clear trends when compared to J_{nr} or percent recovery. However, the areas under the load-displacement curve are sensitive to the percent by volume of modifier added in the asphalt binders.
- GPC has been successful in determining whether or not a polymer is present within a binder, but not in determining the amount or type of polymer used.
- FTIR has the potential to be used in conjunction with GPC to be able to take any sample of polymer modified binder and find the type and concentration of polymer within that sample.
- Elvaloy and PPA significantly impact the non-linear viscoelastic component of the strains.

- Dynamic complex modulus and MEPDG did not appear to be sensitive to polymer modification
- Mixes with a non-recoverable creep compliance (J_{nr}) lower than 0.5 kPa^{-1}performed well, while mixes with higher J_{nr} performed poorly in the flow-time test.

7.2 Conclusion

The conclusions based on the summary of findings are as follows:

1) Upon testing a variety of binders it has been determined that MSCR binder testing is sensitive to asphalt mix performance. Binders with non-recoverable compliance value (J_{nr}) of less than 0.5 kPa^{-1} appear to show better high temperature performance. The results are in line with the AASHTO MP 19-10 specification. It should be noted that the scope of this study was limited to binder selection and many other parameters impact the performance of roadways.
2) The MSCR elastic curve requirement appears to be the most stringent of the requirements to evaluate elastic response as compared to elastic recovery at 25ºC and phase angle of 75.
3) An MSCR recovery at 3.2kPa greater than 40% will ensure that it is above the MSCR elastic recovery curve. This could serve as an alternative specification to the MSCR elastic recovery curve.
4) Additional linear and non-linear visco-elastic binder properties can be determined from the analysis of the MSCR curve. These provide invaluable in-sight into how the polymer modification influences different types of mechanical responses.
5) Some modified binders with a lower PG-grade (-28 versus -22) may grade high on the AASHTO MP-19, which could be misleading that they can withstand heavy traffic.
6) New Jersey DOT is limited in its selection of modified binders as the NJDOT currently requires styrene-butadiene or styrene-butadiene-styrene to be incorporated in all modified binder, causing supply shortages and rising cost. This limitation is imposed by the NJDOT to ensure performance, while the underlining issue is; there currently is not a simple and effective test to predict modified asphalt performance. However, using the MSCR parameter in the binder specification will have the potential to allow the state to open the market to abroad range of modified binders.
7) The MSCR test for non-recoverable creep compliance (J_{nr}) is a simple and quick test to perform and does not require the purchase of an additional testing apparatus since it uses the Dynamic Shear Rheometer (DSR), which is already a common piece of lab equipment in the asphalt industry. Current test method such as Elastic Recovery (ER) and Force Ductility (FD) are time intensive and require the purchasing of additional testing apparatus and are not necessary to evaluate polymer modified binders.

7.3 Recommendations

After conducting a thorough literature review, executing the proposed research plan and subsequent analysis of the results it is the recommendation of this paper for MSCR testing using the parameter J_{nr}, to become a standard means to evaluate polymer modified binders in New Jersey. The guidelines set forth by AASHTO MP 19-10, in which the binders are graded according to traffic (ESALs) by using J_{nr} is recommended. Additionally:

- The New Jersey DOT should use the access database system as a prescreening process for binder selection, alleviating extraneous binder testing and the cost associated with them.

- New Jersey DOT could eliminate the use of elastic recovery, thus saving almost $15,000 dollars on capital cost of equipment and up to $500 per binder characterization considering labor and depreciation cost. These could lead to considerable savings of thousands of dollars over several years.
- Additional testing, including field performance should be conducted on binders with low J_{nr} (less than 0.5 kPa^{-1}) and with a lower PG-grade, such as PG 64-28 versus PG64-22.
    - This can be addressed by closely looking at the ODSR result of binders. For example, at 64˚C, if the G*/sin(δ) is below 2.0 kPa, it is unlikely to pass a higher grade and withstand heavy traffic.
- Low non-recoverable creep compliance (J_{nr} < 0.5 kPa^{-1}) coupled with high MSCR recovery at 3.2 kPa (recovery greater than 40%) and G*/sin(δ) high enough to pass the next high grade will ensure that the binder selected will withstand heavy and extreme traffic levels.
- Most of the binders provided by the refinery do not have specific compositions. Some binders may have several polymers meeting the target specifications. Therefore, it is not known how other polymers influence the non-recoverable compliance. A detailed evaluation of the impact of a broad range of polymer modification on the non-recoverable compliance is needed. However, appropriate interlocking should be evaluated using direct measurement tools, such as the fluorescent microscope.

Bibliography

[1] "N-heptane," 2013. [Online]. Available: http://pubchem.ncbi.nlm.nih.gov/summary/summary.cgi?cid=8900&loc=ec_rcs.

[2] A. Pérez-Lepe, F.J. Martínez-Boza, C. Gallegos, O. González, M.E. Muñoz, A. Santamaría, "Influence of the Processing Conditions on the Rheological Behaviour of Polymer-Modified Bitumen," Science Direct. European Polymer Journal 41 (2005) 2831-2844. 22 July 2005. Elsevier Ltd. 2005.

[3] O. González, M.E. Muñoz, A. Santamaría, M. García-Morales, F.J. Navarro, P. Partal "Rheology and Stability of Bitumen/EVA Blends," Science Direct. European Polymer Journal 40 (2004) 2365-2372. 20 July 2004. Elsevier Ltd. 2004.

[4] G. Airey, "Rheological Properties of Styrene Butadiene Styrene Polymer Modified Road Bitumens", vol. 14, n. 14, Ed., October, 2003, pp. 1709-1719.

[5] Gina M. Hrdlicka, Vivek Tandon, Jorge Prozzi, Andre Smit, Yetkin Yildrim, "Evaluation of Binder Tests for Identifying Rutting and Cracking Potential," Center for Transportation Infrastructure Systems. Research Report 0-4824-1. Conducted for Texas Department of Transportation. February 2007.

[6] Sengoz B. and Isikyakar G., "Evaluation of the Properties and Microstructure of SBS and EVA Polymer Modified Bitumen," Science Direct. Construction and Building Materials 22 (2008) 1897-1905. 29 August 2007. Elsevier Ltd. 2007.

[7] Y. Yildirim, "Polymer Modified Asphalt Binders", vol. 21, Construction and Building Materials, January, 2007, pp. 66-72.

[8] G. D. Airey, "Rheological Evaluation of Ethylene Vinyl Acetate Polymer Modified Bitumens," *Construction and Building Materials*, vol. 16, no. n 8, pp. 473-487, December 2002.

[9] S. Diefenderder, "Evaluation of Polymer Detection Methods for Binder Quality Assurance," in *Proceedings of the 2006 Airfield and Highway Pavement Specialty Conference*, 2006.

[10] K. A. Maccarrone, "High Performance Bitumens," in *Conference of the Australian Road Research Board, Transport*, 1998.

[11] G. G. Maccarrone, "Properties of Polymer Modified Binders and Relationship to Mix And Pavement Performance," in *Association of Asphalt Paving Technologists-Proceedings of the TechnicalSessions*, 1996.

[12] Gina M. Hrdlicka, Vivek Tandon, Jorge Prozzi, Andre Smit, Yetkin Yildrim, "Evaluation of Binder Tests for Identifying Rutting and Cracking Potential of Modified Asphalt Binders," *Center for Transportation. Research Report 0-4824-1*, 2007.

[13] Becker. Y., Mendendez. M. P. and Rodriguez, Y. "Polymer modified asphalt," *Science Direct.Vision Technologica*, vol. 9 (1), pp. 39-50. 2001.

[14] Wen G, *Zhang Y, Zhang Y, Sun K, Fan Y*, "Rheological Characterization of Storage-Stable SBS-Modified," *Polymer Testing 21*, pp. 295-302, 2002.

[15] Dou D, Fu H, Li L, Xie L, Yao S, Yu M., "Storage Stability and Compatibility of Asphalt Binder Modified by SBS Graft Copolymer," Science Direct. Construction and Building Materials 21 (2007) 1528-1533..

[16] Stastna , L. Zanzotto , O.J. Vacin, "Viscosity Function in Polymer-Modified Asphalts," *Science Direct.Journal of Colloid and Interface Science 259*, pp. 200-207, 2002.

[17] Kamiya, S; Tasaka, S; Zhang, XM; Dong, DW; Inagaki, N, "Compatibilizer Role of Styrene-butadiene-styrene Triblock Copolymer," *Polymer Journal*, vol. 33, no. 3, pp. 209-213, 2001.

[18] S. B. a. I. G., "Analysis of Styrene-Butadiene-Styrene Polymer," *Science Direct. Journal of Hazardous Materials*, pp. 424-432, 2008.

[19] HADDADI S., GHORBEL E. & LARADI N., "Effects of the Manufacturing Process on the Performances of the Bituminous Binders Modified with EVA," Science Direct. Construction and Building Materials 22 (2008) 1212-1219. 16 April 2007. Elsevier Ltd. 2007.

[20] Aflaki S. and Tabatabaee N., "Proposals for Modification of Iranian Bitumen to Meet the Climatic Requirements of Iran," Science Direct. Construction and Building Materials 23 (2009) 2141-2150. 8 January 2009. Elsevier Ltd. 2008..

[21] A. Ghavibazoo, "Mechanism of Crumb Rubber Modifier (CRM) dissolution into asphalt matrix and its effect on final physical properties of CRM binder," in *TRB*, 2013.

[22] J. C.-A. M.Sc., "Tests Modification of the Particulate Additive Test 1 (PAT), for the," in *TRB*, 2013.

[23] 2. Asphalt Institute.

[24] H. A. Tabatabaee, "Critical Problems with Using the Asphalt Ductility Test as a Performance Index for Modified Binders," in *TRB*, 2013.

[25] "NCAT Superpave prsentation," [Online]. Available: http://www.ncat.us/education/training/superpave-mix.html.

[26] W. S. Mogawer, "Evaluating the Effects of Ground Tire Rubber (GTR) Modified Asphalt and Dry Added 1 Treated GTR on the Performance Characteristics of RAP Mixtures," in *TRB*, 2013.

[27] T. K., "Polymer-Modified Asphalt Comes of Age," *Better Roads Magazine,* November 2005.

[28] D. J, "www.apao.org/docs/BeneModBindMar06.ppt".

[29] A. Institute, 2006. [Online]. Available: www.asphaltinsitute.org .

[30] N. J.K, "Dynamic Shear Rheological Properties of Polymer-Modified Asphalt Binders," *Journal of Elastomers and Plastics,* vol. 30, no. 3, pp. 245-263, 1998.

[31] AASHTO, Multiple stress Creep Recovery (MSCR) Test of Asphalt Binder using a Dynamic Shear Rheometer (DSR).

[32] H. C., "Development and Numerical Implementation of Nonlinear Viscoelastic-Viscoplastic Model for Asphalt Materials," *PH.D Thesis Texas A & M University ,* 2009.

[33] S. R.A., "Nonlinear Viscoelastic Solids," *International Journal of Soolids and Structures,* vol. 37, pp. 359-366, 2000.

[34] AASHTO Standard Specifications for Transportation Materials and Methods of Sampling and Testing.

[35] Lee S.J., Kim H., Akisetty C.K., and Amirkhanian S.N., "Laboratory Characterization of Recycled Crumb-Rubber-Modified Asphalt Mixture After Extended Aging," *NRC Research Press Web site at cjce.nrc.ca,* 2008.

[36] Shen J., Amirkhanian S., and Xiao F., "High-Pressure Gel Permeation Chromatography of Aging of Recycled Crumb Rubber-Modified Binders with Rejuvenating Agents," *Transportation Research Record: Journal of the Transportation Research Board, No. 1962. Transportation Research Board of the National Academies.,* 2006.

[37] Masson J.F., Collins P., Bundalo-Perc S., Woods J.R., and Al-Qadi I.L., "Early Thermodegradation of Bituminous Sealants Resulting from Improper Installation," *Transportation Research Record: Journal of the Transportation Research Board, No. 1991,* pp. 119-123, 2007.

[38] Bianchetto H., Miro R., Perez-Jimenez F., and Martinez A. H., "Effect of Calcareous Fillers on Bituminous Mix Aging," *Transportation Research Record: Journal of the Transportation Research Board, No. 1998,* pp. 140-148, 2007.

[39] AASHTO, AASHTO T 342 2010, "Standard Practice for Developing Dynamic Modulus MasterCurve for Hot Mix Asphalt (HMA)", Washington, DC, 2010.

[40] "Mechanistic Empirical Design of New and Rehabilitated Pavement Structures Guide.", NCHRP I-37, 2012.

[41] Bonemazzi, "Characteristics of Polymers and Polymers and Polymer-Modified Binders," *Transportation Research Record,* no. n 1535, pp. 36-47, September 1996.

[42] Da Silva, "Study of Rheological Properties of Pure and Polymer-Modified Brazilian Asphalt Binders," *Journal of Materials Science,* vol. 39, no. 2, pp. 539-546, 2004.

[43] G. Polacco, J. Stastna, D. Biondi and L. Zanzotto, "Relationship Between Absolute Viscosity of Polymer-Modified Bitumens and Rutting Resistance of Pavement," *Materials and Structures/Materiaux et Constructions,* vol. 27, no. 166, pp. 110-120, 1994.

[44] Cortizo, M.S., Larsen, D.O. BIanchetto, H. and Alessandrini, J.L. "Effect of the Thermal Degradation of SBS Copolymers during the Ageing of Modified Asphalts," Science Direct. Polymer Degradation and Stability 86 (2004) 275-282.

[45] C.-S. Wu, Handbook Of Size Exclusion Chromatography And Related Techniques: Revised And Expanded, 2005.

[46] Mouillet V. et al. "Infrared Microscopy Investigation of Oxidation and Phase Evolution in Bitumen Modified With Polymers"., "Infrared Microscopy Investigation of Oxidation and Phase Evolution in Bitumen Modified With Polymers," Science Direct. Fuel 87 (2008) 1270-1280. 13 August 2007. Elsevier Ltd. 2007.

[47] Lee Soon-Jae, Amirkhanian Serji N, Kim Kwang W, "Laboratory Evaluation of the Effects of Short-Term Oven Aging on Asphalt Binders in Asphalt Mixtures Using HP-GPC," Science Direct. Construction and Building Materials 23 (2009) 3087-3093. 18 April 2009. Elsevier Ltd. 2009.

[48] Ruan, Y., Davison, R. R., and Glover, C. J., "The Effect of Long-Term Oxidation on the Rheological Properties of Polymer Modified Asphalts," Science Direct. Fuel 82 (2003) 1763-1773. 28 May 2003. Elsevier Ltd. 2003.

[49] Khodaii A. and Mehrara A., "Evaluation of Permanent Deformation of Unmodified and SBS Modified Asphalt Mixtures Using Dynamic Creep Test," Science Direct. Construction and Building Materials 23 (2009) 2586-2592. 16 March 2009. Elsevier Ltd. 2009.

[50] S. Tayfur, *H. Ozen, A. Aksoy.*, "Investigation of Rutting Performance of Asphalt Mixtures Containing Polymer Modifiers," Science Direct. Construction and Building Materials 21 (2007) 328-337. 28 November 2005. Elsevier Ltd. 2005.

[51] G. Amir, A. Magdy and R. MohyElDin, "Effect of CRM dissolution on storage stability of CRM modified asphalt," 2013.

[52] Guian Wen, Yong Zhang, Yinxi Zhang, Kang Sun, Yongzhong Fan, "*Rheological Characterization of Storage-Stable SBS-Modified Asphalts,* Polymer Testing" 21 (2002) 295-302. 7 August 2001. Elsevier Ltd. 2002.

[53] Z. F. a. Y. J, "The Research for High-Performance SBR Compound Modified Asphalt," Science Direct. Construction and Building Materials (2009). Article in Press. Elsevier Ltd. 2009.

[54] SIRIN, O; KIM, H J; TIA, M; CHOUBANE, B, "Comparison of Rutting Resistance of Unmodified and SBS-Modified Superpave Mixtures by Accelerated Pavement Testing," Science Direct. Construction and Building Materials 22 (2008) 286-294. 24 October 2006. Elsevier Ltd. 2007.

[55] "Pavement Interactive," 2008. [Online]. Available: http://www.pavementinteractive.org/article/stone-matrix-asphalt. [Accessed March 2013].

[56] Roberts F.L., Hot Mix Asphalt Materials, Mixture Design and Construction, NAPA Research and Education Foundation, 2000.

[57] NCHRP, "Ruggedness Testing of Dynamic Modulus and Flow Number Test with the Simple Performance Tester," *Transportation Review Board ,* 2008.

[58] M. W. Witczak, K. Kaloush, T. Pellinen, M. E. Basouny and H. V. Quintus, "Simple Perfrormance Test for Superpave Mix Design," *National Cooperative Highway Research Program Report No.465,*

Transportation Review Board.

[59] FHWA. [Online]. Available: http://www.fhwa.dot.gov/pavement/asphalt/pubs/hif13005.pdf. [Accessed 2013].

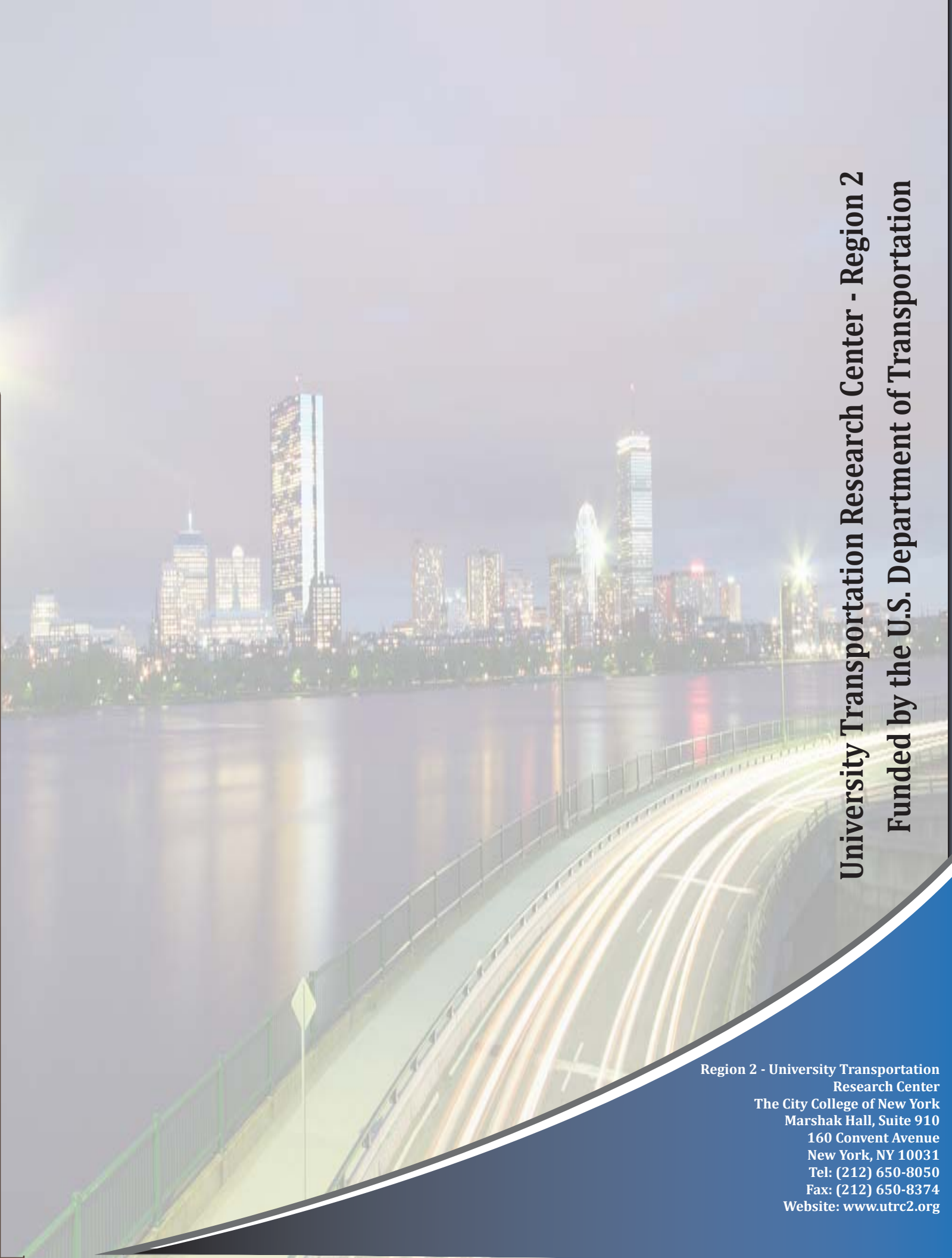

University Transportation Research Center - Region 2

Funded by the U.S. Department of Transportation

Region 2 - University Transportation
Research Center
The City College of New York
Marshak Hall, Suite 910
160 Convent Avenue
New York, NY 10031
Tel: (212) 650-8050
Fax: (212) 650-8374
Website: www.utrc2.org